MULTI-SCALE APPROACHES TO GLOBAL CHALLENGES IN A TELECOUPLED WORLD

By

Zhenci Xu

A DISSERTATION

Submitted to
Michigan State University
in partial fulfillment of the requirements
for the degree of

Fisheries and Wildlife – Doctor of Philosophy

2019

ABSTRACT

MULTI-SCALE APPROACHES TO GLOBAL CHALLENGES IN A TELECOUPLED WORLD

By

Zhenci Xu

Global challenges such as water crisis, energy insecurity, biodiversity loss, land use change and climate change pose threats to the world's sustainability. Globalization enhances the connection of distant areas through various environmental and socioeconomic interactions. To solve the increasing challenges of achieving global sustainability in the context of globalization, the new telecoupling framework (socioeconomic and environmental interactions over distances) is proposed (Liu et al. 2013).

A growing body of research has been exploring the dynamics, impacts, mechanisms, and structure of distant interactions involving global challenges. However, based on the telecoupling framework, we find no research that studies the evolution of multiple global environmental and socioeconomic interaction networks together. Also, the interactions between two kinds of distant virtual resource transfers simultaneously and the drivers of virtual resource transfers at the national scale are still unknown. Little research explores the evolution of virtual resource transfers at a national scale. The impacts of distant interactions on sending systems' sustainability at the regional scale has rarely been quantified and systematically analyzed.

To address these knowledge gaps, I did the following work: First, I assessed the evolution of global telecouplings such as water, energy, land, CO_2 emission, nitrogen emission and financial capital transfer networks and discussed how they have impacts on global water scarcity, energy crisis, land use change, global warming and nitrogen pollution. Second, I evaluated the interactions across two kinds of national telecouplings (interregional water and energy networks), and discussed their implications for the trading region's water scarcity and energy security, and explore

the drivers of national telecouplings. Third, I studied the evolution of national virtual energy network. Fourth, I explored the water and food sustainability in a sending system of telecoupling (food transfer aimed at ensuring food security in the receiving system) at the regional scale. These four works have been accomplished in four chapters, respectively.

Main findings from this dissertation include: At the global scale, the volumes of all these flows, except for land flow, increased over time. Financial capital flows increased most (188.9%), followed by flows of CO_2 (59.3%), energy (58.1%), water (50.7%) and nitrogen (10.5%), while land transfer decreased by 8.8%. At the national scale using China as a demonstration, 40% of provinces gained one kind of resource (either water or energy) through trade at the expense of losing the other kind of internal resource (energy or water), and 20% of provinces suffered a double loss of both water and energy. The remaining provinces gained both water and energy. Over time, the total virtual energy transferred from energy-scarce to energy-abundant provinces increased from 43.2% to 47.5% from 2007 to 2012. At a regional scale, irrigated agriculture's annual water footprint in the North China Plain increased from 53 billion m^3 in 1986 to 78 billion m^3 in 2010. All counties faced unsustainable water use – local water consumption was greater than local renewable freshwater – even as the average crop water productivity increased from 0.90 $kg.m^{-3}$ to 1.94 $kg.m^{-3}$.

These findings provide useful information for policy making to address environmental and socioeconomic challenges and build distant cooperation across multiple scales.

ACKNOWLEDGEMENTS

I thank many people for shaping my PhD study and my life.

I am grateful for the help and instructions from committee members. I thank my advisor Dr. Jianguo (Jack) Liu for his insightful instructions about proposing ideas and writing papers, valuable comments and careful edits. I thank Dr. Ken Frank for his helpful social network analysis class. I thank Dr. Rafael Auras for his patience and passion in discussing with me about life-cycle assessment. I also thank Dr. Jinhua Zhao for his insightful suggestions in revising my dissertation proposal.

I also thank Yunkai Li and Xiuzhi Chen for collecting part of the data.

I greatly thank Jing Sun for his daily talks with me at the beginning of my PhD study when I knew nothing about research. From these talks I learned many tips about how to construct good ideas and write papers. I also appreciate the insightful comments and careful edits from many members in Center for Systems Integration and Sustainability, especially Shuxin Li, Yingjie Li, Sophia Chau, Anna Herzberger, Ying Tang, Thomas Connor, Jinyan Wang, Di Zhang, Mimi Gong, Dapeng Li, Kelly Kapsar, Ciara Hovis, Susie (Ruqun) Wu, Paul McCord, Julia Whyte, Sue Nichols and Franco Ruzzenenti.

I would like to thank my family and friends. I thank all my family members for their unconditional support and care. I would also like to thank my best friend Dequ Hong who was always willing to hear my emotions, trust me and comprehend me.

Finally, I acknowledge financial supports from the National Science Foundation, College of Agriculture and Natural Resources, and Graduate School at Michigan State University.

TABLE OF CONTENTS

LIST OF TABLES

LIST OF FIGURES

CHAPTER 1. INTRODUCTION

BACKGROUND

Global challenges such as water crisis, energy insecurity, biodiversity loss, land use change and climate change pose threats to the world's sustainability (Liu et al. 2015). Globalization enhances the connection of distant areas through various environmental and socioeconomic interactions (Liu et al. 2013). The stronger connections also affect the pattern of global challenges (Figure 1.1). For example, inter-basin water transfer projects are planned to alleviate water crises. The total amount of water moved through inter-basin water transfer projects accounts for 14% of total global annual water withdrawal (Liu, Yang and Li 2016). Distant energy transmission projects are also constructed to support sustainable development of energy-scarce areas (Chen, Li and Wu 2010). International trade drives global land use change and biodiversity loss (Meyfroidt, Rudel and Lambin 2010, Lenzen et al. 2012). Also, global challenges such as food insecurity drive international events like food trade and have significantly strengthened distant interactions worldwide.

To solve the increasing challenges of achieving global sustainability in the context of globalization (Figure 1.1), the new telecoupling framework (socioeconomic and environmental interactions over distance) is proposed (Liu et al. 2013). For each telecoupling, systems represent coupled human and natural systems in which humans and nature interact, and may involve distant interactions. Systems can be classified as sending systems, receiving systems, or spillover systems. Sending systems act as origins, or donors and receiving systems as recipients or destinations. Of course, which system is considered as sending and which as receiving depends on the distant interactions being analyzed. Spillover systems refer to systems which affect and/or are affected by the distant interactions between sending systems and receiving systems. The causes of a telecoupling refer to factors that affect its emergence and dynamics. Effects are environmental and socioeconomic consequences of the telecoupling. The telecoupling framework connects distant systems as one united telecoupled system through interactions and feedbacks, and seeks to understand various components driving distant interactions at different coupled human and natural systems across multiple scales. It helps to detect hidden mechanisms and facilitates a comprehensive understanding of distant interactions for creating effective solutions to achieve sustainability and improve human well-being (Liu et al. 2013, Liu et al. 2015).

The increasing international trade aiming at alleviating regional food insecurity and energy crisis leads to global land use change, carbon emission, nitrogen pollution, and water scarcity (Lambin and Meyfroidt 2011, Peters et al. 2011, Oita et al. 2016, Dalin et al. 2017). The information about the relationships between global challenges and telecoupling are critical in this telecoupled world.

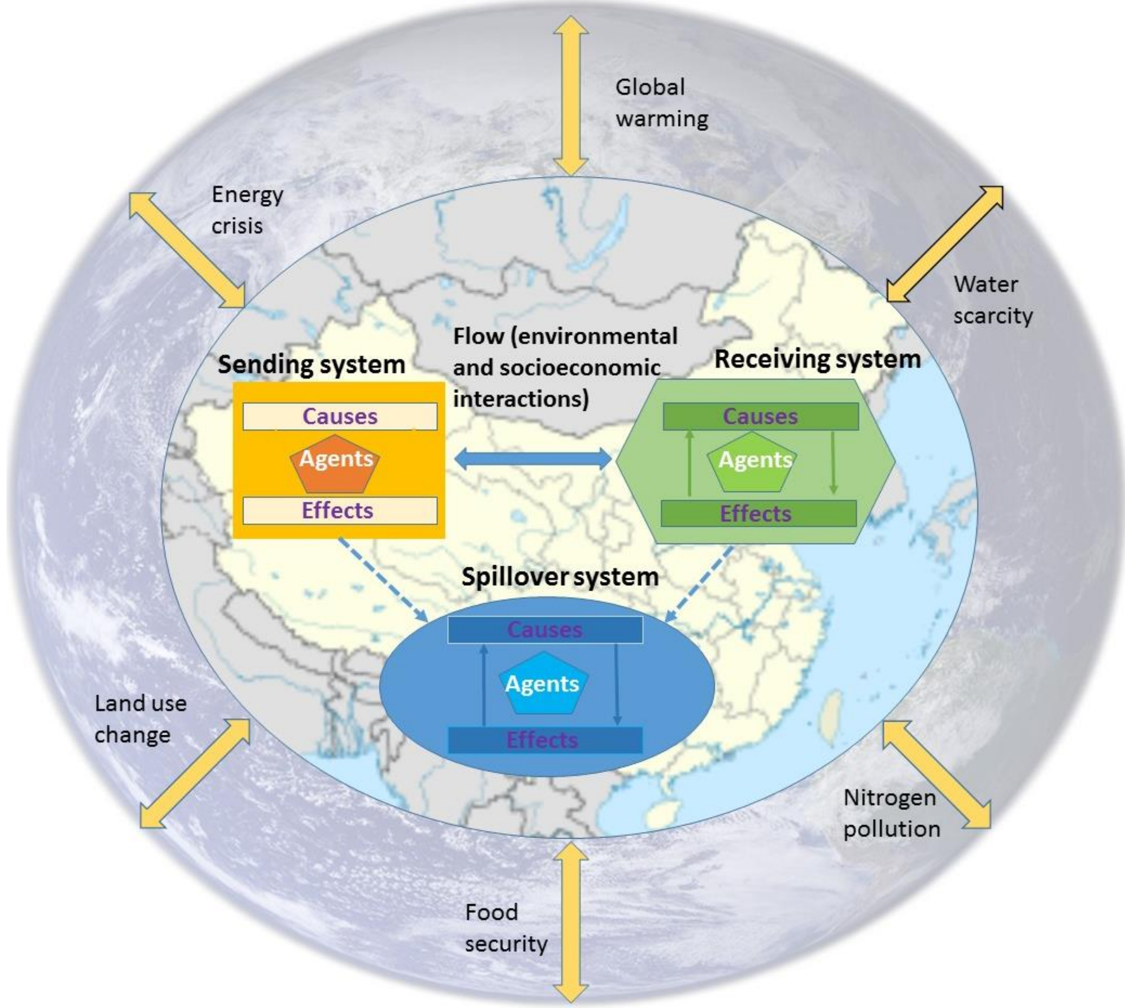

Figure 1.1. Conceptual framework of studying global challenges in a telecoupled world.

A growing body of research has been exploring the dynamics, impacts, mechanisms, and structure of distant interactions involving global challenges (Dalin et al. 2012, Qiang et al. 2013, Dalin et al. 2014, Tamea et al. 2014, Zhang and Anadon 2014, Liu et al. 2015, Zhang et al. 2016). However, based on the telecoupling framework, we find no research that studies the evolution of multiple global environmental and socioeconomic interactions networks together. Also, the interaction between two kinds of distant virtual resource transfer simultaneously and the drivers of virtual resource transfer at the national scale are still unknown. Little research explores the impacts of physical water transfer projects at the inter-basin level on spillover systems and global challenges. The impacts of distant interactions on sending systems' sustainability at a regional scale has rarely been quantified and systematically analyzed.

Such information is urgently required for the following reasons: First, global challenges such as water scarcity, energy crisis, biodiversity loss, and global warming pose great threats to sustainable development in the context of global population growth and economic development. Second, increasing telecouplings (e.g., increasing international trade) connect the challenges in local systems with mechanisms in distant systems, thus affecting global challenges. Third, a multi-scale approach could facilitate the understanding of cross-scale interactions between global challenges and telecouplings. Fourth, the telecoupling framework can help detect hidden local environmental and socioeconomic woes affected by distant systems, which may be escalated to national or even global catastrophes (Scheffer et al. 2015, Vörösmarty et al. 2015).

RESEARCH OBJECTIVES

To address these knowledge gaps, I will do the following work (Figure 1.2). First, I assess the evolution of global telecouplings such as water, energy, land, CO_2 emission, nitrogen emission and financial capital transfer networks and discuss their impacts on global water scarcity, energy crisis, land use change, global warming and nitrogen pollution. Second, I evaluate the interactions across two kinds of national telecouplings (interregional water and energy networks), and discuss their implications for the trading region's water scarcity and energy security, and explore the drivers of national telecouplings. Third, I study the impacts (e.g., CO_2 emissions) of telecoupling (e.g., inter-basin physical water transfer to alleviate the receiving system's water scarcity) on spillover systems. Fourth, I explore the water and food sustainability in a sending system of telecoupling (food transfer aimed at ensuring food security in the receiving system) at the regional scale. These four works will be accomplished in four chapters, respectively.

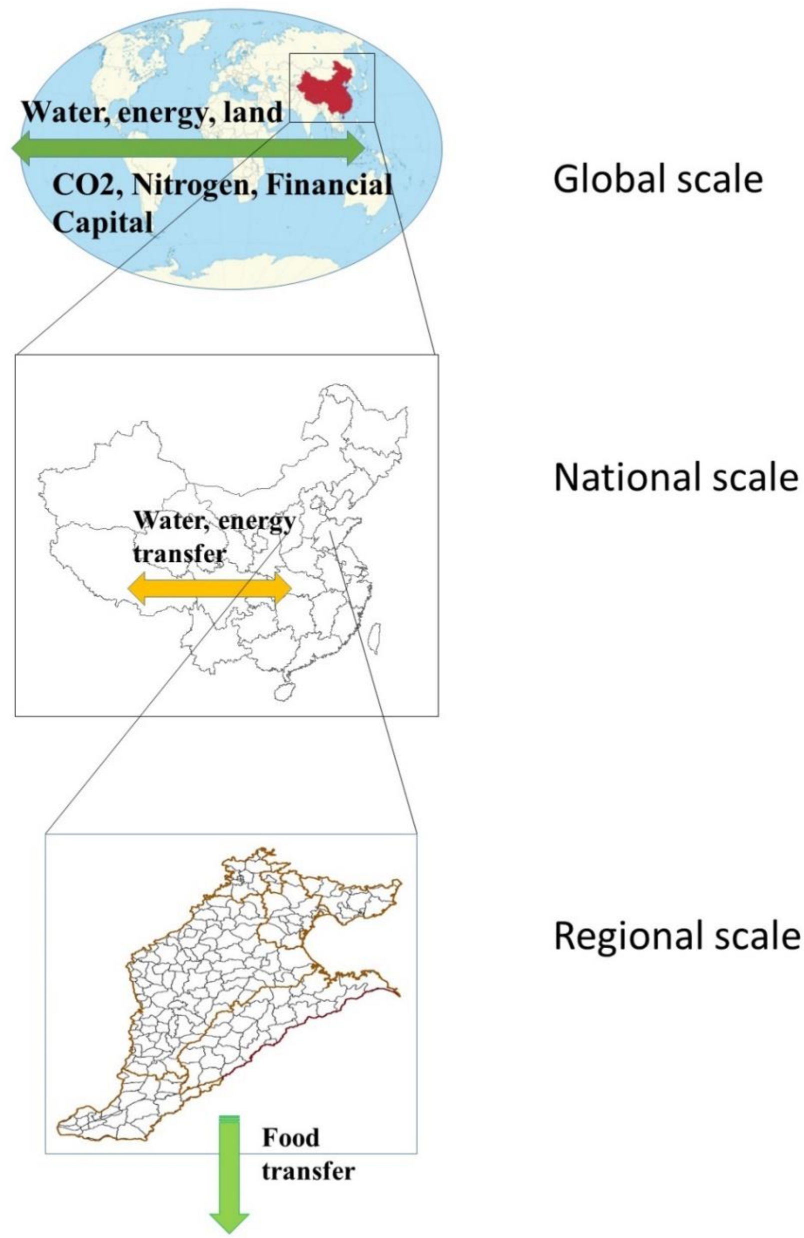

Figure 1.2 Interactions between telecouplings and global challenges cross multi-scales

The study area consists of the world, China, regions of China encompassing the South-to-North Water Transfer Project, and the North China Plain.

To study the global telecoupling, I collected data from the World Input-Output Database (Timmer et al. 2015), performed multi-regional input-output analysis (MRIO) to build these global networks.

To explore interactions across national water-energy network and understand the drivers of these two telecouplings, I performed an analysis in China's interprovincial water-energy networks. China faces a serious water crisis and pressure on energy in the 21 century (Crompton and Wu 2005, Zhao et al. 2015). Even though China possesses the world's fourth-largest amount of fresh water resources, its renewable water resource per capita only equals to about one quarter of world's average water resource per capita due to its largest population (Liu and Yang 2012). The uneven water resource distribution causes a barrier to development across China (Liu and Yang 2012). Moreover, China has become the world's largest energy consumer after surpassing the United States in 2009 (Swartz and Oster 2010, Chen et al. 2013). The energy resource distribution in China is also largely uneven and has negative impacts on China's development. Understanding the interaction, interaction type, and impacts of indirect interactions of China's interprovincial virtual water and energy (water, energy consumed in the production process of commodities traded) transfer networks can provide useful information for enhancing water security and energy security through virtual resource transfer in other developing countries.

To explore evolution of national virtual energy network, I chose China's interprovincial virtual energy networks over time as the first demonstration. With the country's economic growth, the national energy consumption and environmental pollutant emissions are growing rapidly. In 2013, nearly 22% of global energy consumption occurred in China (Cui, Peng and Zhu 2015). Consequently, China has surpassed the United States to be the world's largest energy consumer and the largest source of CO_2 emissions (Yuan et al. 2013, Cui et al. 2015). China's uneven energy resource distribution has negative impacts on China's development (Ma and Oxley 2012). As China is still in the industrialization and urbanization process, energy consumption and pollutant emissions will increase in the near future (National Development and Reform Commission of the People's Republic of China 2013). Developing strategies to maintain energy supplies while achieving economic and social sustainable development will be important issues to policy makers.

To assess water and food sustainability of a sending system at the regional scale involved in telecoupling (e.g., food transfer), I chose the North China Plain (NCP) with 207 counties as a demonstration site for the comprehensive sustainability assessment. The NCP is the national agricultural base and main grain production area in China (Qin et al. 2015), which provides more than one quarter of national food supply. Much of the food produced there was transferred to other areas of China through food trade such as north-to-south food transfer (Pietz 2015). Ninety-six percent of grain areas in NCP are planted with winter wheat and summer maize, which produces approximately 50% of the national wheat and maize production in total (Wang et al. 2001, Qin et al. 2015). But the average per capita freshwater resource in the plain is only 302 m^3 per year (Zhang et al. 2011), less than 1/24 of the global average (Kang, Yang and Pei 2013). Water-conserving irrigation technology is planned by the government to be applied in NCP to alleviate pressure on water while ensuring food production (Ministry of water resources of China 2014). Using such limited water resources to support large amounts of food production is a great challenge. Addressing the challenge in NCP can have significant implications for not only China, but also for other developing countries worldwide.

CHAPTER 2. EVOLUTION OF MULTIPLE GLOBAL VIRTUAL MATERIAL FLOWS

Xu, Z., S. Chau, F. Ruzzenenti, T. Connor, Y. Li, Y. Tang, D. Li, M. Gong & J. Liu (2018) Evolution of multiple global virtual material flows. *Science of The Total Environment,* 658, 659-668.

ABSTRACT

The world is connected through multiple flows of material, but a comprehensive assessment of their temporal dynamics and interactions is rare. To address this knowledge gap, we assessed the evolution and interactions of global flows of virtual water, energy, land, CO_2, nitrogen as well as financial capital embodied in international trade from 1995 to 2008. We found that the volumes of all these flows, except for land flow, increased over time. Financial capital flows increased most (188.9%), followed by flows of CO_2 (59.3%), energy (58.1%), water (50.7%) and nitrogen (10.5%), while land transfer decreased by 8.8%. Volumes of virtual material flows among distant countries were much higher than those among adjacent countries. The top five countries accounted for a surprisingly large proportion (47% to 80%) of total flow volumes. Different kinds of virtual material flows tended to enhance each other through synergistic effects, and CO_2 and nitrogen flows tended to have stronger positive synergetic impacts on the other virtual material flows. Our results suggest that it is important to pay particular attention to such fast-growing material flows, promote cooperation between distant countries and target countries with the largest flows to achieve global sustainable development goals.

INTRODUCTION

The world has become increasingly connected (Lambin and Meyfroidt 2011, Liu et al. 2015). The proliferation of material flows (e.g., international food trade, and energy trade across borders) is increasingly connecting adjacent and distant places into integrated systems (Liu 2017). Such material flows may continue to proliferate and intensify with global population growth, lifestyle changes, growing resource consumption, and the uneven distribution of resources (Liu et al. 2015).

Virtual resources consumed in commodity production have attracted global attention since their transfer affects environmental system in trading areas (Liu et al. 2015, Wiedmann and Lenzen 2018). For instance, importing food allows China to gain virtual land from other countries, enabling China to meet its food demand while not increasing the areal extent of its domestic agricultural land for food production (Qiang et al. 2013). Water, energy and land are critical resources for environmental conservation and socioeconomic development (Xu et al. 2017), and the world faces great threats from their shortage and uneven distribution (Lambin and Meyfroidt 2011, International Energy Agency 2015, Mekonnen and Hoekstra 2016). Four billion people suffer from severe water scarcity (Mekonnen and Hoekstra 2016); more than one billion people lack electricity (International Energy Agency 2015); and a growing world population may need an additional 2.7–4.9 Mha of cropland per year to ensure food security. This cropland shortage threatens forests that provide biodiversity and vital ecosystem services (e.g., oxygen production and carbon sequestration) (Lambin and Meyfroidt 2011). However, this process also displaces environmental burdens such as CO_2 and nitrogen emissions via natural capital transfers. For example, importing food has allowed China to become a global leader in carbon sequestration since its CO_2 emissions from deforestation are displaced to distant, exporting countries such as Brazil (Torres, Moran and Silva 2017). CO_2 plays a major role in global warming, and nitrogen emissions pose various threats to environmental and human health such as biodiversity loss, stratospheric ozone depletion and chronic respiratory and heart disease (Kampa and Castanas 2008, Erisman et al. 2013). Both CO_2 and nitrogen pollution have increased over the past decades (Peters et al. 2011, Crippa et al. 2016). Furthermore, large increases in virtual resource flows have increased financial capital flows between countries (Forbes and Warnock 2012).

Water, energy, land, CO_2, nitrogen, and financial capital are highly interconnected (Conway et al. 2015, Maris et al. 2015, Rulli et al. 2016). For example, water is used to produce energy (e.g., hydropower production), and in turn, energy is required to produce and distribute water (e.g., desalination, water diversion). All of these processes generate CO_2 and nitrogen emissions. Land can be used to store water and grow crops for bioenergy, a process that also produces nitrogen emissions. National and local economies affect, and are also affected by, these highly interconnected processes.

Despite a growing body of research on spatial pattern and impacts of distant virtual material flows (e.g., water, CO_2, and energy embodied in traded goods) (Konar et al. 2011, Dalin et al. 2012, Liu et al. 2013, Ji, Zhang and Fan 2014, Zhang et al. 2016, Zhong et al. 2016, Wiedmann and Lenzen 2018), there is little research focused on the evolution and interactions of multiple material flow networks. Moreover, no study has assessed multiple major networks of natural capital, financial capital and environmental burdens simultaneously over time. Also, the evolution of land, CO_2 and nitrogen flow networks has rarely been studied. While several studies have analyzed the typology of the global virtual water trade network and energy trade network separately (Peters et al. 2011, Dalin et al. 2012), a comparison of trade interactions between distant and adjacent countries is lacking. Furthermore, the evolution of trade volume of top trade countries in such transfer networks has not been examined (Dalin et al. 2012, Zhong et al. 2016). Such an assessment is urgently required (Liu et al. 2013) because ignoring these cross-border interactions leads to an incomplete understanding of the mechanisms behind global environmental and socioeconomic changes, thereby hindering global sustainability efforts. Comparing interactions between distant countries and adjacent countries can reveal potential key partners in international cooperation. The comparison also can help show socioeconomic and environmental impacts from trade with distant and adjacent countries, particularly since distant trade often consumes more energy for transport and therefore emits more CO_2. Also, assessing multiple kinds of material flows simultaneously can generate cross-sectoral knowledge to inform more effective policies, overcoming the shortcomings of most policies which focus on a single sector and neglect interrelationships (e.g., synergies, trade-offs) among different kinds of material flows (Liu et al. 2015, Liu 2017).

To fill these knowledge gaps, we simultaneously assessed the evolution and interactions of six global flows of virtual water, energy, land, CO_2, and nitrogen as well as financial capital embodied in international trade from 1995 to 2008 (when the most recent data are available). In the following text, for the sake of simplicity, we also considered financial capital flow as a type of virtual material flow since financial capital flow refers to the capital value embedded in the international trade. Therefore, there were six kinds of virtual material flows. Guided by the integrated framework of intercoupling (environmental and socioeconomic interactions between adjacent and distant places (Liu 2017)), we addressed several related questions. First, how did the total volume of these global virtual material flows change over time? Second, was the transfer volume of virtual material flows greater between distant countries than between adjacent countries over time? Third, what was the temporal pattern in intensity and dominance of top trade countries (measured by the ratio between the trade volume of top trade countries and the total trade volume of all countries analyzed)? Fourth, how did multiple global virtual material flow networks interact with each other (e.g., synergies, trade-offs)? Using data from the World Input-Output Database (WIOD) (Timmer et al. 2015), we performed multi-regional input-output analyses and network analysis to address these questions. Finally, we discussed the implications of these findings for global sustainability.

MATERIALS AND METHODS

Our analysis covered 35 sectors across environmental, economic and social dimensions such as "agriculture, hunting, forestry and fishing" and "mining and quarrying", in all countries with available data, giving our study a broader scope than other studies focusing only on a single or few sectors (Dalin et al. 2012, Zhong et al. 2016).

Data.

We obtained multi-regional input-output tables for all sectors' material inputs and outputs (water, energy, land, CO_2, nitrogen, and financial capital output for all 35 sectors) from the World Input-Output Database (WIOD) (Timmer et al. 2015). WIOD is one of the most developed global databases. It shows the trade flows between countries, has homogeneous sectors for all countries, and allows direct comparison between sectors (e.g., agriculture, hunting, forestry and fishing, mining and quarrying, education etc.) in different countries. It also provides a reasonable coverage of countries (40 countries accounting for 97% of world's GDP; see Supplementary Table S1 for country names) and temporal range (1995-2011) (Kander et al. 2015). Data for environmental impacts (water, energy, land consumption, CO_2, and nitrogen) were available through 2008, while data for financial flows were available through 2011. To keep all the datasets consistent, 2008 was the last year of data included our analyses.

Construction of global material flow networks.

Global material flow networks are composed of nodes (each representing a country) and links (each representing a material flow such as virtual land between trading countries) between pairs of nodes. The weight of a link indicates the volume (e.g., hectares of virtual land) of a flow from one country to another, and the weight of a node indicates the total flow volume that is imported or exported by a given country. Two kinds of directed weighted networks exist, each representing one of two potential flow directions. Import-directed networks are those in which links represent imports, and export-directed networks are those in which links represent exports. Either kind of network represents the total global material flows for a given network because each flow is associated with both an import country and an export country. Thus, a certain flow is represented in both kinds of networks.

For each kind of material flow, we constructed a global network by applying multi-regional input-output analysis, a method commonly used to determine interdependencies between countries by tracking monetary flows. Assuming there are m countries and each country has n sectors, we can calculate the monetary output of sector i in country R by:

$$x_i^R = \sum_{S=1}^{m} \sum_{j=1}^{n} x_{ij}^{RS} + \sum_{S=1}^{m} y_i^{RS} \qquad (1)$$

Where the x_{ij}^{RS} represents the money flow from sector i of country R to sector j of country S, and y_i^{RS} indicates country S's final demand provided by sector i in country R.

The direct input coefficient a_{ij}^{RS} is calculated by:

$$a_{ij}^{RS} = x_{ij}^{RS} / x_j^S \qquad (2)$$

where a_{ij}^{RS} indicates the amount of monetary flow from sector i of country R that results in one monetary output in sector j in country S.

Letting X=[x_i^R], A=[a_{ij}^{RS}] and Y=[y_i^{RS}], we obtained the following matrix based on Eq. (1) and (2):

$$X = A.X + Y \qquad (3)$$

In the following consumption driven equation, $(I-A)^{-1}$ is the Leontief inverse matrix indicating both direct and indirect monetary flows from other countries to meet one unit of final monetary demand:

$$X = B.Y$$

$$B = (I-A)^{-1} \tag{4}$$

To calculate the virtual material flow embodied in international trade, we applied the direct material consumption coefficient. The direct material consumption coefficient of sector i in country R can be expressed as Eq. (5):

$$e_i^R = \frac{w_i^R}{x_i^R} \tag{5}$$

where w_i^R represents total material consumption in sector i of country R, therefore e_i^R represents the amount of material consumed to increase one monetary unit of output in sector i in country R.

Letting $E=[e_i^R]$, we obtained the following material transfer matrix (Feng et al. 2013):

$$\text{Material} = E.B.Y \tag{6}$$

Network analysis

We analyzed the temporal change of trade flow volumes of all kinds of material flow networks by tracking the sum of the volumes of each material flow network over time. We compared flow volumes between distant countries (not sharing a border) and adjacent countries (sharing a border) over time. On average, each of the 40 countries was linked with 35 distant and 4 adjacent countries.

In both the export-directed and import-directed networks, we assessed each country's node strength (total volume of a country's trade links) and designated the top five countries (top five highest node strengths) as "trade hubs". We then tracked the node strength of these hubs over time in both export-directed and import-directed networks. For example, country *a*'s node strength in an export-directed network is $O_a = \sum_b P_{ab}$, where P_{ab} represents the virtual material flows exported from country *a* to country *b*. The ratio between the combined strength of the world's five trade hubs in a given network and the total global network's volume quantifies the dominance of these hubs.

We used the "multiplexity" and "multireciprocity" index developed by Gemmetto et al. (2016) to explore two kinds of synergies between two or more global material flow networks: multiplexed synergies and multireciprocated synergies (Ruzzenenti et al. 2015, Gemmetto et al. 2016). The first kind of synergy occurs when a link (trade flow) between two nodes (countries) in one network is paralleled by a link that flows in the same direction between the same two nodes in another network (Ruzzenenti et al. 2015, Gemmetto et al. 2016). The second kind occurs when the link between two nodes in a network flows in the opposite direction between the two nodes in another network. We created a null model to clear the spurious effects of chance in the correlation analysis (Gemmetto et al. 2016). Z-score tests were used to determine the significance of synergistic effects between global networks (Ruzzenenti et al. 2015, Gemmetto et al. 2016).

RESULTS

Global virtual versions of water, energy, CO_2, nitrogen and financial capital transfers intensified from 1995 to 2008, while virtual land transfers decreased during that time (Figure 2.1). The virtual transfer of financial capital increased the most (188.9%), followed by CO_2 (59.3%), energy (58.1%), water (50.7%) and nitrogen (10.5%). Virtual land transfer declined by 8.8%.

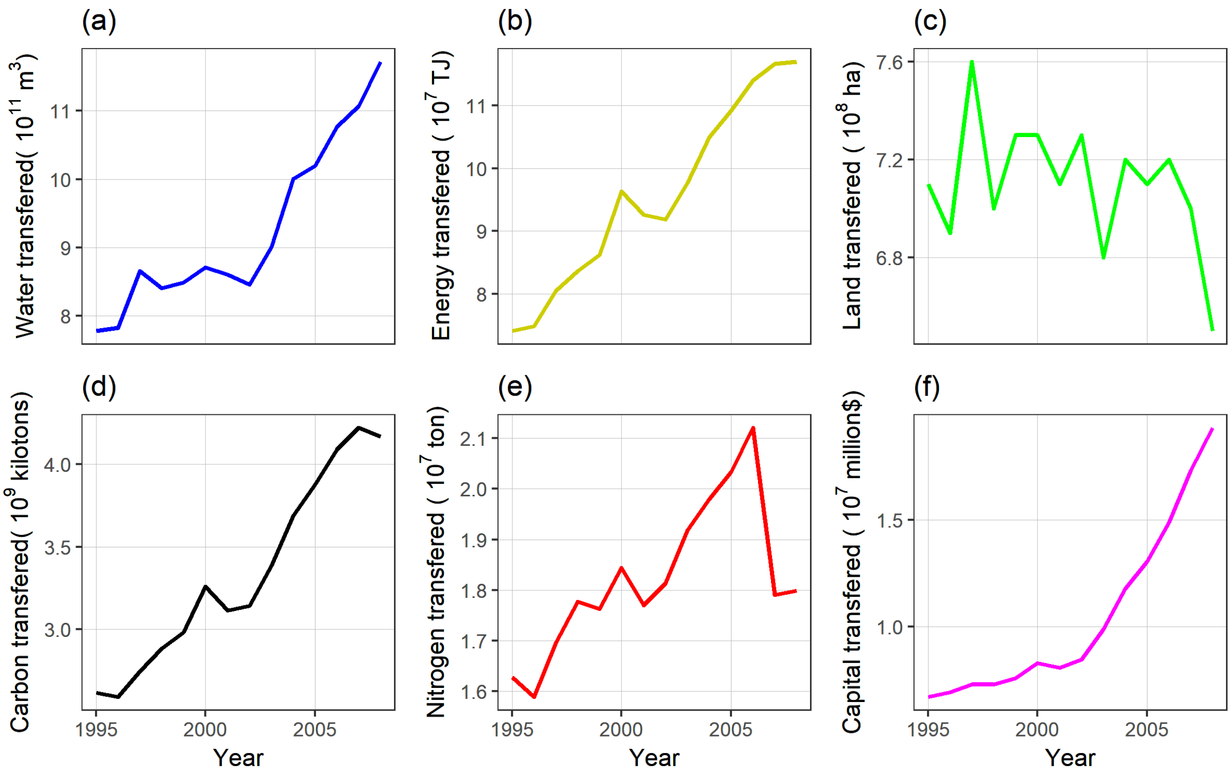

Figure 2.1 Temporal changes in total transfer volume of global (a) virtual water, (b) virtual energy, (c) virtual land, (d) virtual CO_2, (e) virtual nitrogen, and (f) financial capital.

In each kind of virtual material network, distant countries had higher total trade volumes with each other than adjacent countries (Figure 2.2). The total flow volumes between distant countries were much more than those between adjacent countries. Over time, all flows between distant countries, except for virtual land, also increased more than those between adjacent countries (Figure 2.2). However, the average flow volume between each pair of adjacent countries was larger than that between each pair of distant countries (Figure 2.3).

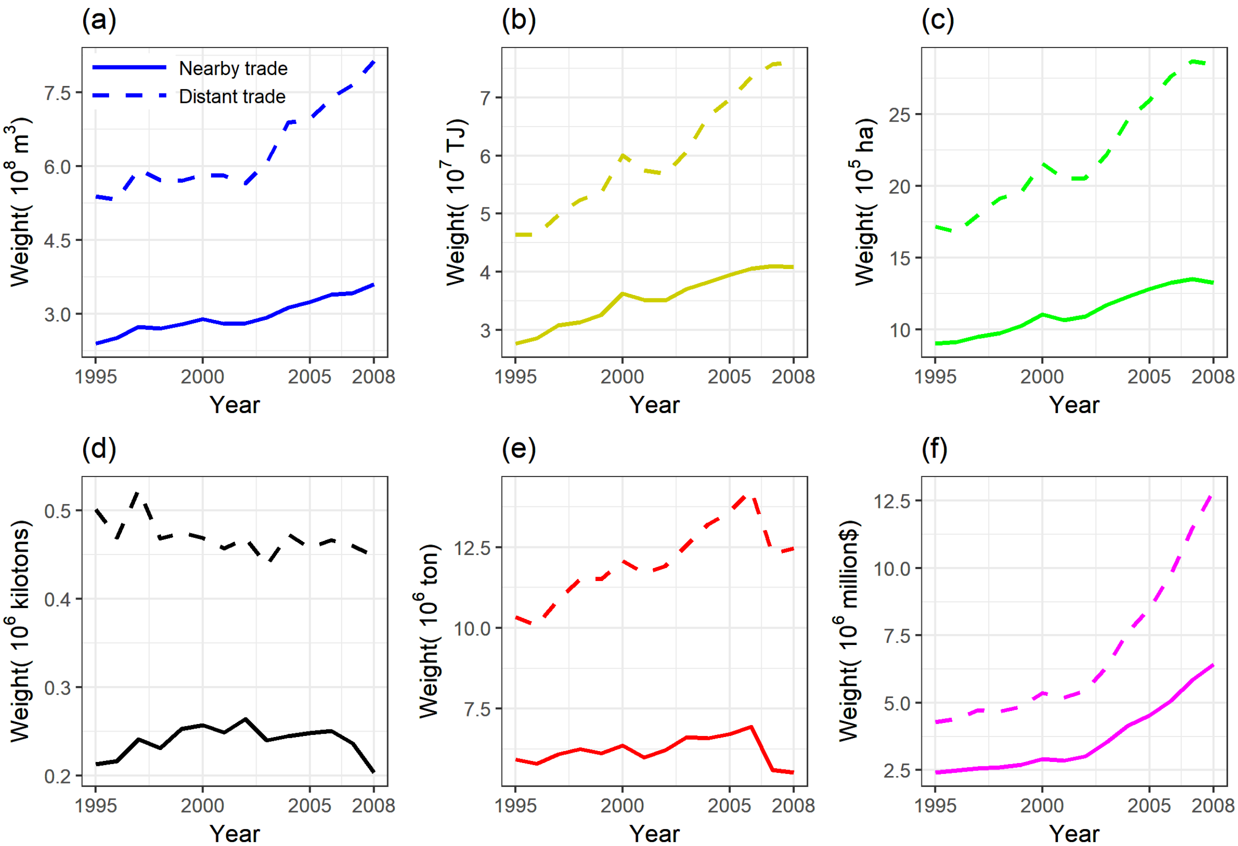

Figure 2.2. Volume of virtual material transfer between distant countries and adjacent countries over time. (a) virtual water. (b) virtual energy. (c) virtual land. (d) virtual CO2. (e) virtual nitrogen. (f) financial capital.

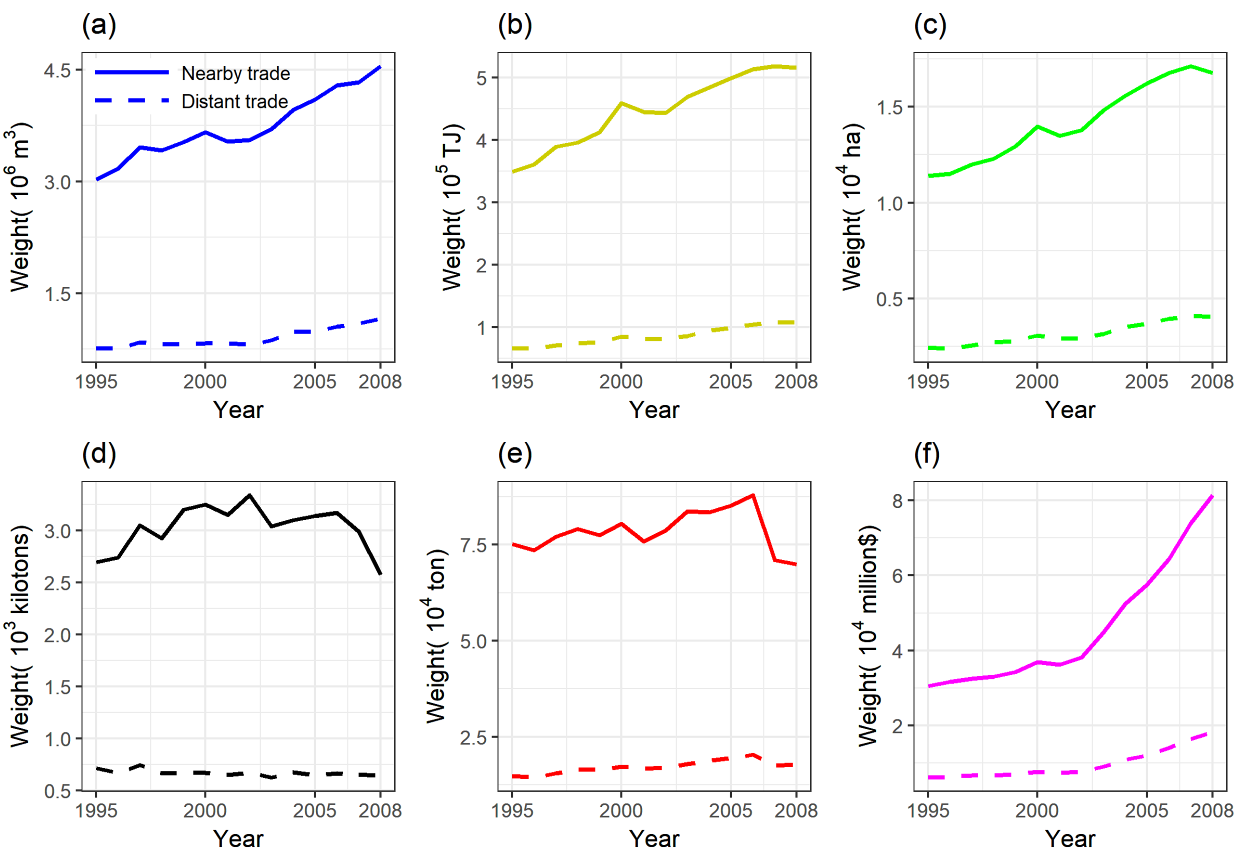

Figure 2.3. Average volume of virtual material transfer between per pair of distant countries or per pair of adjacent countries over time. (a) virtual water. (b) virtual energy. (c) virtual land. (d) virtual CO_2. (e) virtual nitrogen. (f) financial capital.

All material flow networks were highly connected, and the US and China were in the top five trading countries of each network (Figure 2.4). Both the US and China had trade relations with all other countries, but China became more influential over time (Figure 2.4). In 1995, the US was the top trading country in all six material flow networks. In 2008, however, China replaced the US as the top trading country of virtual CO_2 and nitrogen transfer. China's virtual trade volumes in all six global networks increased over time, although the US continued to dominate the virtual water, energy, land and financial capital networks.

（1）

(a) (b)

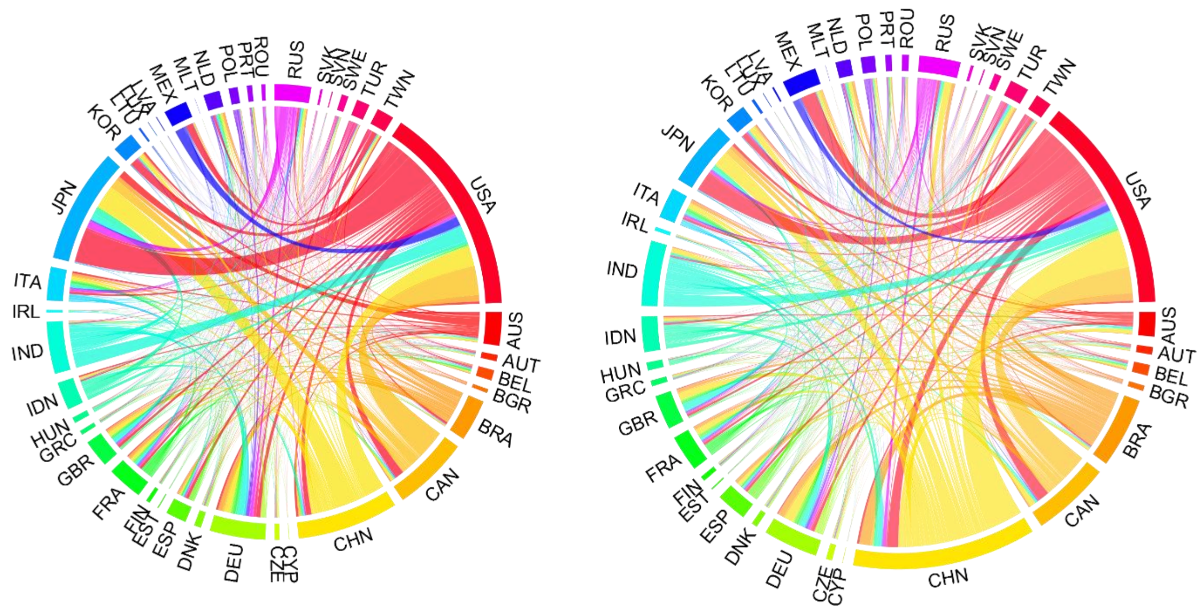

Figure 2.4. Transfer of virtual (1) water, (2) energy, (3) land, (4) CO_2, (5) nitrogen, and (6) financial capital between individual countries (a: in 1995; b: in 2008). The arc length of an outer circle indicates the sum of exports and imports in each country (See Supplementary Table S1 for the acronyms of country names). Ribbon colors suggest the country of export.

Figure 2.4. (cont'd.)

（2）

(a)

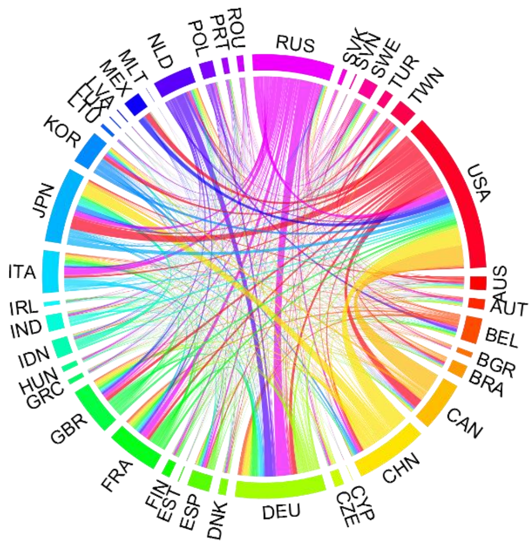

(b)

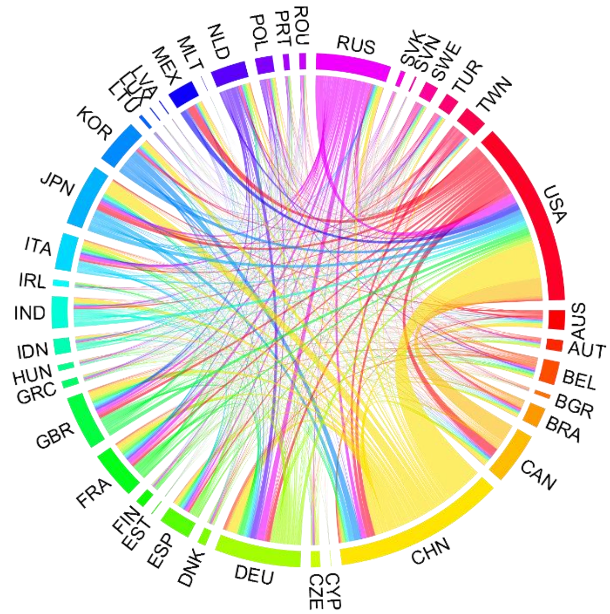

（3）

(a)

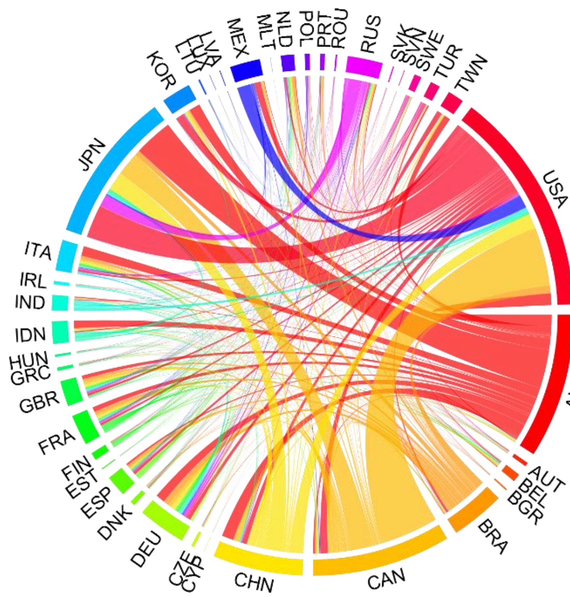

(b)

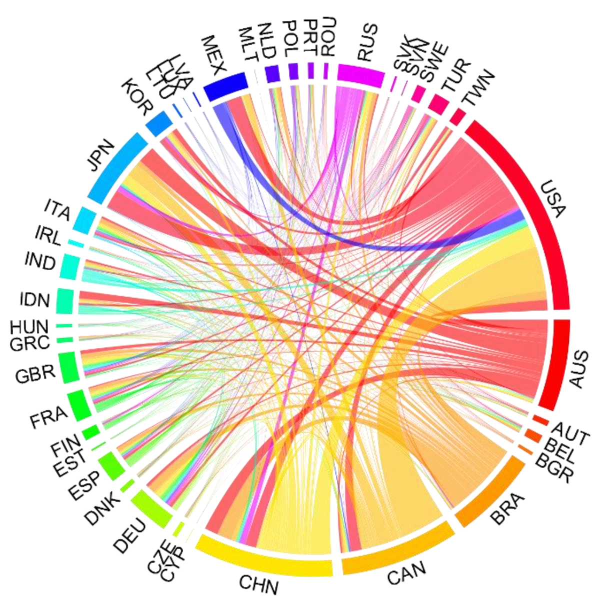

Figure 2.4. (cont'd.)

(4)

(a)

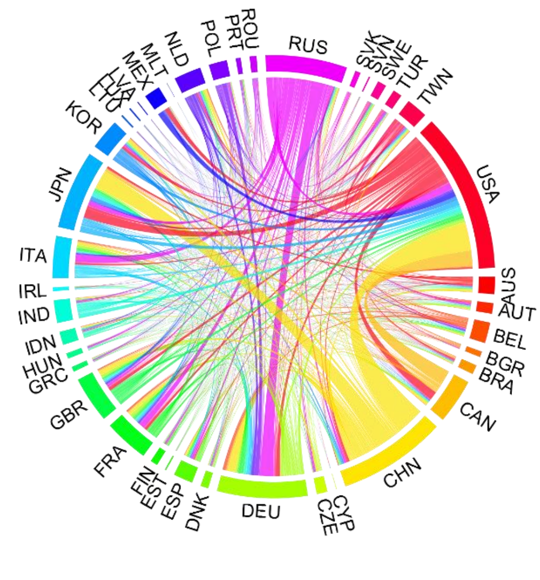

(b)

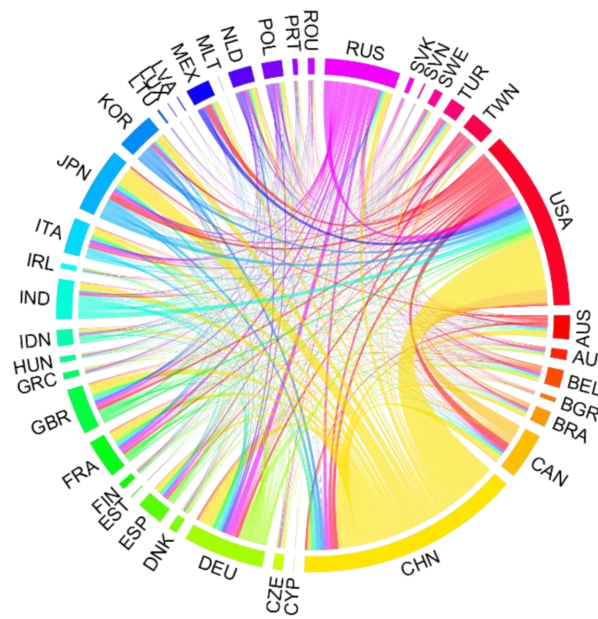

(5)

(a)

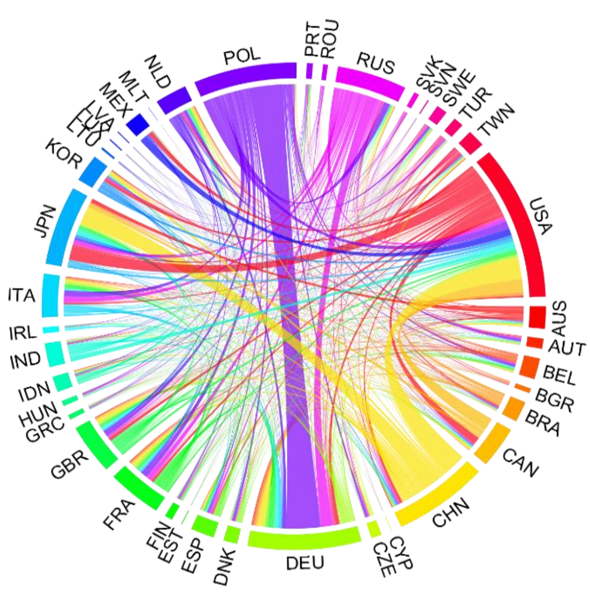

(b)

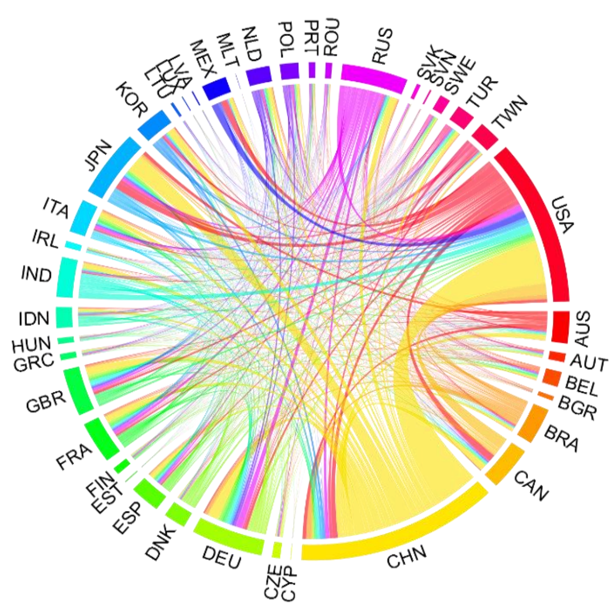

Figure 2.4. (cont'd.)

（6）

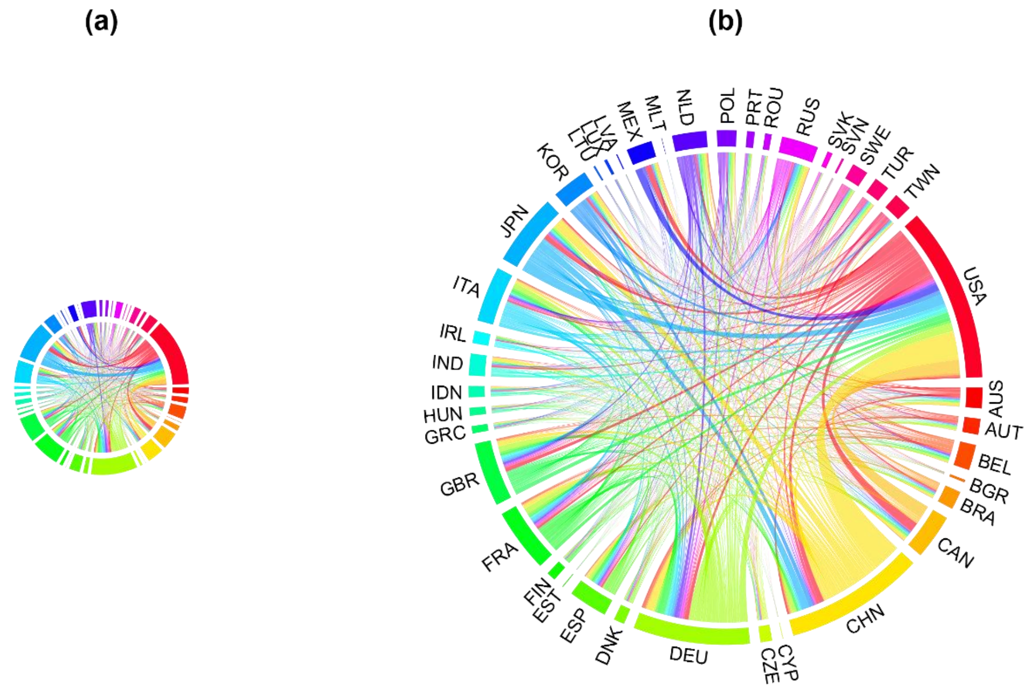

The top five countries that dominated global networks accounted for 47% to 80% of the total volume in various material flows over time (Figure 2.5). In both import-directed networks (in which flow links represent imports) and export-directed networks (in which flow links represent exports), the sum of virtual material flows of the top five countries increased over time (Figure 2.5). Their dominance increased in all export-directed networks except for virtual land network, and decreased in all import-directed networks. In 1995, the top five countries' dominance in virtual energy, CO_2, nitrogen and financial capital in export-directed networks was weaker than that in their corresponding import-directed networks. Interestingly, their dominance in all export-directed networks surpassed their dominance in their corresponding imported-directed networks over time (Figure 2.5h and 2.5j). The US and China were the top trading countries in all networks, accounting for a large percentage of total trade volumes (Figure 2.4).

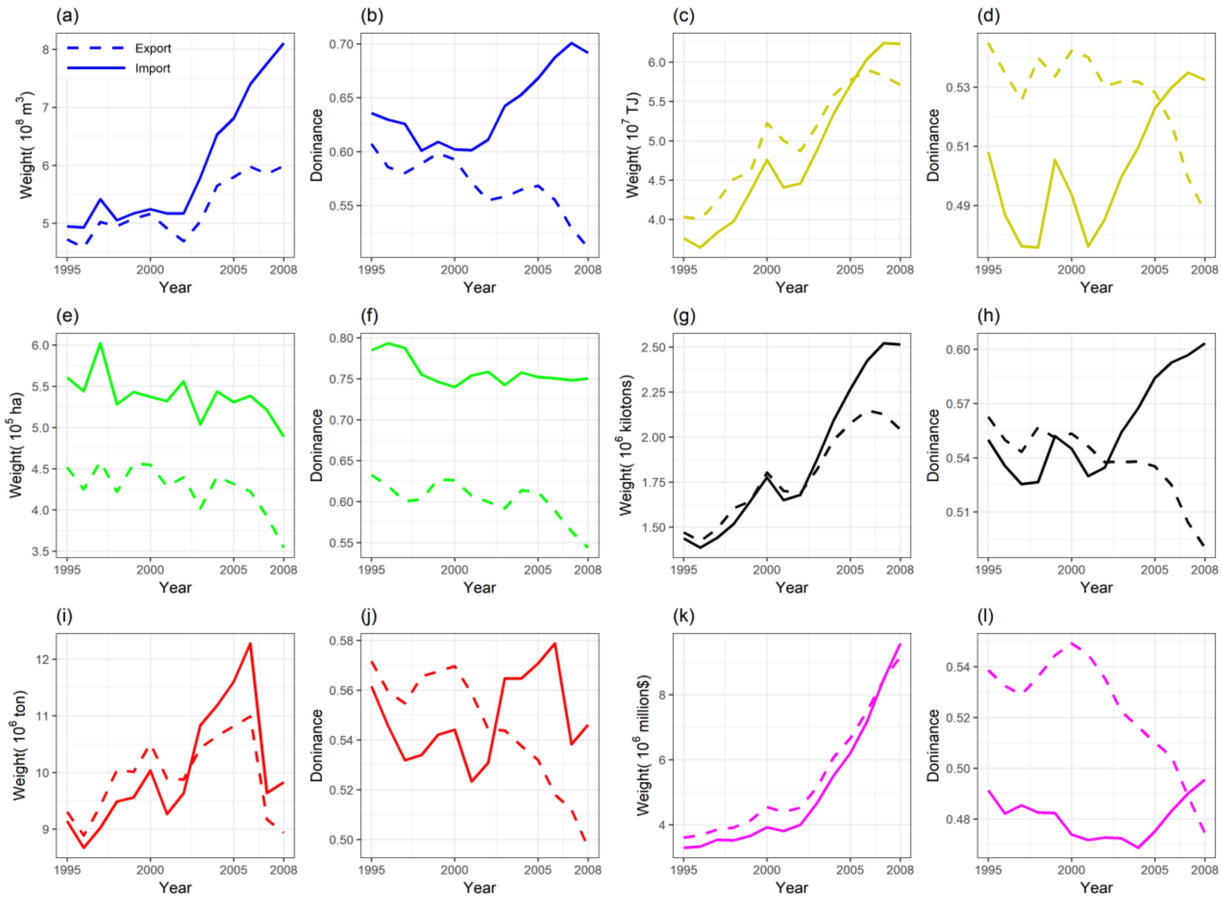

Figure 2.5. Weight and its dominance (measured by the ratio between the trade volume of top trade countries and the global total trade volume) of virtual material flows in top five countries. (a-b) water. (c-d) energy. (e-f) land. (g-h) CO_2. (i-j) nitrogen. (k-l) financial capital. Solid line indicates import and dashed line refers to export

Different kinds of material flows tended to enhance each other through synergistic effects (Figure 2.6), and the synergistic effects between different material flows in the opposite direction have generally strengthened over time. The synergistic also varied among different pairs of material flows. Virtual CO_2 and nitrogen flows tended to have stronger, positive synergetic impacts on the other material flows. The synergistic effect between CO_2 and energy flows was the strongest and intensified with time.

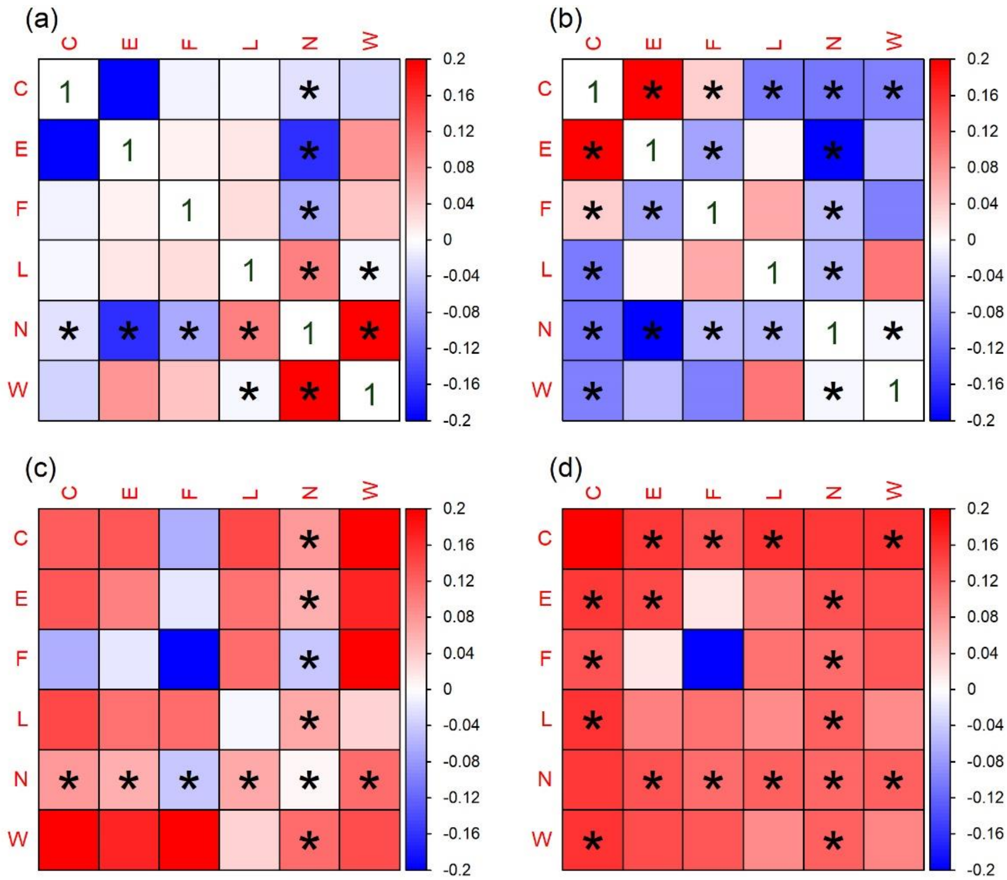

Figure 2.6. Interrelationships among different kinds of virtual material flows. Note: C-CO_2, E-energy, F-financial capital, L-land, N-nitrogen pollution, W-water. (a) and (b) indicate synergistic effects for trade flows with the same direction in 1995 and 2008 while (c) and (d) indicate synergistic effect for trade flows with the opposite direction in 1995 and 2008, respectively. Synergistic effect means flows with the same direction or flows with the opposite direction enhance each other. * refers to analysis with statistically significant Z-score. We have cleared the spurious effects of chance in the correlation analysis.

DISCUSSION

Flow volumes of all virtual materials embodied in international trade, except for virtual land, intensified over time. Distant countries had larger total flow volumes than adjacent countries, partially because there were more distant countries than adjacent countries. But adjacent countries had greater average transfer volumes per country due to the ease of trading over shorter distances. Improvements in land use efficiency, such as agricultural intensification, are likely partially responsible for the decline in virtual land flow (Rudel et al. 2009, FAO 2016). Thus, despite rapid growth in international agricultural trade, the virtual land embodied in trade commodities has not increased accordingly. The virtual energy network had very strong synergistic effects with the virtual CO_2 network because countries tended to import virtual energy with a higher CO_2 content (e.g., developed countries tended to displace manufacturing industries with high energy consumption and low energy efficiency and large CO_2 emissions to developing countries (Cherniwchan, Copeland and Taylor 2016).

The world's population is expected to reach nine billion by 2050 (Evans 2009), bringing with it an exponential rise in global demand for natural resources and accompanied environmental burden. In response, global material flows would continue to intensify and play increasingly important roles in shaping environmental and socioeconomic conditions at multiple scales. For example, large increases in the international trade of soybeans have lowered soy prices in China and caused farmers in northeast China to shift the types of crops they plant (Sun, Tong and Liu 2017, Sun et al. 2018). This, in turn, affects water use and gross primary productivity (Viña et al. 2017). Enhancing environmental sustainability and human wellbeing therefore requires a multi-scale perspective that encompasses global cross-border interactions (Liu et al. 2013).

Global trade hubs such as the US and China dominate global networks. Environmental and socioeconomic shifts in these hubs result in consequences worldwide. For example, the 2008 financial crisis that originated in the US resonated across the globe; exceptionally rapid economic development in China led to increased importation of forest products, which led to deforestation in the Asia-Pacific region and many other regions (Zhang 2007, Liu 2014) as those countries harvested large forest areas to meet China's demands for forest products. To manage global flows of virtual materials, policy makers could consider forces from these hubs which can exert strong power over global trade dynamics. Safeguarding the environment through sustainable resource use will require a better understanding of the existing international mechanisms and structures of trade networks to target top trading countries.

More governance aiming at virtual material trade should be developed to enforce trade regulations (Lenzen et al. 2012, Zhao et al. 2015). Though some institutions and agreements like the Word Trade Organization and the Kyoto Protocol are able to promote the multilateral trade governance, there has been little focus on virtual material trade. Additional institutions should be established to promote multilateral and bilateral trade governance aimed at virtual material trade across national borders (Frankel 2009). Consumption-based virtual material consumption/emission should be measured and then responsibility of consumption could be partly allocated to consumers (Frankel 2009, Peters 2010). And more consumption-based policies should be built to manage the virtual material trade.

By examining the temporal pattern of multiple virtual material flow networks simultaneously, the environmental and socioeconomic interdependencies between countries, driven by trade, can be better clarified. Research and policy-making should not be limited to a single sector like water or energy or CO_2, but consider synergies and trade-offs between two or more sectors (Liu et al. 2015, Wicaksono, Jeong and Kang 2017, Miglietta, Morrone and De Leo 2018). While nexus approaches (e.g., food, energy, and water nexus) have gained increasing attention to understand interactions among sectors, they mainly focus on sectors in a specific place such as within a country (Liu et al. 2018). To gain a comprehensive understanding of interactions among sectors and identify previously overlooked environmental and socioeconomic harms and benefits, more studies that assess these sectors among different countries simultaneously are needed. Such integration would enhance our understanding of complex system dynamics and chart a path towards achieving human well-being and global sustainability (Liu et al. 2015, Lamastra et al. 2017).

CONCLUSIONS

Here we present the first comprehensive assessment of the evolution and interactions of six kinds of global environmental and socioeconomic interaction networks -- global trade of three kinds of virtual natural capital (water, energy, land), two kinds of virtual environmental burdens (CO_2 and nitrogen emissions) and one kind of financial capital (money). All global networks increased over time, with the exception of virtual land transfer. Financial capital transfer increased much more sharply (188.9%) than other material networks. Distant countries generated greater volumes of material flow than adjacent countries. Surprisingly, the top five trade countries in each material network accounted for a considerable proportion (47% to 80%) of the total transfer volume. Different networks tend to enhance each other. We suggest policy-makers consider the influence of powerful material flow networks between trading countries for achieving the United Nations Sustainable Development Goals.

CHAPTER 3. INTERACTIVE NATIONAL VIRTUAL WATER-ENERGY NEXUS NETWORKS

Xu, Z., Y. Li, A. Herzberger, X. Chen, M. Gong, K. Kapsar, C. Hovis, J. Whyte, Y. Tang & Y. Li (2019) Interactive national virtual water-energy nexus networks. *Science of The Total Environment,* 673, 128-135.

ABSTRACT

Across the globe, many regions import virtual resources to support their development. Althoug h many researchers have studied transfers of a single virtual resource, interactions across two types of virtual resource transfer networks – energy and water, for example – have rarely been explored simultaneously. To address these knowledge gaps, we constructed and analyzed interprovincial virtual water and energy transfer networks, using China (the largest energy consumer and is undergoing severe water scarcity) as a demonstration. The results unexpectedly showed that more than 40% of provinces gained one kind of resource (either water or energy) through trade at the expense of losing the other kind of internal resource (energy or water), and 20% of provinces suffered a double loss of both water and energy. The remaining provinces gained both water and energy. Surprisingly, approximately 40% of transferred water/energy was from relatively water/energy-scarce provinces to water/energy-abundant provinces, further deepening resource inequality. Moreover, 33.3% and 26.7% of the provinces relied more on cross-border trade than on internal resources to support their water and energy consumption, respectively. Furthermore, 83.3% and 73.3% of provinces depended more on distant provinces via trade than adjacent ones to support their water and energy consumption, respectively. Overall, virtual water-energy networks tended to enhance each other. Trade largely shaped the nexus relationship between water and energy consumption in provinces. Our study suggests the urgent need to assess multiple virtual resource networks simultaneously in other countries to uncover unintended consequences and to develop cross-sectoral and holistic policies to achieve global sustainability and human well-being.

Key words: virtual water, virtual energy, nexus, trade, China, network

INTRODUCTION

Economic development and population growth substantially increase global resource demand (e.g., water and energy) (Liu et al. 2015, Steffen et al. 2015), resulting in resource scarcity that becomes a barrier for sustainability (Yergin 2006, Mekonnen and Hoekstra 2016). The Virtual resources, such as water and energy, that are consumed in commodity production processes have gained global attention as a key mechanism for alleviating resource scarcity in a receiving system (e.g., a region, a city) through commodity trade (Novo, Garrido and Varela-Ortega 2009, Wiedmann 2009, Steinmann et al. 2017, Xu et al. 2018). Today, transfers of virtual resources such as water and energy have been intensified by globalization (Dalin et al. 2012, Chen et al. 2018). For example, the volume of global virtual water transfers embodied in international food trade has substantially increased over time (Dalin et al. 2012). The virtual energy flows embodied in international trade have also evolved into a highly interconnected network (Chen et al. 2018).

Many studies have evaluated trade within a single virtual resource trade network (e.g., water). These analyses focus on virtual resource trade's spatial pattern, structure, and impacts on sending and receiving systems (Hoekstra and Hung 2002, Chapagain and Hoekstra 2003, Chapagain et al. 2006, Dabrowski, Masekoameng and Ashton 2009, Wiedmann 2009, Konar et al. 2011, Zhang, Yang and Shi 2011, Mubako, Lahiri and Lant 2013, Zhang and Anadon 2014, Zhao et al. 2015, Oita et al. 2016). However, based on the integrated framework of metacoupling (Liu 2017), we found little research has simultaneously explored the interactions between trading systems in two types of virtual resource transfer networks from a nexus perspective (von Braun and Mirzabaev 2016), as different kinds of virtual resource transfer may influence each other and cross-sectoral impacts may happen. The cross-sectoral impacts mean changes in one sector influences another sector. For example, while China constructed more hydropower stations to develop hydropower and satisfy energy demand, substantial water loss occurred when water evaporated from reservoirs, resulting in regional water scarcity (Liu et al. 2015). Current water-energy nexus studies mainly focus on one specific place instead of the relationship between multiple distant places (Liu et al. 2018). Also, there is little research comparing trade between distant systems with trade between geographically adjacent systems. Furthermore, little research has explored drivers of two types of virtual resource transfer simultaneously by using gravity equation (Duarte, Pinilla and Serrano 2018). Such information is urgently required as the world demand for various natural resources in different places may change at differing rates. A more holistic understanding of multiple types of virtual resource trade should be developed to improve resource management efficiency. Moreover, comparing the influences from adjacent and distant provinces can help reveal influential places in different geographical regions. This comparison can also help unveil socioeconomic and environmental impacts from trade with adjacent and distant provinces (e.g., distant trade often consumes more energy for transportation and therefore emits more CO_2) (Liu et al. 2018).

To address these knowledge gaps, we studied China's interprovincial virtual water and energy transfer networks simultaneously. Water and energy are strongly interrelated in human activities and play significant roles in both environmental conservation and socioeconomic development (Liu et al. 2015). Therefore, analyzing virtual water and energy transfer networks together can help us better understand the interactions between provinces in different virtual resource transfer networks. China is facing a serious water crisis and energy shortage in the 21st century (Crompton and Wu 2005, Zhao et al. 2015). Even though China ranks fourth in the world for freshwater resources, its high population makes its per capita renewable freshwater resources levels only one quarter of the world average (Liu and Yang 2012). Furthermore, uneven water resource distribution within China is a barrier to development (Liu and Yang 2012). China has also become the world's largest energy consumer after surpassing the United States (U.S.) in 2009 (Swartz and Oster 2010, Chen et al. 2013). The distribution of coal, natural gas and electricity in China is largely uneven and has negative impacts on China's development (Ma and Oxley 2012). Understanding the interactions between China's interprovincial virtual water and energy transfer networks and their impacts can provide useful information and lessons for enhancing water and energy security through virtual resource transfer in other developing countries.

Based on the most recently available multiregional input-output table for developing interprovincial energy and water trade networks simultaneously in China (Zhang et al. 2013, Zhao et al. 2015), we used network analysis to study interactions across virtual water and energy networks between provinces. We also constructed a "without trade" scenario to study the impact of trade on the nexus between water and energy consumption across provinces. Furthermore, we used the augmented gravity model to explore the drivers of China's virtual water/energy transfer.

MATERIAL AND METHODS

Data sources. We used the most recently available multiregional input-output table for developing energy and water networks simultaneously in China (Zhang et al. 2013, Zhao et al. 2015). The Chinese 2007 interprovincial input-output table was constructed by the Chinese National Bureau of Statistics. Being consistent with previous research (Zhao et al. 2015), water withdrawal data in sector at the provincial level were derived from Water Resource Bulletin at the provincial level and Chinese Economic Census Yearbook 2008 (Provincial Water Resources Bureau 2007, Census 2008, Zhao et al. 2015). The sources of water withdrawal were surface water, groundwater, and transferred water (Ministry of water resources of China 2007, Zhao et al. 2015). The energy consumption data for sectors in provinces were obtained from the 2008 energy balance table (National Bureau of Statistics 2008).

Construction of virtual water/energy trade network. We quantified the interprovincial virtual water and energy transfer network by applying multi-region input-output analysis and direct water/energy consumption coefficients. We considered each trading province as one node (or a coupled human and natural system) (Liu et al. 2007), thus all provinces construct the interprovincial virtual water/energy trade network. A direct link existing between any pair of nodes represents a virtual water/energy flow between provinces, and the weight of the link reflects the volume of the virtual water/energy flow.

First, we used multi-region input-output analysis to study interdependencies between different provinces' economies by tracing capital flows. This method shows the contribution from production of sectors in a particular province to the intermediate and final consumption of all sectors in all provinces in the form of monetary value. Intermediate consumption is represented by the monetary value of goods and services consumed as inputs by a process of production, while final consumption is represented by the monetary value used for direct satisfaction of individual needs or collective needs of members of a community.

Assuming the number of provinces is m, and each province has n sectors. The output in sector i of province R can be represented by Eq. (1) as follows:

$$x_i^R = \sum_{S=1}^{m} \sum_{j=1}^{n} x_{ij}^{RS} + \sum_{S=1}^{m} y_i^{RS} \qquad (1)$$

where x_{ij}^{RS} is the intermediate consumption in sector j of province S provided by sector i of province R. The y_i^{RS} is the final consumption in province S directly provided by sector i of province R.

The direct input coefficient a_{ij}^{RS} can be represented by Eq. (2):

$$a_{ij}^{RS} = x_{ij}^{RS} / x_j^S. \qquad (2)$$

where x_j^S represents the total output in sector j of province S. a_{ij}^{RS} represents the amount of monetary input in sector i of province R needed to increase the output in sector j of province S by one monetary unit.

Based on Eq. (2), we converted Eq. (1) into matrix notation as follows:

$$X^* = A^* X^* + Y^* \qquad (3)$$

$X^*=[x^1, x^2, \dots, x^m]^T$ represents the vector of total output for all m provinces. A is matrix for direct input coefficient. Y^* is the vector of final consumption in all provinces.

Then we transformed Eq. (3) into the following format:

$$X^* = BY^*, B = (I - A)^{-1} \qquad (4)$$

The term $(I - A)^{-1}$ is the Leontief inverse matrix, which represents the amount of output from other provinces that is required to meet one monetary unit of final consumption. To link the monetary transfer with virtual water/energy transfer, we defined the direct water/energy consumption coefficients. The direct water/energy consumptions coefficient of sector j in province R can be expressed as Eq. (5):

$$e_j^R = \frac{w_j^R}{x_j^R} \qquad (5)$$

where the w_j^R represents total water/energy consumption in sector j of province R, and x_j^R is the output of sector j of province R. e_j^R represents the amount of water/energy used to produce one monetary unit of output in sector j of province R.

For a particular province R, the total water/energy footprint WF^R which is equal to the sum of net virtual water/energy import and internal water consumption (Hoekstra and Hung 2002) can be calculated by Eq. (6):

$$WF^R = E\ B\ Y^R \tag{6}$$

where $E=[e^1, e^2, \dots, e^N]$ is a $1 \times n \times m$ vector of all provincial sectors' direct water/energy consumption coefficient, Y^R represents the final consumption in province R.

Drivers of water/energy transfer. We determined the drivers of national virtual water/energy transfer by using the gravity model.

The general pattern of the gravity model is represented as follows (Bergstrand 1985):

$$X_{ij} = \beta_0 Y_i^{\beta_1} Y_j^{\beta_2} N_i^{\beta_3} N_j^{\beta_4} D_{ij}^{\beta_5} A_{ij}^{\beta_6} u_{ij} \tag{11}$$

Where X_{ij} represents the volume of virtual water/energy that flows from province i to province j. Y_i and Y_j represent the gross domestic product (GDP) in province i and j, respectively. N_i and N_j indicates population of province i and province j. D_{ij} represents the distance between province i and province j. And A_{ij} is a dummy variable indicating whether provinces are adjacent to each other. If they are adjacent to each other, $A_{ij}=1$ and, conversely, $A_{ij}=0$. u_{ij} indicates the error term.

Eq.(11) was transformed into linear equation by log function as follows:

$$\log(X_{ij})=\beta_0+ \beta_1.\log(Y_i)+ \beta_2.\log(Y_j)+ \beta_3.\log(N_i)+ \beta_4.\log(N_j)+ \beta_5.\log(D_{ij})+ \beta_6.\log(A_{ij})+ u_{ij}$$

(12)

We added the cropland area per capita (CAP) in the gravity equation, to investigate the impacts of land use on interprovincial virtual water/energy flow. This variables was added since agricultural development can largely drive water and energy consumption (Foley et al. 2005).

After model specification, the augmented model can be represented by Eq.(13) as follows:

$$\log(X_{ij})=\log(\beta_0)+\beta_1.\log(Y_i)+\beta_2.\log(Y_j)+\beta_3.\log(N_i)+\beta_4.\log(N_j)+\beta_5.\log(CAP_i)+\beta_6.\log(CAP_j)+\beta_7.\log(D_{ij})+\beta_8.\log(A_{ij})+u_{ij} \quad (13)$$

We ran the multivariate analysis to explore drivers associated with virtual water/energy transfer. Firstly, we performed the homogeneity test of variance for the virtual water and energy transfer data to evaluate the degree of heteroskedasticity of the variables included in the analysis. The P-values for the homogeneity test of variance for virtual water and energy transfers are 0.080 and 0.162, respectively, indicating that the degree of heteroskedasticity in the data is not significant. Ordinary Least Square (OLS) regression was then applied in order to explore the drivers of virtual water or energy transfers. We used the ratio between internal water consumption (W_C) and energy consumption (E_C) (equation (14)) as the measurement for water-energy nexus relationship.

$$\text{nexus ratio}=Wc/Ec \quad (14)$$

We defined this index ourselves based on our understanding of the water-energy nexus. In Liu et al. (2015), nexus relationships refer to the interdependency between multiple issues and are addressed together (Liu et al. 2015). Water and energy are consumed in most of the human activities involved in the sectors of the multiregional input-output table. Additionally, the consumption of water and energy coincides with each other. For example, in agriculture, the water consumed in the food production process requires energy to pump the water. In industry, energy production requires the use of water to cool down machines and plants, or produce the materials used to generate the energy (e.g., biofuel). In order to represent the interdependency between water and energy consumption, we calculated the ratio between their consumption.

Following previous research (Zhao et al. 2015, Wood et al. 2018), we created a hypothetical without-trade scenario to estimate the influence of current interprovincial trade on the water-energy nexus relationship in provinces. The nexus ratio* under the "without-trade" scenario refers to the hypothetical water-energy nexus in a province in which no virtual water and energy were imported (equation (15)). Previous research assumes that under a "without-trade" scenario a given province would use more domestic resources to meet the total resource demand since no resources were imported, resulting in more domestic resource consumption (Zhao et al. 2015, Wood et al. 2018). Provinces' water-energy nexus ratio* under a without-trade scenario were therefore calculated by adding the trade balance (net import in our case) back to provinces in previous research (Zhao et al. 2015, Wood et al. 2018). To simulate the "without-trade" scenario, we followed Zhao et al (2015) and Wood et al (2018)'s methods by assuming that additional domestic production would supplement the original imported materials (Zhao et al. 2015, Wood et al. 2018). For example, the original nexus ratio under the "with-trade" scenario was evaluated using the ratio of domestic water consumption to domestic energy consumption for a province in reality. Under the "without-trade" scenario, there is no virtual water/energy trade to support domestic demand for water and energy. The province depends entirely on water and energy from local sources.

$$\text{nexus ratio}^* = (W_C+VW_{\text{net import}}) / (E_C+VE_{\text{net import}}) \qquad (15)$$

where $VW_{\text{net import}}$ and $VE_{\text{net import}}$ are the net imported virtual water/energy (Zhao et al. 2015, Wood et al. 2018). Admittedly, this approach must be seen as a simplified estimation given the complex environmental and socioeconomic dynamics that might unfold in the absence of trade. However, this without-trade scenario has been used in other fields to evaluate the impacts of trade on water scarcity and nutrient supply (Zhao et al. 2015, Wood et al. 2018), since it provides a useful approximation for measuring the impacts of trade on environmental systems.

RESULTS

Interactions across water-energy nexus network

In interprovincial virtual water-energy flow network, more than 40% of the provinces gained in trading water at the expense of losing their own energy or gained in trading energy at the expense of losing their own water (Figure 3.1). Almost a quarter (23%) of the provinces (Guangxi, Hunan, Jiangxi, Fujian, Anhui, Hebei, Heilongjiang) gained virtual energy but lost water, while 20% (Guizhou, Guangdong, Jiangsu, Shandong, Liaoning, Inner Mongolia) gained virtual water but lost energy. Twenty percent of the provinces (Xinjiang, Sichuan, Chongqing, Hubei, Shanxi, Jilin) lost both their water and energy. The remaining 36.7% of the provinces gained both water and energy at no cost.

Virtual water and energy networks tended to enhance each other (Figure 3.2). The total exported water and exported energy for all provinces were significantly positively correlated, as were the total exported water and imported energy, the total imported water and imported energy, and the total imported water and exported energy (Figure 3.2).

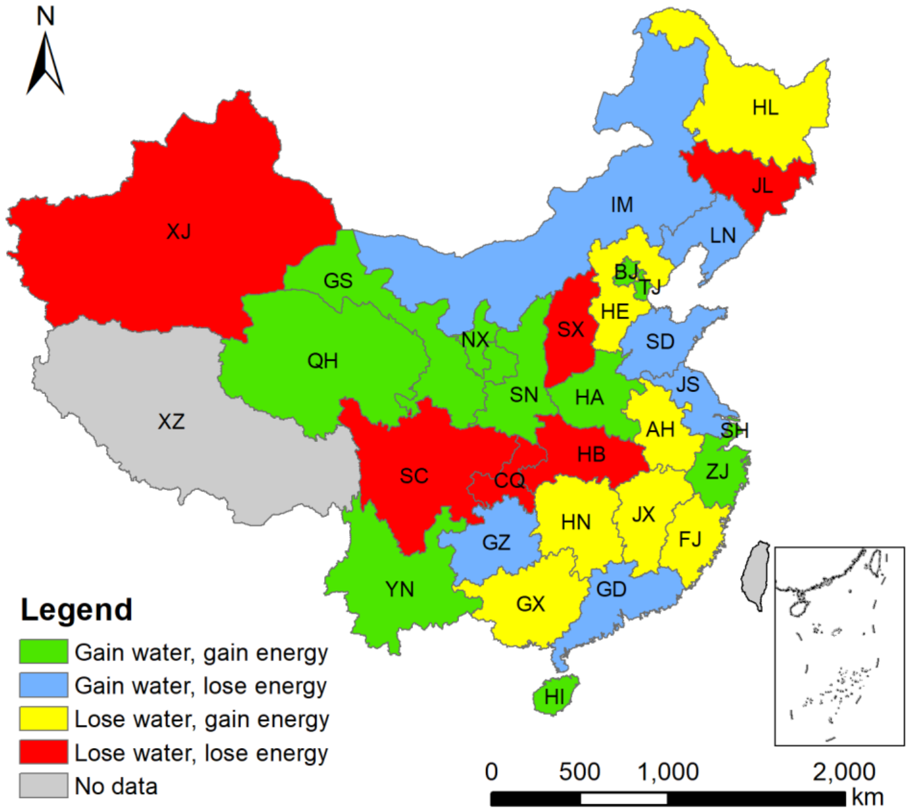

Figure 3.1. Concurrent impact of interprovincial virtual water-energy transfer network on provinces

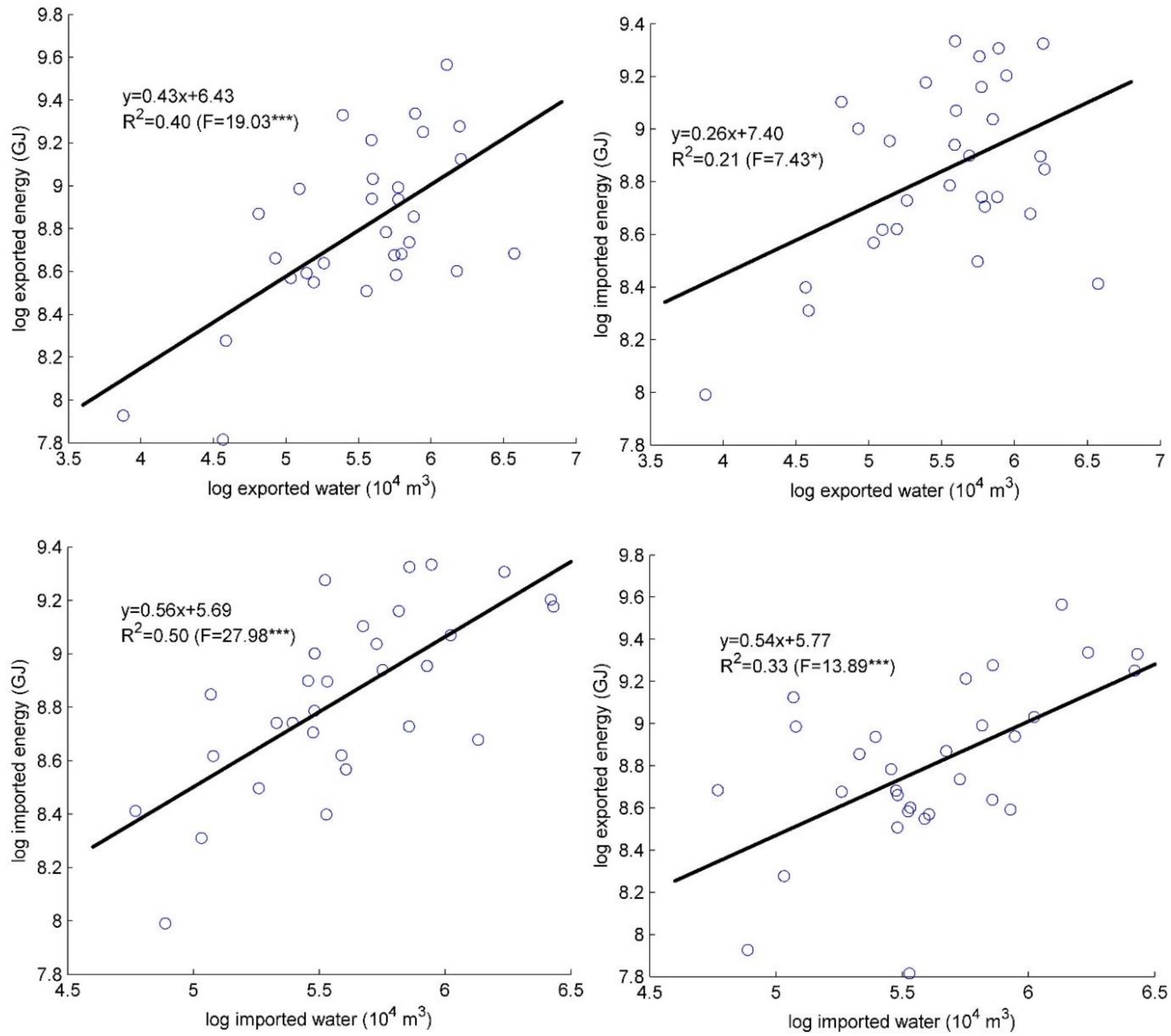

Figure 3.2. Relationship between exported/imported water and exported/imported energy. The F-value represents the significance testing result from the fitting process. ***, and * reflects significance under significant level *a*=0.01 and *a*=0.05, respectively.

Surprisingly, 39.4% and 40.6% of interprovincial trade for energy and water trade, respectively, were from relatively resource-scarce provinces to resource-abundant provinces (Figure 3). Furthermore, 33.3% and 26.7% of the provinces depended more on cross-border trade than their own internal resources to support their water and energy consumption, respectively (Table 3.1).

Moreover, 83.3% and 73.3% of the provinces depended more on distant trade than adjacent trade to support their water and energy consumption, respectively.

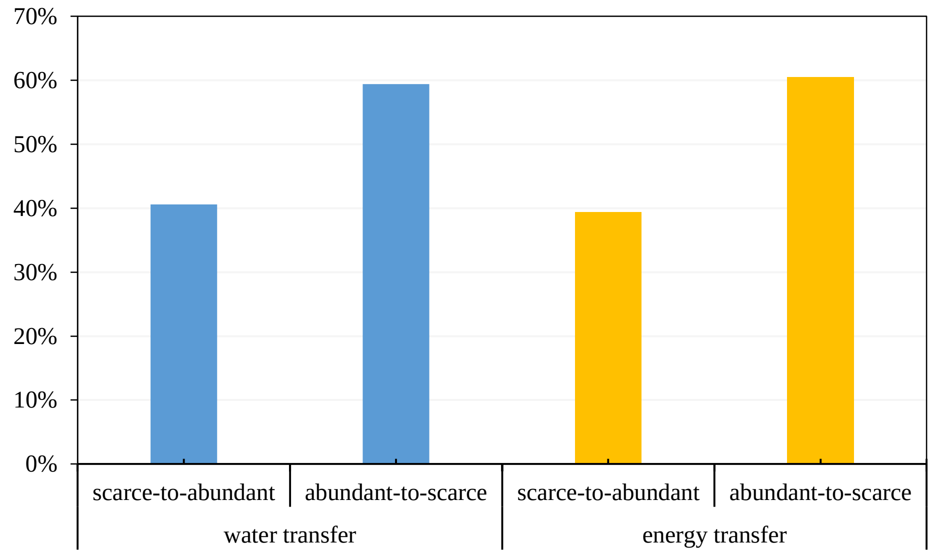

Figure 3.3. Percentage of virtual water/energy transfer between relatively water/energy-scarce provinces and water/energy-abundant provinces.

Table 3.1. Volume of provinces' resource consumption supported by internal, adjacent and distant systems.

Provinces	Water (10^4 m^3)			Energy (GJ)		
	From internal system	From adjacent system	From distant system	From internal system	From adjacent system	From distant system
Beijing	1.82×10^5	7.59×10^4	3.96×10^5	9.23×10^8	2.59×10^8	1.01×10^9
Tianjin	1.24×10^5	4.35×10^4	2.59×10^5	5.85×10^8	2.25×10^8	7.79×10^8
Hebei	5.01×10^5	2.04×10^5	5.19×10^5	2.75×10^9	1.47×10^9	6.46×10^8
Shaanxi	3.69×10^5	4.07×10^4	7.92×10^4	1.76×10^9	2.09×10^8	2.06×10^8
Inner Mongolia	6.88×10^5	1.22×10^5	1.23×10^6	5.21×10^9	2.54×10^8	2.24×10^8
Liaoning	8.21×10^5	3.28×10^5	2.37×10^5	2.49×10^9	4.35×10^8	4.37×10^8
Jilin	8.81×10^5	4.98×10^4	6.75×10^4	8.82×10^8	4.7×10^8	2.35×10^8
Heilongjiang	6.29×10^5	1.26×10^5	2.07×10^5	1.25×10^9	9.77×10^8	9.14×10^8
Shanghai	7.56×10^5	2.46×10^5	6.36×10^5	1.48×10^9	5.67×10^8	1.59×10^9
Jiangsu	3.59×10^6	3.54×10^5	2.28×10^6	2.83×10^9	4.35×10^8	1.16×10^9
Zhejiang	6.86×10^5	2.75×10^5	3.80×10^5	1.22×10^9	4.55×10^8	9.92×10^8
Anhui	8.63×10^5	1.82×10^5	3.52×10^5	1.03×10^9	5.39×10^8	5.52×10^8
Fujian	7.29×10^5	8.77×10^4	2.11×10^5	1.16×10^9	1.65×10^8	3.43×10^8
Shanxi	1.15×10^6	1.31×10^5	1.71×10^5	8.6×10^8	2.77×10^8	3.34×10^8
Shandong	1.92×10^6	6.94×10^5	2.00×10^6	4.08×10^9	3.31×10^8	1.17×10^9
Henan	1.11×10^6	1.71×10^5	8.81×10^5	2.71×10^9	3.58×10^8	8.17×10^8
Hubei	1.22×10^6	5.56×10^4	1.92×10^5	1.94×10^9	1.79×10^8	3.73×10^8
1Hunan	1.59×10^6	1.29×10^5	1.57×10^5	1.81×10^9	3.75×10^8	4.19×10^8
Guangdong	2.50×10^6	1.00×10^6	7.21×10^5	2.75×10^9	3.75×10^8	1.65×10^9
Guangxi	1.31×10^6	1.50×10^5	1.90×10^5	8.77×10^8	3.76×10^8	4.12×10^8
Hainan	2.84×10^5	0	3.38×10^5	2.11×10^8	0	2.51×10^8
Chongqing	4.05×10^5	6.69×10^4	1.15×10^5	7.16×10^8	98564763	2.16×10^8
Sichuan	1.52×10^6	4.19×10^4	1.72×10^5	1.79×10^9	1.73×10^8	3.79×10^8
Guizhou	5.93×10^5	2.97×10^5	1.06×10^5	9.68×10^8	1.91×10^8	1.79×10^8
Yunnan	8.34×10^5	2.06×10^5	1.81×10^5	1.37×10^9	1.7×10^8	2.47×10^8
Shaanxi	4.40×10^5	1.51×10^5	6.97×10^5	8.77×10^8	5.25×10^8	3.77×10^8
Gansu	5.85×10^5	6.53×10^5	6.58×10^4	6.06×10^8	2.61×10^8	2.74×10^8
Qinghai	7.61×10^4	2.47×10^4	5.26×10^4	2.47×10^8	4.97×10^7	4.83×10^7
Ningxia	2.67×10^5	9.32×10^3	9.83×10^4	3.19×10^8	9.96×10^7	1.05×10^8
Xinjiang	2.96×10^5	6.26×10^3	5.26×10^4	8.11×10^8	4.91×10^7	2.1×10^8

Trade largely shaped the nexus ratio between internal water and energy consumption in provinces (Figure 3.4). Trade increased the ratio between water and energy consumption in 47% of the provinces, while decreased the ratio in 53% of the provinces. The three provinces that increased most-are Xinjiang (840%), Heilongjiang (140%) and Guangxi (122%). The provinces that decreased most are Shandong (-58%), Beijing (-50%) and Qinghai (-43%).

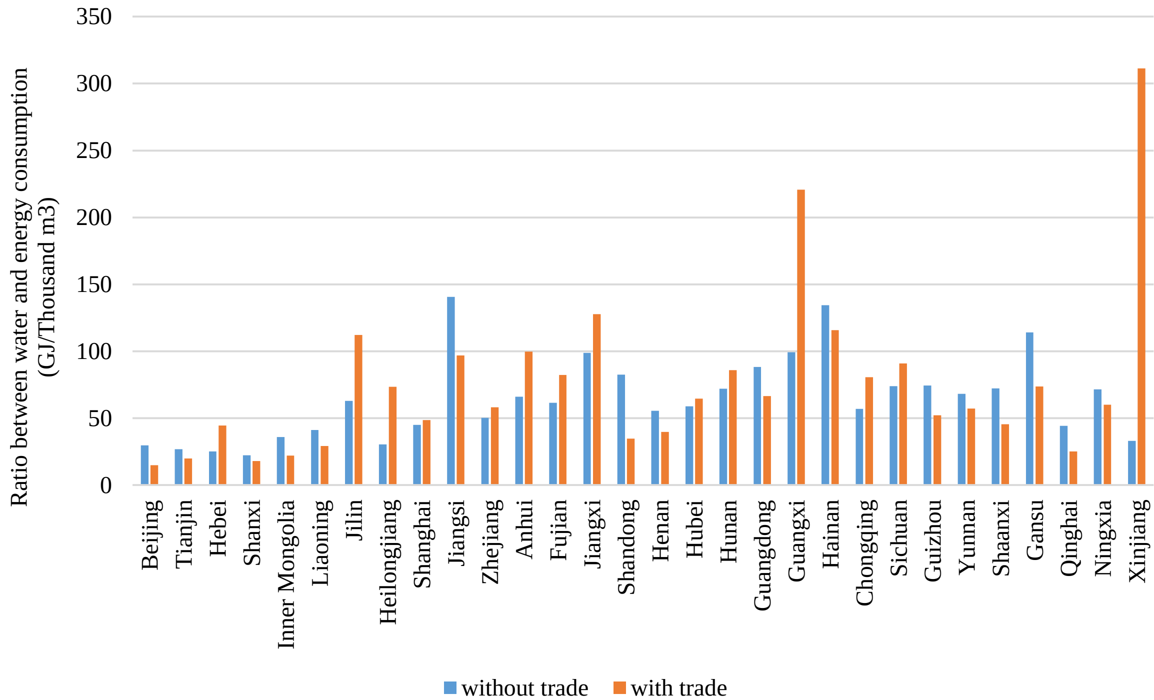

Figure 3.4. Water-energy nexus ratio (the ratio between internal water and energy consumption) in each province under with trade and without trade scenarios

Drivers of virtual water and energy trade

GDP per capita, precipitation, cropland area per capita of both the sending and the receiving provinces, distance between provinces, whether or not provinces shared a border, population, and percent of industrial GDP in total GDP in the receiving province all significantly affected both the virtual water and energy flows. Population in sending provinces significantly affected the virtual energy flows, but no virtual water. Only the percent of industrial GDP in total GDP in sending provinces affected virtual water flows rather than energy (Table 3.2). There are more variables in receiving than sending areas that significantly affect the virtual water/energy transfer, indicating that receiving areas may be more determinant than sending areas in a virtual water/energy trade network, which is consistent with the previous research (Tamea et al. 2014).

These results indicate that the volume of bilateral virtual water and energy flows tends to be large between two provinces with strong economic bases and scales. The scale of the economy reflects the resource demand capacity and trade demand potential of the region, as well as the combined production capacity and export potential of the region. The larger the economic scale is, the greater the outside trade flow is, the greater the flows of virtual water and energy are. Therefore, the relationship between the economic scale and virtual water and energy trade of the two regions is positive. Population size has a significant positive correlation with virtual water and energy export and import. Population is the basis for economic development, and resource demand. So provinces with greater population sizes tend to have more trade interactions with other provinces.

For trade flow between provinces, as distance between provinces increases, the amount of virtual water and energy trade declines. When provinces share borders, they tend to transfer more virtual water and energy to each other. The reason is that greater distance increases transportation cost, which significantly decreases the amount of trade. Also, while trading provinces share borders with each other, it tends to have a short distance and low transportation cost and therefore there may be more trade interaction between nearby provinces. In addition, the effects of proportion of industrial GDP on sending and receiving systems is different. The greater the proportion of industrial GDP in the exporting province, the more restricted the flows of virtual water and energy were. However, virtual water and energy flows increased with increases in the proportion of industrial GDP in the importing province. The reason may be that the virtual water and energy trade is driven more by demand than supply (Tamea et al. 2014). Provinces with greater local industry would have greater internal resource consumption and import more resources but provide less resources to other provinces.

We also found that land use (cropland area per capita) significantly affects virtual water and energy trade. More cropland area per capita in the sending province tends to be associated with increased virtual water and energy trade. But in receiving provinces, more cropland per capita leads to less virtual water and energy trade. This may be because the surplus of cropland area can be used to produce food for export, which is one type of economic benefit that accelerates virtual water/energy export. Also, surplus cropland area may be indicative of less demand for trade since the province can feed itself to an extent. For precipitation, it has positive effects on trade in export provinces but negative effects on trade in receiving provinces. The reason may be that precipitation increases water of local areas, therefore local area would demand less resource from trade but can export more resource outside for profits.

Table 3.2. OLS results for augmented gravity model about drivers of water and energy transfer

Variables	Water	Energy
Population_sending	0.158	0.749**
	(0.126)	(0.086)
Population_receiving	1.433**	1.354**
	(0.100)	(0.068)
GDP per capita_sending	1.497**	1.211**
	(0.126)	(0.086)
GDP per capita_receiving	0.471**	0.436**
	(0.077)	(0.052)
Cropland area per capita_sending	1.037**	0.304**
	(0.107)	(0.073)
Cropland area per capita_receiving	-0.425**	-0.404**
	(0.072)	(0.049)
Percent of industrial GDP in total GDP_sending	-1.327**	-0.024
	(0.107)	(0.191)
Percent of industrial GDP in total GDP _receiving	0.769**	0.480*
	(0.280)	(0.191)
Precipitation_sending	0.320**	0.475**
	(0.118)	(0.080)
Precipitation_receiving	-0.352**	-0.560**
	(0.113)	(0.077)
Distance between sending system and receiving systems	-0.696**	-0.833**
	(0.094)	(0.064)
Border dummy (whether provinces share border or not)	0.262**	0.248**
	(0.067)	(0.064)
Constant	-1.581	4.729**
	(0.853)	(0.583)
R^2	0.577	0.712
F	97.368	176.743
P-value for homogeneity test of variance	0.08	0.16

Dependent variable: Virtual water and energy transfer. Standard deviations were put in parentheses.

Notes: The number in table represents the coefficients of variables. *, ** denotes significance at 0.05, and 0.01 level.

DISCUSSION

Our study finds that in this virtual water and energy network, more than 40% of provinces gained in trading water at the expense of losing their own energy or gained in trading energy at the expense of losing their own water. Twenty percent of provinces suffered a double loss of both their own internal water and energy, while the rest of provinces gained both trading water and energy at no cost of internal water and energy. GDP is one important driver of virtual water and energy transfer. After China's "reform and opening up", China's GDP grew about 10% annually from 1979 to 2013 (Morrison 2014), with associated growth in the demand for water and energy. This growing economic development likewise drives virtual water and energy transfer and increases their impacts on trading systems.

Virtual water and energy flows are driven by economic development rather than motivated by alleviating water or energy scarcity, as virtual water and energy transfers are embodied in commodity trade. Distance between trading systems has a significant negative impact on the transfer of virtual water and energy, most likely due to the increasing transportation cost. Cropland area per capita in a sending province is another important driver of virtual water/energy trade. This may be because the surplus of cropland area can be used to produce food for export, which is one type of economic benefit that accelerates virtual water/energy export.

Cross-sectoral impacts should be considered in future analyses (Liu et al. 2015). The virtual water and energy networks are highly positively interrelated. Provinces with large amounts of imported and exported virtual water tend to also have substantial amounts of imported and exported amounts of virtual energy and vice versa. Benefits in water or energy trade in one place may be associated with impacts on energy or water in a distant place, which may lead to unexpected costs and inefficiency of management. Therefore, more holistic policies considering cross-sectoral impacts over distances should be developed to maximize the efficiency of integrated management.

Considering distant interactions in trading networks helps local governments find hidden factors affecting local water and energy systems. In the case of virtual water-energy networks, distant areas have even more impacts on a focal area than adjacent areas. The reason may be that there are more distant provinces than adjacent provinces, thus the trade interactions between distant provinces were greater than those between adjacent provinces. Furthermore, in many provinces, cross-border virtual resource trade is greater than domestic resource consumption. Thus more cooperative resource management with distant systems should be developed (Liu et al. 2013).

Our driver analysis revealed that virtual water/energy trade may be motivated more by the demand side than by the supply side. Therefore, more demand-side policies should be developed to reduce resource consumption and environmental burden. For example, in virtual water trade, the false perception of limitless water availability due to low water usage cost in a virtual water-receiving province (demand side) would encourage the receiving province to promote water-intensive activities (Zhao et al. 2015), thus leading to water pressure on virtual water-exporting provinces (supply side). Ignoring such an issue may trigger a series of unexpected changes (e.g., water scarcity, biodiversity loss, and vulnerable economy) in both the water-receiving and water-exporting systems. Developing demand-side policies can avoid such negative consequences. For example, if the government considers charging a virtual water tax on imported commodities in virtual water receiving provinces, this could motivate more efficient water use and virtual water importing provinces could take more responsibility for water consumption in virtual water exporting provinces (Zhong and Mol 2010, Lenzen et al. 2012). Thus, water waste and water scarcity due to virtual water trade can be controlled. Our driver analysis also provides useful information for predicting the virtual resource trade and choosing potential partners to develop collaborative relationships for managing virtual resource trade. Based on our analysis, if provinces were to develop collaborations and policies to control the virtual resource trade, it would be advantageous to choose receiving provinces with a strong economic base, particularly with a high industrial GDP and large population. Additionally, the results of the driver analysis can also supply information for dividing responsibility for virtual resource consumption and management when trading partners debate about who should take more responsibility and how to control the virtual resource trade based on the significant drivers.

In our study, the interactions between provinces across the virtual water and energy nexus network at the national scale are further revealed, contributing to a more holistic understanding of virtual resource studies. Future research should extend this study by assessing the interactions across multiple types of virtual resource/material flows beyond virtual water and energy, for example, to include virtual land and carbon across spatial and temporal scales (Lu et al. 2015). This could further reveal the relationships (e.g., trade-offs, synergies) between more complex virtual resource/material transfer networks and their impacts on national sustainability and result in a more in-depth understanding of the mechanism of interactions within and between adjacent and distant systems (Liu 2018). Our study on two types of distant resource transfer networks could improve our understanding of cross-border interactions, uncover hidden problems that could give rise to national crises, and facilitate an increased understanding of the importance of adjacent and distant interactions and their associated implications for policy.

CONCLUSIONS

Our paper investigated the interactions across two types of virtual resource transfer networks – energy and water at the national scale, using China as a case. The results showed that more than 40% of provinces gained one type of resource (either water or energy) by trade at the expense of losing the other type of internal resource (energy or water), and 20% of the provinces suffered a double loss of both water and energy. The rest of provinces gained both water and energy. Moreover, 33.3% and 26.7% of the provinces depended more on cross-border trade than on internal resources to support their water and energy consumption, respectively. Furthermore, most of provinces relied more on distant provinces via trade than adjacent ones to support their water and energy consumption. Unexpectedly, approximately 40% of virtual water/energy flow was from relatively water/energy-scarce provinces to water/energy-abundant provinces, leading to resource inequality. Virtual water-energy networks tended to enhance each other. Our study suggests the urgent need to study multiple virtual resource networks simultaneously and to build cross-sectoral and holistic policies to achieve sustainable resource use.

CHAPTER 4. SHIFT IN A NATIONAL VIRTUAL ENERGY NETWORK

Xu, Z., D. Zhang, P. McCord, M. Gong & J. Liu (2019) Shift in a national virtual energy network. *Applied Energy,* 242, 561-569.

ABSTRACT

Energy is one of the most fundamental resources for humans and nature. Virtual energy transfer is considered one potential mechanism to alleviate energy shortages and support socioeconomic development in energy-scarce regions. However, little research has explored the change in flow pattern of national virtual energy trade since the 2008 global financial crisis. To fill this knowledge gap, we choose China's interprovincial virtual energy transfer network as a demonstration, since China is the world's biggest energy consumer and features a starkly uneven spatial distribution of energy resources. Surprisingly, the total virtual energy transferred from energy scarce to energy-abundant provinces increased from 43.2% to 47.5% from 2007 to 2012. In particular, the virtual oil which transferred from energy-scarce to energy-abundant provinces grew from 51.5% in 2007 to 54.0% in 2012. The percentage of provinces that transferred a greater amount of total virtual energy than was consumed internally increased from 23.3% in 2007 to 36.7% in 2012. Unexpectedly, the total virtual energy flowing from west China to east China was much greater than physical energy transferred through the West-To-East Electricity Transmission Project (WTEETP). This study suggests that it would be interesting to study patterns of interactions of virtual energy networks in other countries.

INTRODUCTION

Global economic development and population growth place large demands on natural resources and contribute to environmental degradation (Liu et al. 2015, Steffen et al. 2015). The sustainability of natural resources and the environment attracts global attention, particularly topics concerning energy availability and production as energy is a fundamental natural resource sustaining human activities (e.g., industry, irrigated agriculture) (Liu et al. 2015, Liu et al. 2018). Many regions face severe energy shortages, posing threats to their sustainable development. More than one billion people lack access to electricity (International Energy Agency 2015).

Due to persistent energy shortages, the virtual consumption and transfer of energy has attracted widespread attention in recent years (Liu et al. 2018, Xu et al. 2018). Virtual energy is energy consumed during the production process of commodities (Zhou and Yang 2006, Chen et al. 2017, Liu et al. 2017). Virtual energy is considered a potential mechanism critical to avoiding regional energy crises since commodities traded from one location to another include virtual energy. This means the importing area can avoid expending the energy to produce the imported commodities. In contrast, physical energy is transferred by energy transmission projects such as China's West-To-East Electricity Transmission Project (WTEETP) to alleviate energy shortages in energy-scarce regions (Chen et al. 2010).

Many studies have explored the spatial structure and impact of virtual energy or other materials like embodied emissions/pollution transfer (Tang, Snowden and Höök 2013, Wu, Lei and Li 2015, Zhang et al. 2015, Mi et al. 2017, Sun et al. 2017, Chen et al. 2018, Xu et al. 2018, Kan et al. 2019). For example, Tang et. al. (2013) analyzed the virtual energy embodied in UK's international trade and found that UK's virtual energy imports had surpassed its virtual energy exports every year since 1997 (Tang et al. 2013). Wu et al. (2015) assessed the spatial pattern of virtual energy flow between provinces in China in 2007 and revealed that huge amount of virtual energy went from western provinces to eastern provinces (Wu et al. 2015). Sun et. al. (2015) studied the energy implications of China's booming regional economies' development. They found that China's three major economic circles (*Pearl-River-Delta, Yangtze-River-Delta*, and *Jing-Jin-Ji*) had large demands for virtual energy trade and more than 50% of interregional trade of virtual energy was induced by the three economic circles (Sun et al. 2017). Mi et al (2017) studied change in China's CO_2 emission flow network between 2007 and 2012, and found that CO_2 flow pattern had changed largely since the financial crisis (Mi et al. 2017). Kan et al (2019) applied the multi-regional input-output (MRIO) analysis to assess the natural gas embodied in international trade, and showed that total amount of natural gas embodied in the international trade accounted for 2722.1 bcm in 2011 (Kan et al. 2019). Chen at al. (2018) used MRIO and complex network analysis to study the structure of embodied energy flow network across multiple scales (Chen et al. 2018). Their results indicated the existence of small-world nature and heterogeneity in the network. Xu et al. (2019) employed MRIO and Multiplexity approach to assess evolution of multiple global virtual material flows and interactions between multiple virtual material networks (Xu et al. 2018). They found that the total amount of most of virtual materials transfer increased over time except for the global virtual land network, and different global virtual material networks tended to enhance each other.

Based on the integrated framework of metacoupling (environmental and socioeconomic interactions within and across borders (Liu 2017)), we identified the following research gaps: (1). little research has assessed the changes in flow pattern of China's interprovincial virtual energy network considering different type of virtual energy (e.g., coal, oil, natural gas and others) since the global financial crisis; (2). few studies have studied the change in pattern of virtual energy transfer considering the different types of energy (e.g., coal, oil, natural gas and others) between energy-scarce and energy-abundant areas; (3). little research has compared virtual energy transfer to physical energy transfer such as the West-To-East Electricity Transmission Project which aims at solving energy shortages; (4). comparisons between internal energy consumption (Our internal energy consumption refers to the internal energy footprint, which encompasses all local energy use (direct and indirect) associated with the final consumption in the studied area), nearby virtual energy trade and distant energy trade have not been undertaken (Liu 2017). Such information is urgently needed given the high energy demand and severely uneven distribution of global energy resources. Addressing these gaps can also help understand the hidden network linkages of interregional virtual energy flow. Assessing the change in flow pattern of virtual energy network since the global financial crisis will result in more updated and accurate information about China's virtual energy transfer. Assessing the changing patterns of virtual energy flows from energy-scarce to energy-abundant provinces will help to clarify the role of virtual energy trade in alleviating regional shortages. Comparing interactions between distant provinces and nearby provinces can reveal potential key partners in cooperation. This comparison may also demonstrate socioeconomic and environmental impacts from trade with distant and nearby provinces (e.g., distant trade often consumes more energy for transport and therefore emits more CO_2).

To fill these knowledge gaps, we focused on China's interprovincial virtual energy networks over time. With the country's economic growth, the national energy consumption and environmental pollutant emissions are growing rapidly. In 2013, nearly 22% of global energy consumption occurred in China (Cui et al. 2015). Consequently, China has surpassed the United States to be the world's largest energy consumer and the largest source of CO_2 emissions (Yuan et al. 2013, Cui et al. 2015). China's uneven energy resource distribution has negative impacts on its own development (Ma and Oxley 2012). As China is still in the industrialization and urbanization process, energy consumption and pollutant emissions will increase in the near future (National Development and Reform Commission of the People's Republic of China 2013). Developing strategies to maintain energy supplies while achieving economic and social sustainable development will be important issues for policy makers.

We proposed the following hypotheses. First, more virtual energy was transferred from energy-scarce to energy-abundant provinces sine the 2008 global financial crisis. Second, provinces tended to have more cross-border (including nearby and distant) virtual energy trade since the global financial crisis. Third, provinces depended more on distant rather than nearby virtual energy trade and this dependence increased over time. Fourth, net virtual energy transferred from the west of China to the east of China was greater than the physical energy transferred through the WTEETP. To test these hypotheses, we investigated China's interprovincial virtual energy networks in 2007 and 2012.

MATERIAL AND METHODS:

Data sources. We applied the recent multiregional input-output table for China: the Chinese 2007 and 2012 interprovincial input-output table. The data source of China's MRIO table is the same as the paper by Mi et al. (2017) which explored changes in China's interprovincial CO_2 network between 2007 and 2012 (Mi et al. 2017). The CEADs (China Emission Accounts & Datasets) has published China Multi-Regional Input-Output Table 2012 on the website (http://www.ceads.net/data/input-output-tables/). The energy consumption data for sectors within provinces were obtained from the energy balance table of the China Energy Statistical Yearbook 2008 and 2013 (National Bureau of Statistics 2008).

Construction of virtual energy trade network. We constructed the interprovincial virtual energy transfer network by applying multi-region input-output analysis and direct energy consumption coefficients. We considered each trading province as one node, therefore all trading provinces constructed one interprovincial virtual energy trade network. A direct link existing between any pair of nodes represents a virtual energy flow between provinces. The weight of the link represents the volume of virtual energy flow.

First, we used multi-region input-output analysis to assess interdependencies between different provinces' economies by tracking capital flow. By using this method, we showed the contribution from production sectors within provinces to intermediate and final consumption of all sectors in all provinces in the form of monetary value. Intermediate consumption is reflected by the monetary value of goods and services consumed as inputs by a process of production, while final consumption is reflected by the monetary value used for direct satisfaction of individual needs or collective needs of members of a community.

Assuming the number of provinces is m, and each province possesses n sectors, the output in sector i of province R can be calculated by Eq.(1) as follows:

$$x_i^R = \sum_{S=1}^{m} \sum_{j=1}^{n} x_{ij}^{RS} + \sum_{S=1}^{m} y_i^{RS} \qquad (1)$$

where x_{ij}^{RS} represents the intermediate consumption in sector j of province S provided by sector i of province R. The y_i^{RS} represents the final consumption in province S directly provided by sector i of province R.

The direct input coefficient a_{ij}^{RS} can be calculated by Eq. (2):

$$a_{ij}^{RS} = x_{ij}^{RS}/x_j^S. \tag{2}$$

where x_j^S is the total output in sector j of province S. a_{ij}^{RS} is the amount of input in sector i of province R to increase one monetary output in sector j of province S.

Based on Eq.(2), we can transform Eq.(1) into a matrix as follows:

$$X^* = A^*X^* + Y^* \tag{3}$$

$X^*=[x^1, x^2, \ldots, x^m]^T$ is the vector of total output for all m provinces. A represents a matrix for direct input coefficient. Y^* represents the vector of final consumption in all provinces.

Then we transformed Eq.(3) into a consumption driven format as follows:

$$X^* = BY^*, B = (I - A)^{-1} \tag{4}$$

The $(I - A)^{-1}$ is the Leontief inverse matrix indicating how much output from other provinces is required to meet one unit of final consumption in monetary value.

To link monetary transfer with virtual energy transfer, the direct energy consumption coefficients are defined and applied. The direct energy consumption coefficient of sector j in province R can be calculated as Eq.(5):

$$e_j^R = \frac{w_j^R}{x_j^R} \tag{5}$$

where w_j^R is total energy consumption for particular type of energy in sector j of province R, and x_j^R represents the output of sector j of province R. e_j^R is the amount of energy used to produce one monetary unit of output in sector j of province R. Here, we divided the virtual energy into different types based on energy sources that used to produce the virtual energy. Based the available data in

China provinces' Energy Balance table in 2007 and 2012, we divided virtual energy into coal produced virtual energy, oil produced virtual energy, natural gas produced virtual energy and others produced virtual energy.

For a particular province R, the total energy footprint WF^{R}, which is equal to the sum of net virtual energy import and internal energy consumption (Hoekstra and Hung 2002), can be expressed by Eq.(6):

$$\mathrm{WF}^{\mathrm{R}} = \mathrm{E} \,.\, \mathrm{B} \,.\, \mathrm{Y}^{\mathrm{R}} \tag{6}$$

where $\mathrm{E}=[e^1, e^2, \dots, e^N]$ represents a $1\times \mathrm{n} \times \mathrm{m}$ vector of all provincial sectors' direct energy consumption coefficients, Y^{R} is the final consumption in province R. Our analyses' calculation is based on the multiregional input-output analysis which catches both the direct and indirect energy use embodied in commodity trade (Kan et al. 2019). Our internal energy consumption refers to the internal energy footprint, which refers to all local energy use (direct and indirect) associated with final consumption in the studied area.

Provincial energy production data were obtained from the China Energy Statistical Yearbook for the years 2008 and 2013 to identify whether or not virtual energy flows from energy-scarce to energy-abundant provinces. If the virtual energy flowed from a province with comparably less energy production to another province with comparably more energy production, the virtual energy trade would be classified as a flow from an energy-scarce to an energy-abundant province, and vice-versa.

China is geographically divided into east, central and west areas. In this paper, 30 provinces were analyzed. Liaoning, Hebei, Beijing, Tianjin, Shandong, Jiangsu, Shanghai, Zhejiang, Fujian, Guangdong, and Hainan belong to the eastern area. Shanxi, Jilin, Heilongjiang, Anhui, Jiangxi, Henan, Hubei and Hunan are located in the central area. Inner Mongolia, Chongqing, Guangxi, Sichuan, Guizhou, Yunnan, Shaanxi, Gansu, Qinghai, Ningxia and Xinjiang are all western provinces. Tibet, Hong Kong, Macau and Taiwan were not analyzed due to data acquisition problems.

We also classified interprovincial virtual energy trade into "nearby virtual energy trade" and "distant virtual energy trade" based on the geographical relationship between provinces. For example, virtual energy trade between provinces that share land borders were deemed as nearby virtual energy trade. In all other cases, virtual energy trade between two provinces were deemed as distant virtual energy trade.

RESULTS.

More virtual energy was transferred from energy-scarce to energy-abundant provinces over time (Figure 4.1-4.2). The total virtual energy transferred from energy-scarce to energy-abundant provinces grew by 63.8% from 2007 to 2012, while the total virtual energy transferred from energy-abundant to energy-scarce provinces grew by only 38% during the same period (Figure 4.1.a). The virtual energy transferred from energy-scarce to energy-abundant provinces of coal, oil, natural gas and other energy grew by 66%, 34.8%, 150% and 81.5%, respectively (Figure 4.1.b-e). Conversely, the virtual coal, virtual oil, virtual natural gas and other virtual energy transferred from energy-abundant to energy-scarce provinces grew by 39.3%, 22.2%, 120% and 38.4%, respectively. The ratio of the amount of virtual energy trade – that flowing from energy-scarce to energy-abundant provinces – to the total amount of virtual energy trade increased from 43.2% to 47.5% over time (Figure 4.2). For virtual coal, this ratio increased from 39.4% to 43.6% (Figure

4.2). For virtual oil, this ratio increased from 51.5% to 54%. For virtual gas, this ratio increased from 47.7% to 50.9%. For other virtual energy, this ratio increased from 42.5% to 49.2%.

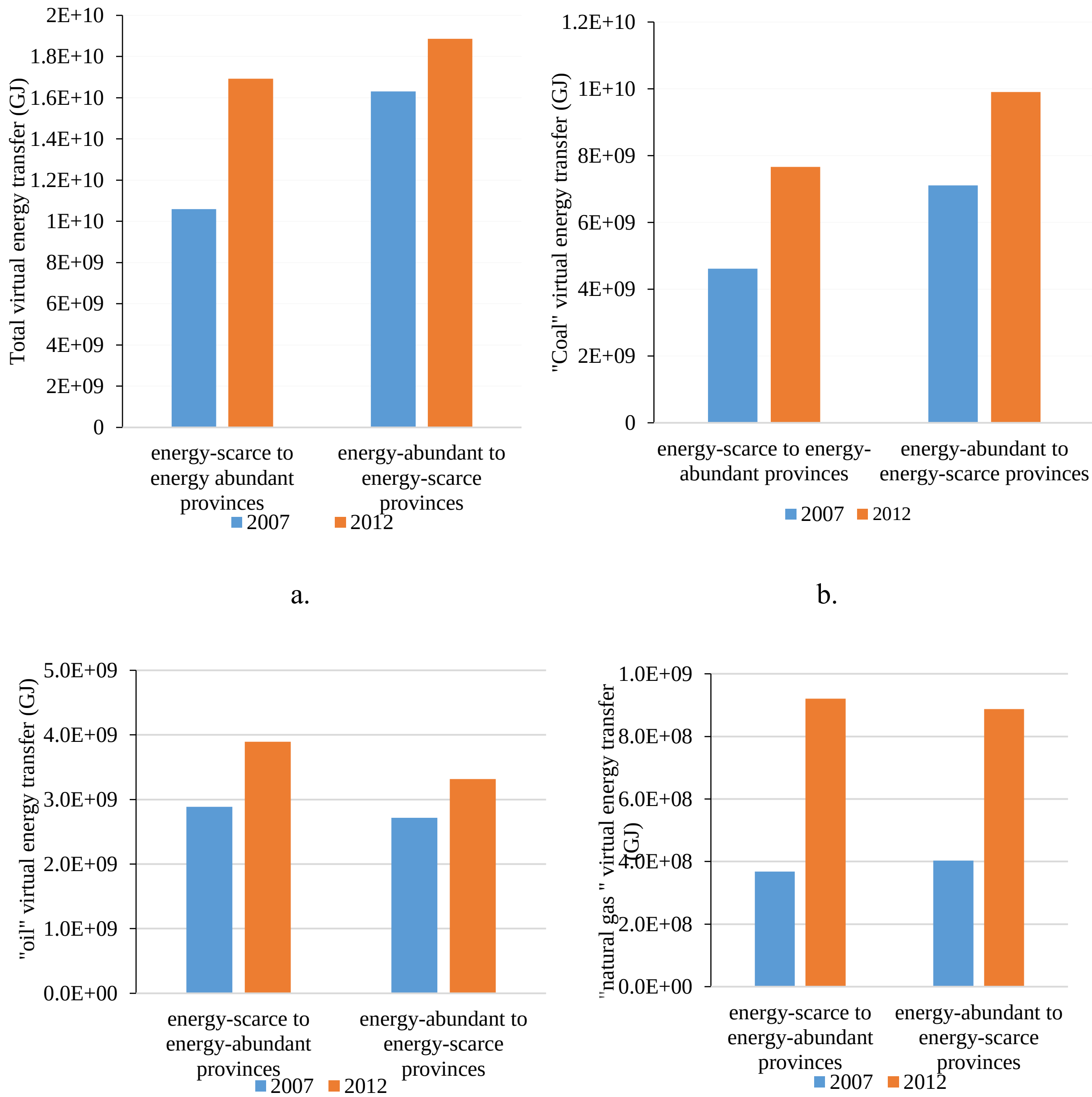

a. b.

c. d.

Figure 4.1. Different types of virtual energy transferred from energy-scarce to energy-abundant provinces: a. total virtual energy; b. virtual coal; c. virtual oil; d. virtual natural gas; e. other virtual energy type.

Figure 4.1 (cont'd)

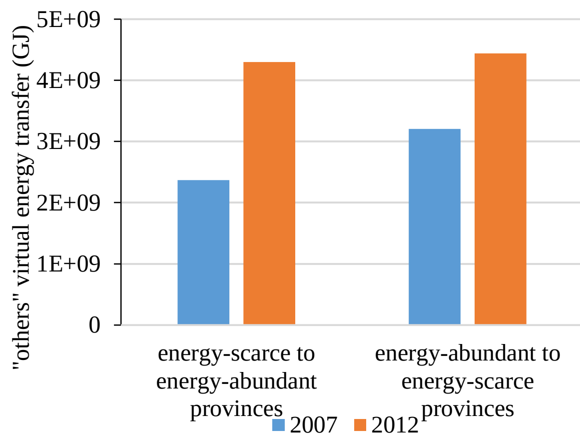

e.

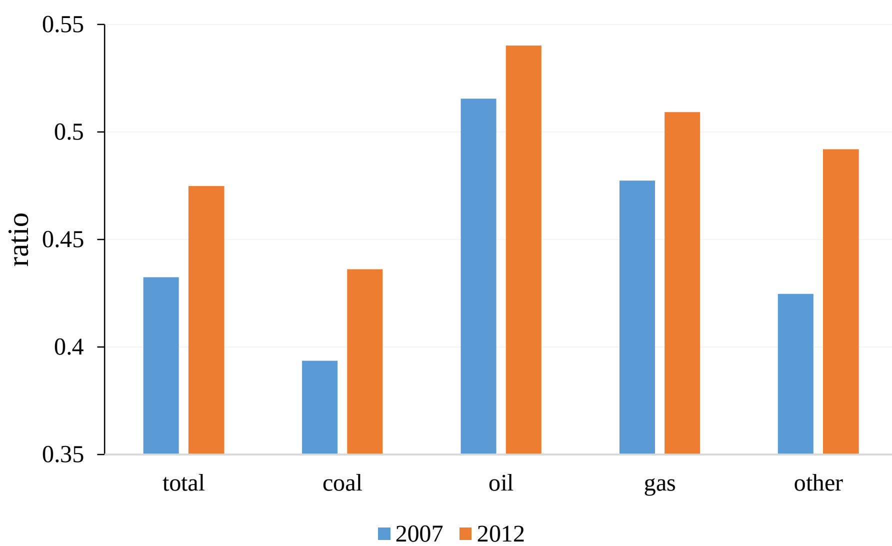

Figure 4.2. Ratio of the different types of virtual energy, which transferred from energy-scarce to energy-abundant provinces, to total amount of the corresponding type of virtual energy transfer.

A majority of the provinces inspected had more imported virtual energy than internal energy consumption over time (Figure 4.3). The percentage of provinces that imported more total virtual energy than total energy consumed internally increased from 23.3% in 2007 to 36.7% in 2012. For virtual coal, virtual oil, virtual natural gas and other virtual energy, this percentage increased by 6.67%, 20%, 6.67% and 6.67%, respectively. The provinces that depend most on imported total virtual energy in 2012 were Beijing, Hainan and Shanghai. However, for specific types of virtual energy, the provinces that depended most on the imported virtual energy varied (Figure 4.3). The provinces that depended most on the imported virtual coal in 2007 and 2012 were Hainan, Beijing and Shanghai. For virtual oil, the top provinces in 2007 were Anhui, Jiangsu and Hebei, while in 2012 the top provinces were Anhui, Inner Mongolia and Jilin. Concerning virtual natural gas, the provinces that depended most on imported virtual natural gas in 2007 were Guangxi, Fujian and Jiangxi, and in 2012 were Yunnan, Guangxi and Guizhou. For other virtual energy types, the top provinces that depended most on imported virtual energy in 2007 were Shanghai, Hainan and Anhui, and in 2012 were Hainan, Shaanxi and Shanghai. The imported total virtual energy in all provinces was equal to 58% and 71% of internal energy consumption in 2007 and 2012, respectively. For specific types of virtual energy, the ratios was 55.2%, 60.6%, 49.8% and 57.3% in 2007, and was 77.3%, 60.5%, 68.6% and 67.5% in 2012, for virtual coal, virtual oil, virtual natural gas and other virtual energy, respectively.

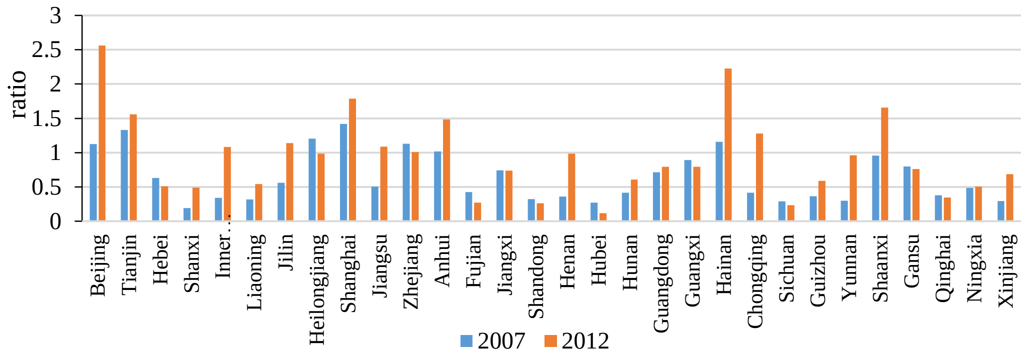

a.

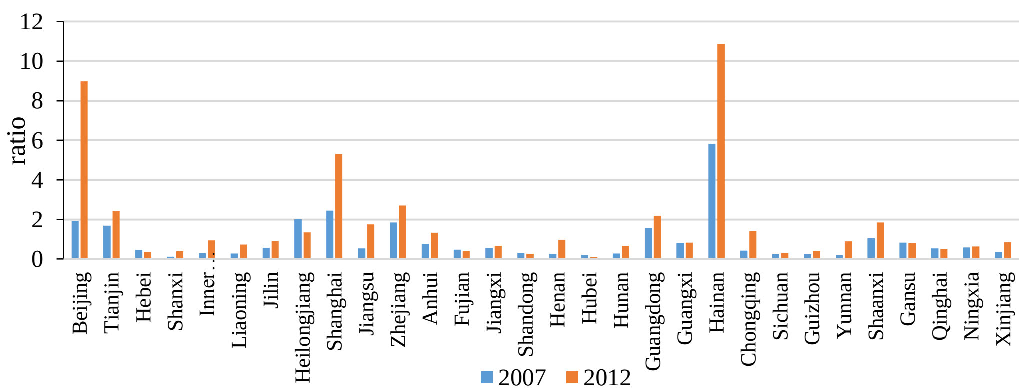

b.

Figure 4.3. Ratio of imported virtual energy to internal energy consumption in each province in 2007 and 2012: a. total virtual energy; b. virtual coal; c. virtual oil; d. virtual natural gas; e. other virtual energy type.

Figure 4.3 (cont'd)

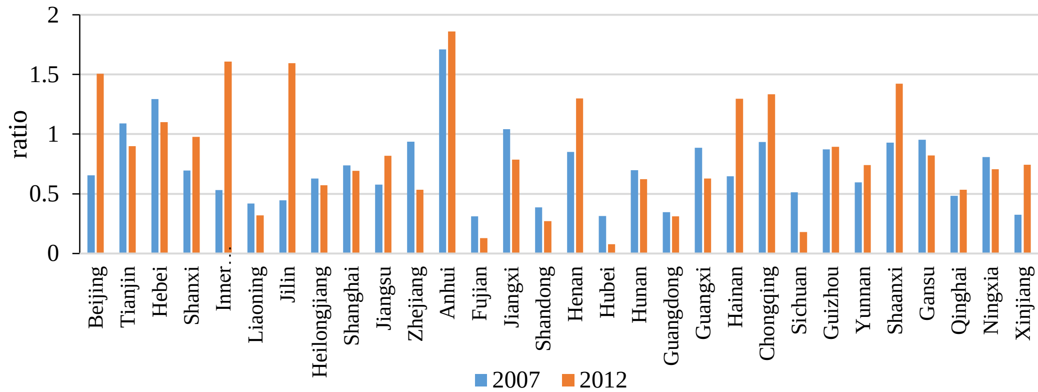

c.

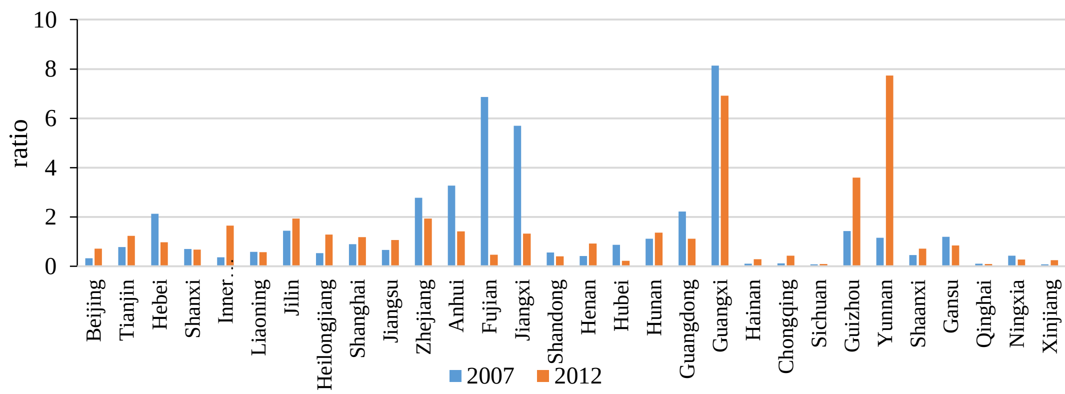

d.

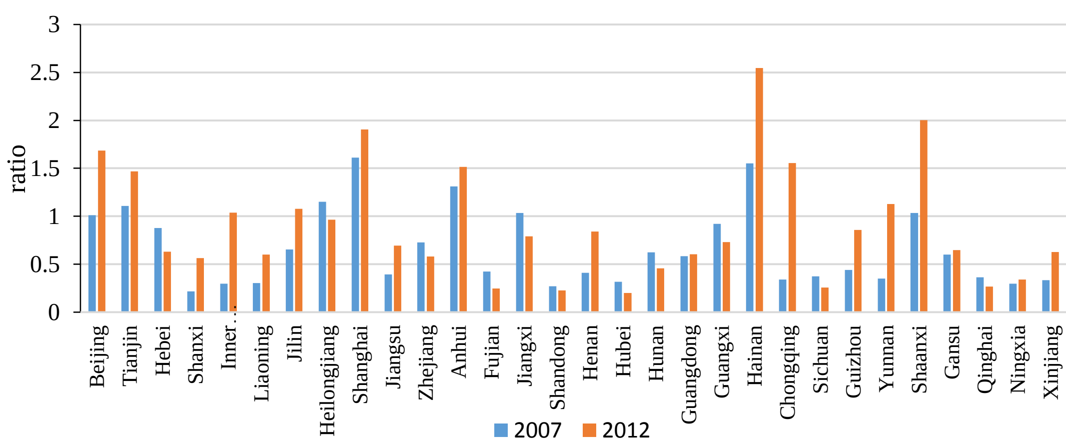

e.

Distant virtual energy trade became more common than nearby virtual energy trade over time (Figure 4.4). Eighty percent of provinces had more distant virtual energy trade over time. In 2007, 73.3% of the provinces had more distant total virtual energy trade than nearby total virtual energy trade (Figure 4.4), and this ratio increased to 100% in 2012. In particular, 83.3% of the provinces in 2007 had more distant virtual oil trade than nearby virtual energy trade, and this ratio increased to 100% in 2012. The provinces with the most distant virtual energy trade were Xinjiang, Fujian and Yunnan in 2012 (Figure 4.4). In 2007, the top provinces dominated by distant total virtual energy trade were Guangdong, Xinjiang and Beijing. The provinces least dominated by distant total virtual energy trade were Hebei, Jilin and Shaanxi. These results varied by the virtual energy type being traded (Figure 4.4). The top provinces dominated by distant virtual coal trade in 2007 were Xinjiang, Guangdong and Shanghai, and in 2012 were Xinjiang, Fujian and Shanghai. The top provinces dominated by distant virtual oil trade in 2007 were Beijing, Shandong and Xinjiang, and in 2012 were Xinjiang, Yunnan and Heilongjiang. The top provinces dominated by distant virtual natural gas trade in 2007 were Guangdong, Fujian and Beijing, and in 2012 were Guangdong, Xinjiang, Fujian and Yunnan. The top provinces dominated by distant trade of other virtual energy in 2007 were Guangdong, Beijing and Tianjin, and in 2012 were Xinjiang, Yunnan and Fujian.

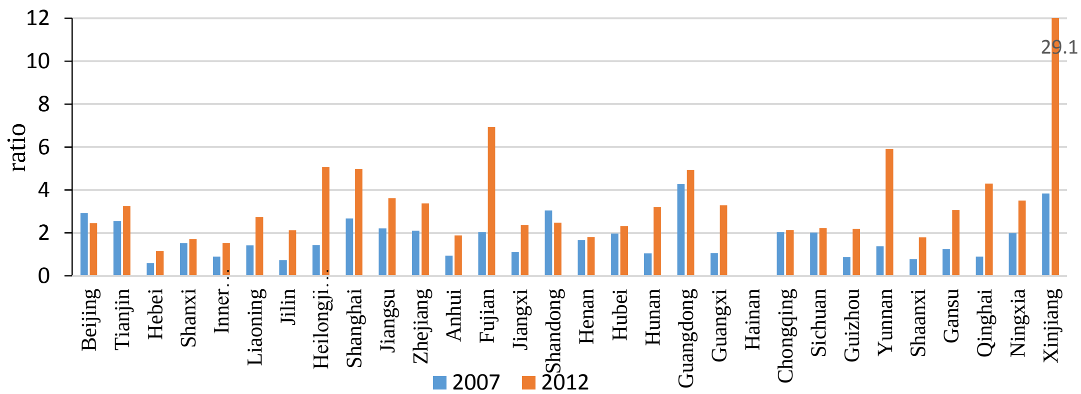

a.

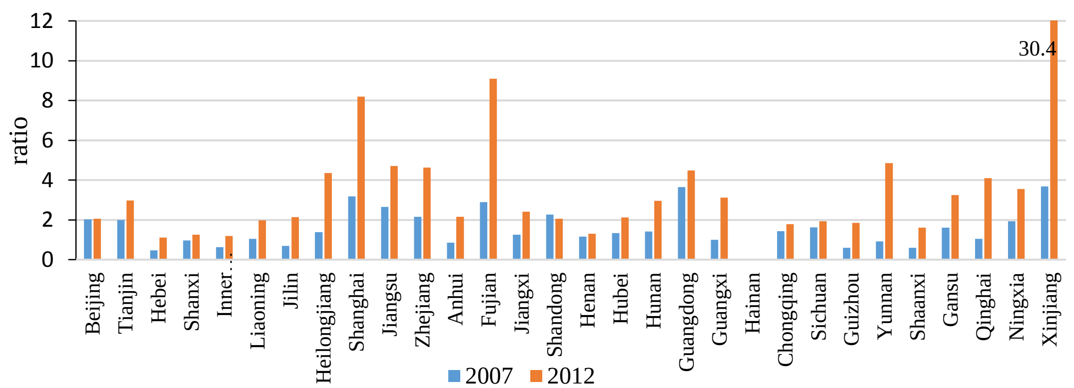

b.

Figure 4.4. Ratio between distant and nearby virtual energy trade in each province in 2007 and 2012: a. total virtual energy; b. virtual coal; c. virtual oil; d. virtual natural gas; e. other virtual energy type.

Figure 4.4 (cont'd)

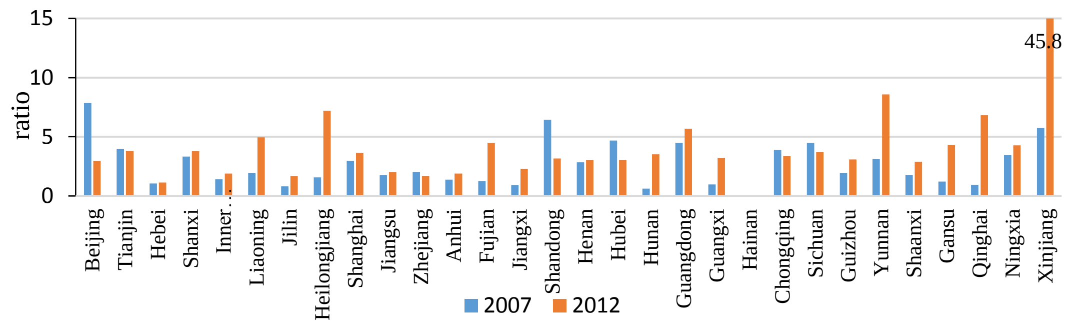

c.

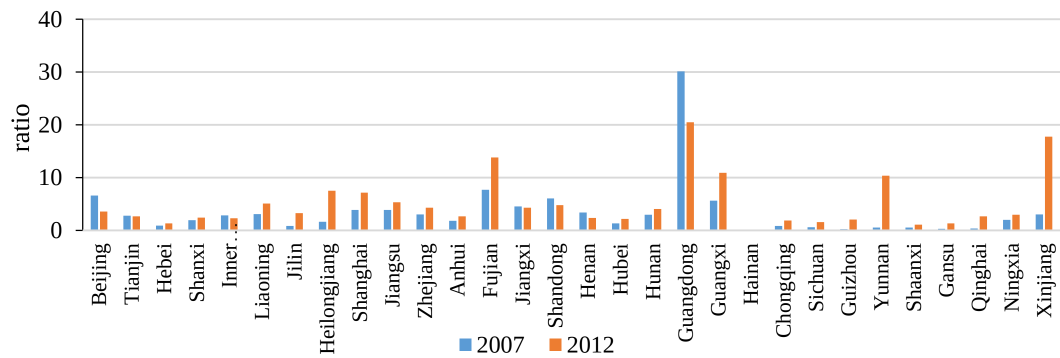

d.

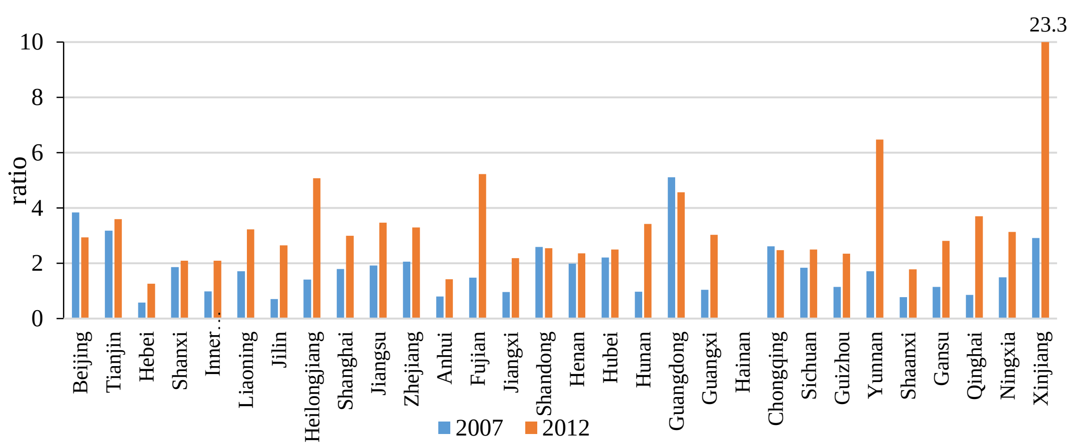

e.

More total virtual energy moved from west to east China than the physical energy that flowed from west to east China through the WTEETP (Table 4.1). In 2007, the total virtual energy from west to east China was 236% as much as the physical energy transferred through the WEETP. And this percentage is 160% in 2012. The flow pattern of virtual energy varied from different types of virtual energy. For both virtual coal and virtual natural gas, more virtual energy was transferred from west China to east China than the virtual energy transfer in the opposite direction in both 2007 and 2012. But more virtual was flowed from east China to west China than the virtual oil that flowed in the opposite direction in both 2007 and 2012.

Table 4.1 (a). Total virtual energy transferred between different parts of China

Total virtual energy transferred (GJ)		*Receiving systems*					
		2007			2012		
		east China	west China	central China	east China	west China	central China
Sending systems	east China	2.76×10^{10}	1.67×10^{9}	3.42×10^{9}	2.78×10^{10}	4.05×10^{9}	5.02×10^{9}
	west China	1.99×10^{9}	1.17×10^{10}	1.05×10^{9}	4.27×10^{9}	1.70×10^{10}	2.49×10^{9}
	central China	3.17×10^{9}	1.08×10^{9}	1.38×10^{10}	4.76×10^{9}	2.55×10^{9}	1.76×10^{10}

Table 4.1 (b). Virtual coal transferred between different parts of China

Virtual coal transferred (GJ)		*Receiving systems*					
		2007			2012		
		east China	west China	central China	east China	west China	central China
Sending systems	east China	1.23×10^{10}	6.37×10^{8}	1.54×10^{9}	1.10×10^{10}	1.72×10^{9}	2.10×10^{9}
	west China	1.03×10^{9}	6.04×10^{9}	5.34×10^{8}	2.27×10^{9}	8.34×10^{9}	1.31×10^{9}
	central China	1.86×10^{9}	6.7×10^{8}	8.35×10^{9}	2.71×10^{9}	1.46×10^{9}	9.41×10^{9}

Table 4.1 (c). Virtual oil transferred between different parts of China

Virtual oil transferred (GJ)		Receiving systems					
		2007			2012		
		east China	west China	central China	east China	west China	central China
Sending systems	east China	7.57×10^9	5.68×10^8	9.45×10^8	8.1×10^9	1.03×10^9	1.37×10^9
	west China	3.46×10^8	1.91×10^9	1.79×10^8	6.44×10^8	3.07×10^9	3.82×10^8
	central China	6.65×10^8	1.82×10^8	2.49×10^9	8.08×10^8	3.95×10^8	3.34×10^9

Table 4.1 (d). Virtual natural gas transferred between different parts of China

Virtual natural gas transferred (GJ)		Receiving systems					
		2007			2012		
		east China	west China	central China	east China	west China	central China
Sending systems	east China	5.96×10^8	3.72×10^7	6.6×10^7	1.2×10^9	2.02×10^8	2.39×10^8
	west China	1.47×10^8	1.05×10^9	8.29×10^7	2.89×10^8	1.46×10^9	1.84×10^8
	central China	4.85×10^7	2.12×10^7	2.66×10^8	1.69×10^8	9.08×10^7	6.19×10^8

Table 4.1 (e). Other virtual energy transferred between different parts of China

Others virtual energy transferred (GJ)		Receiving systems					
		2007			2012		
		east China	west China	central China	east China	west China	central China
Sending systems	east China	7.11×10^9	4.25×10^8	8.69×10^8	7.56×10^9	1.1×10^9	1.32×10^9
	west China	4.69×10^8	2.66×10^9	2.52×10^8	1.06×10^9	4.17×10^9	6.07×10^8
	central China	5.99×10^8	2.06×10^8	2.72×10^9	1.08×10^9	6.05×10^8	4.19×10^9

DISCUSSION

This study explored the shift in national virtual energy transfer patterns since the financial crisis. In particular, considering the potential differences in the flow pattern of different virtual energy types, this paper analyzed the virtual coal, virtual oil, virtual natural gas and other virtual energy types based on the available data. Based on our analysis of these flow pattern in China's virtual energy network in 2007 and 2012, we found that more total virtual energy flowed from energy-scarce to energy-abundant regions since the global financial crisis, especially for the virtual oil. The reason for this may be that virtual energy transfer does not aim to alleviate regional energy shortages; rather, it is motivated by commodity trade which seeks to promote economic growth since the financial crisis. After the "reform and opening up" policy, China's GDP grew about 10% annually from 1979 to 2013 (Morrison 2014), with associated growth in energy demand across provinces. The geographical separation between production and consumption of products across provinces continues to drive this virtual energy transfer embodied in commodity trade (Kan et al. 2019).

Provinces depend more on cross-border trade, especially trade taking place over great distances. Based on our analyses in 2007 and 2012, the proportion of provinces with imported virtual energy exceeding the internal consumption had increased over time, and the growth rate of total imported virtual energy in China exceeded the internal consumption. Among them, the ratio of virtual oil to the oil internal energy consumption greatly exceeds other types of virtual energy. In 2012, the amount of distant trade of all types of virtual energy was greater than their respective nearby trade. For local governments, looking to distant suppliers within trading networks helps them find "hidden" energy resources. In the case of virtual energy networks, our results demonstrate that distant areas have greater impacts on focal areas than adjacent areas. More cooperation with distant provinces should be encouraged since they play more important roles in meeting resource demands. In the case of virtual energy networks, our results demonstrate that distant areas have greater impacts on focal areas than adjacent areas. As China's economic development, population growth and technological progress continue, it is encouraged to guide the development of long-distance virtual energy trade, strengthen effective cooperation among different regional provinces to satisfy people's demand, support economic development and further shaping the regional environmental mechanism. Especially for Xinjiang which greatly depends on distant energy transfer, it is important for Xinjiang to develop cooperation with trading partners

In this study, we found virtual energy transfer to have a greater impact on sending and receiving systems than physical energy transfer. The virtual energy flowing from west to east China is much greater than the physical energy transferred through the WTEETP. Currently, energy policy primarily focuses on physical supplies, not virtual energy. This may overlook the important influence that virtual energy has on the regional energy mechanism, thus leading to less efficient policy management. Because the total virtual energy flowing from west China to east China was much greater than physical energy transferred through the West-To-East Electricity Transmission Project (WTEETP). If government only applied physical energy transmission projects to alleviate the energy scarcity, it would overlook the virtual energy's function and therefore the efficiency of policy for saving energy shortage in focal areas may not be maximized. Therefore, besides physical energy transmission project, government can also consider managing virtual energy trade to alleviate energy shortage in energy-scarce areas. For example, they can consider applying the virtual energy subsidy to motivate virtual energy trade from energy-abundant area to energy-scarce area for alleviating energy scarcity (Cherniwchan et al. 2016) so that the efficiency of policy can be maximized and energy shortage in focal areas can be better solved. The interregional results provide a quantitative basis to assign sound reduction targets for specific regions and help facilitate binding commitments of interprovincial cooperation for energy conservation. According to our results, the eastern regions such as Guangdong should take more responsibility due to the large share of virtual energy this province uses. The eastern regions can play an important role in energy saving and emission reduction by leveraging its favorable economic conditions and advanced technologies. In addition, future analyses using enhanced energy monitoring and updated input–output tables at the national and sub-national levels are encouraged in order to gain a more robust understanding of the implications energy transfers may have on China's resource consumption, expanding economy and population.

Energy management should target at specific type of virtual energy, since the flow pattern of different types of energy differed from each other. This was especially true for virtual oil as more than half of the virtual oil was flowed from energy-scarce to energy abundant provinces. Therefore, government should consider policies (e.g., applying oil virtual energy export tax) that may regulate the virtual oil flows to change their spatial patterns (Cherniwchan et al. 2016).

By placing this study under the metacoupling framework, the temporal patterns of interaction between trading provinces across the virtual energy network at the national scale are further revealed, contributing to a more holistic understanding of virtual resource studies. Future research should extend this study by applying complex network analysis to study typology of national virtual resource transfer networks (Chen et al. 2018), and assessing the interactions across multiple types of virtual resource/material flows beyond virtual energy, for example, to include virtual water, land and carbon across spatial and temporal scales (Lu et al. 2015). This could further reveal the relationship (e.g., trade-offs, synergies) between more virtual resource/material transfer networks and their impacts on national sustainability and thereby result in a more in-depth understanding of the mechanism of interactions within and between adjacent and distant systems. By utilizing the metacoupling framework, we believe a series of metacoupling studies could improve our understanding of cross-border interactions across multiple scales and multiple organizational levels, and help uncover hidden problems which give rise to national and global sustainability challenges. These studies could also facilitate an increased understanding of the importance of adjacent and distant interactions as well as their associated implications for policy, thereby aiding efforts to improve human well-being and ensure the sustainability of coupled human and natural systems.

CONCLUSIONS

We conducted the assessment concerning the changes in flow pattern of national virtual energy trade in China since the financial crisis. And flow patterns of different types of virtual energy (coal, oil, natural gas and others) were compared. We demonstrated a persistent flow of total virtual energy from energy-scare to energy-abundant provinces as the percentage of total virtual flows between such provinces increased from 43.2% in 2007 to 47.5% in 2012. Especially for virtual oil, its transfer from energy-scarce to energy-abundant provinces grew from 51.5% in 2007 to 54.0% in 2012. Further, net total virtual energy flowing from west China to east China greatly exceeded physical energy transferred by way of the West-to-East Electricity Transmission Project. Provinces were also increasingly trading with distant locations as 73.3% of all investigated provinces had more distant than nearby total virtual energy trade in 2007; yet, in 2012, this ratio increased to 100%. We hope these findings will assist policymakers in crafting more efficient energy policy since the current focus on physical energy supplies may overlook potential solutions virtual energy trade can offer in addressing regional energy deficit.

CHAPTER 5. SPATIAL-TEMPORAL ASSESSMENT OF WATER FOOTPRINT, WATER SCARCITY AND CROP WATER PRODUCTIVITY AT THE COUNTY LEVEL IN CHINA'S MAJOR CROP PRODUCTION REGION

Xu, Z., X. Chen, S. R. Wu, M. Gong, Y. Du, J. Wang, Y. Li & J. Liu (2019) Spatial-temporal assessment of water footprint, water scarcity and crop water productivity in a major crop production region. *Journal of Cleaner Production,* 224, 375-383.

ABSTRACT

Irrigated agriculture has had an enormous influence on food security, water security and human well-being. Water footprint (how much water is used), water scarcity (how scarce water is), and crop water productivity (how much productivity irrigation adds) are important indicators for evaluating sustainability in irrigated agriculture. Yet these interrelated indicators have not been studied simultaneously at the county level – the basic administrative unit of agricultural planning and water management in countries such as China, India and Japan. To fill this knowledge gap, we performed a demonstration in China's major crop production region, the North China Plain (NCP)'s 207 counties from 1986-2010. The results show that the irrigated agriculture's annual water footprint in the North China Plain increased from 53 billion m^3 in 1986 to 78 billion m^3 in 2010. All counties faced unsustainable water use - local water consumption was greater than local renewable freshwater – even as the average crop water productivity increased from 0.90 $kg.m^{-3}$ to 1.94 $kg.m^{-3}$. The 173 NCP counties suffering severe water scarcity still produced significant crop yield with a high water footprint, a red flag of unsustainable irrigated agriculture. This study has implications for revealing potential unsustainable conditions in irrigated agriculture worldwide.

Keywords: water footprint, water scarcity, crop water productivity, irrigated agriculture, food security, sustainability, China, county level, North China Plain.

INTRODUCTION

Global challenges involving food and water play significant roles in sustainability and human well-being worldwide. The Earth's freshwater resources have been facing tremendous pressure due to increasing consumptive use and water pollution (Steffen et al. 2015, Mekonnen and Hoekstra 2016). For example, global water withdrawal increased 630 percent during 1900-2010 (Food and Agriculture Organization of the United Nations 2018). Global food production also faces great challenges since by 2050 9 billion people will need to be fed. (Godfray et al. 2010).

Irrigated agriculture has important implications for both water security and food security. It accounts for more than 70% of the total water use, and more than 90% of total consumptive water use worldwide (*Consumptive water use* is *water* removed from available supplies without return to a *water* resource system) (Döll 2009, Food and Agriculture Organization of the United Nations 2018) . Forty percent of global agricultural production requires irrigation (Viala 2008).

Much effort has been made to improve irrigated agriculture's performance on water consumption and crop yields for more sustainable development. Many public policies have been applied and billions of dollars spent to save water in irrigated agriculture (Ward and Pulido-Velazquez 2008). The water footprint, water scarcity and crop water productivity are used as indicators to assess water and food sustainability. A product's water footprint (WF) is the total volume of freshwater consumed to produce the product (Liu, Zehnder and Yang 2009, Mekonnen and Hoekstra 2011). WF includes not only direct water consumption of products, but also indirect water consumption – water indirectly consumed and water polluted throughout the production chain. Water scarcity is a shortage of renewable fresh water compared to water demand (Raskin, Hansen and Margolis 1996, Damkjaer and Taylor 2017). We measure agricultural water use against renewable agricultural water resources to represent the extent of water scarcity in agriculture (Raskin et al. 1996, Damkjaer and Taylor 2017). Crop water productivity refers to the amount of crop produced per unit of water used. China is challenged to increase crop water productivity to relieve pressures that agriculture puts on water resources while increasing crop production (Wang et al. 2014). Evaluating water footprints presents a comprehensive picture of the relationship between water consumption and human appropriation, because a water footprint includes both direct water consumption of products and water indirectly consumed and polluted during production. Assessing the impacts of water scarcity helps pinpoint vulnerable hotspots for solving problem. Exploring crop water productivity can facilitate understanding the trade-offs between food production and water consumption. Holistically, understanding all three variables can illuminate pathways to alleviate conflicts between water security and food security.

Many studies have focused on water footprint, water scarcity and crop water productivity separately (Hoekstra and Mekonnen 2011, Hoekstra and Mekonnen 2012, Jaramillo and Destouni 2015, Zhao et al. 2015, Ashraf Vaghefi et al. 2017, Sun et al. 2017). Hoekstra and Mekonnen (2012) has quantified and mapped the water footprint of humanity with high spatial resolution and found that agricultural production accounted for almost 92% of global WF footprint during 1996-2005 (Hoekstra and Mekonnen 2012). Jaramillo et al. (2015) studied the global effects of flow regulation and irrigation on global freshwater conditions and revealed the two can raise the global water footprint of humanity by approximately 18% (Jaramillo and Destouni 2015). Hoekstra and Mekonnen (2011) defined the blue water scarcity index as the ratio of blue water footprint to blue water availability, and applied this index in the world's major river basins (Hoekstra and Mekonnen 2011). They found that the blue water scarcity level in 55% of the basins studied exceeded 100% at least one month of the year, meaning the blue water footprint surpassed available blue water in these study basins. Zhao et. al. (2015) used the water scarcity index to investigate impacts of interprovincial virtual water flow on trading provinces' water scarcity, and found the virtual water flow could exacerbate trading provinces' water scarcity level (Zhao et al. 2015). Vaghefi et al (2017) assessed the crop water productivity of irrigated maize and wheat in Karheh River Basin by using a hydrological model and a river basin water allocation model (Ashraf Vaghefi et al. 2017). Their results indicated a close linear relationship between crop water productivity and yield. Sun et. al (2017) explored crop water productivity of wheat in the Hetao irrigation district at the field scale and analyzed the impacts of agricultural and climatic factors on crop water productivity (Sun et al. 2017). Their results showed that crop water productivity was highly sensitive to relative humidity, wind speed and irrigation efficiency, while lowly sensitive to sunshine hours and the amount of fertilizers used.

Yet to our knowledge water footprint, water scarcity, and crop water productivity (the amount of crop produced per unit of water used) have not been assessed simultaneously at the county level in large plains over a temporal scale. Such information is urgently needed since the global irrigated agriculture area has nearly tripled from 1900 to 2005 amid growing population, water crisis and food shortage. Assessing them together can show a more comprehensive interrelationship among food production, water consumption and water scarcity. This will help to construct targeted policies to achieve both food security and water security in irrigated agriculture. Different from most water footprint studies at coarse spatial scales (e.g., global and national scales) or focused on geographic units (e.g., 5' × 5' or 30' × 30' grid), a study at the county level helps to better understand and manage water conservation and food production because much of agricultural planning and water management (e.g., sown area, planned total crop yield, and permits of water use) is done at the county level in countries such as China, India and Japan.

To fill this knowledge gap, we chose the North China Plain (NCP), with 207 counties, as a demonstration site for integrated assessment. The NCP is the national agricultural base and main grain production area in China. The region includes the plain of Beijing, Tianjin City, Hebei Province, and part of Henan and Shandong provinces with 133 million people (Zhang et al. 2012). Approximately 80% of the seeded areas of all crops are grain areas, 96% of which are planted with winter wheat and summer maize (Wang et al. 2001). From 1986 to 2010, the total wheat production in the NCP had increased from 1.58 to 2.49 million tons, while the total maize production had grown from 1.07 to 2.97 million tons in the NCP over this time period. While the NCP needs water for agriculture, the available freshwater per capita annually in the plain – 302 m^3 per year (Zhang et al. 2011) – is less than 1/24 of the global average. This is far below the international standard of freshwater resource shortage with the 1,000 m^3 threshold (Kang et al. 2013). Using such limited water resources to support large amounts of agricultural production and socioeconomic development is a great challenge, implicating significant impacts on national food security, water security and sustainable development. Many policies and technology investments have been applied in the NCP to solve the water crisis and ensure sustainable water use for food production, but the outcome has not been assessed comprehensively. Exploring this problem in the NCP can have implications for not only China, but also other irrigated areas worldwide.

The aim of this study was to assess the water footprint, water scarcity and crop water productivity of irrigated agriculture at the county level in the NCP from 1986 to 2010. We calculated the blue, green, and grey water footprint to illustrate the dynamics of total water footprint (WF_{total}) in the whole NCP; applied the water scarcity index to study the impacts of water consumption from irrigated agriculture on water scarcity in each county; and measured the grain yield per unit water use to represent crop water productivity (Mekonnen and Hoekstra 2011).

MATERIALS AND METHODS

Data sources

We compiled a set of data for our analyses, including agrometeorological data, basic agricultural data, and geographic information system (GIS) data. We obtained the agrometeorological data from the Meteorological Data Sharing Service System of National Meteorological Information Center of China. These data covered 69 meteorological stations in Beijing, Tianjin, Hebei Province, Shandong Province, and Henan Province and included average air temperature, maximum air temperature, minimum air temperature, hours of sunshine, and daily precipitation data from 1986 to 2010. These factors were used to calculate the reference evapotranspiration (ET_0) based on Penman-Monteith equation (Xu et al. 2017). The ET_0 were used for calculating water footprint. We also used data on the crop growth periods, estimation of accumulated temperature, and solar radiation of winter wheat and summer maize from the cited literature, to define crop water production function in different areas. We obtained basic county-level agricultural production data – the cultivated area, nitrogen use, amount of production of winter wheat and summer maize – from the Agricultural Information Institute of Chinese Academy of Agricultural Sciences, to help calculate effective rainfall and grey water footprint, and to explore the relationship between crop production and water footprint. The empirically measured data of ETc (crop evapotranspiration) were derived from Luancheng Agro-Eco-Experimental Station of the Chinese Academy of Sciences in Shijiazhuang City, Hebei Province. We also acquired the digitized soil organic matter map data (at a scale of 1:14,000,000) in 2005 from the Data Center for Resources and Environmental Sciences of Chinese Academy of Sciences, to help define crop water functions in different areas. Furthermore, we received GIS shape files for provinces, counties, main cities, and the Yellow River. Our unit of analysis was the county. For agrometeorological data that were not at the county level, we used the ordinary Kriging method to interpolate data at agrometeorological stations to counties. Specifically, we converted vector data of stations into raster data and then calculated the sum value by zonal statistics for each county in ArcGIS (version 10.1 ESRI). Crop Water Production Function (CWPF) is the mathematical expression that describes the relationship between water use and crop production for a certain kind of crop. The function is mainly influenced by sunshine and heat factors such as photo synthetically active radiation and effective accumulated temperature, and agricultural production factors such as soil organic matter, crop types and varieties (Kang 2007) (see details in Supplementary Information).

WF assessment

We assessed the WF for the entire grain production chain, which included both the consumptive water usage for crop growth (WF_{cons}) and the fresh water to dilute associated pollutants (WF_{grey}). According to the sources of water, WF_{cons} were further divided into WF_{blue} (the volume of surface water, shallow and deep groundwater used for irrigation) and WF_{green} (the volume of rainwater used for growing crops). More detailed procedures for the WF assessment methods (including all calculation equations) can be found in Supplementary Information.

WF_{cons}

WF_{cons} of a crop production is the total actual consumption of water within its whole production chain. Often, it is difficult to directly measure WF_{cons} and thus the indirect water requirement method is used. The crop water requirement is assumed to be the needed water via crop evapotranspiration under optimal conditions, which is calculated by multiplying the reference crop evapotranspiration with a crop coefficient. Because actual crops are not always grown under optimal conditions, actual evapotranspiration should be less than optimal crop evapotranspiration and thus a water stress coefficient is introduced. The main factors that affected crop evapotranspiration include precipitation, air temperature, pressure, sunshine hours, wind speed, crop type, soil condition, and planted time. The calculation functions are given below (Allen et al. 1998; Hoekstra et al. 2011).

$$WF_{cons} = \frac{1000 \times ET_0 \times A}{Y} \tag{1}$$

$$ET_{\boldsymbol{c}} = K_c \times ET_0 \tag{2}$$

$$ET_0 = \frac{0.408\delta(R_n - G) + \gamma\frac{900}{T+273}U_2(e_s - e_a)}{\delta + \gamma(1 + 0.34U_2)} \tag{3}$$

Where ET_a (mm) is the actual crop evapotranspiration; A(km^2) is the total planation area; Y (kg) is the total crop yield; K_c is crop coefficient comparing to reference crop evapotranspiration; ET_0 (mm) is reference crop evapotranspiration; R_n (MJ m^{-2} d^{-1}) is net radiation on surface of crop; G (MJ m^{-2} d^{-1}) is soil heat flux; T (℃) is average air temperature; U_2 (m s^{-1}) is wind speed at 2 meters above ground; e_s (kPa) is saturation vapor pressure; e_a (kPa) is measured vapor pressure; δ (kPa $℃^{-1}$) is the slope of the curve between saturation vapor pressure and temperature; γ (kPa $℃^{-1}$) is hygrometer constant.

For our proposed water consumption method, the actual crop evapotranspiration in Eq. (1) was calculated from the crop water production function (CWPF) shown below.

$$y = aET_a^2 + bET_a + c \tag{4}$$

$$ET_a = min(-\frac{b}{2a} \pm \sqrt{\frac{y}{a} + \frac{b^2}{4a^2} - \frac{c}{a}}) \tag{5}$$

Where *a*,*b*,*c* are regression coefficients; and y(kg/ha) is unit area crop yield.

Considering that the actual crop water consumption might differ from the estimated amount in the conventional water requirement method, we proposed a new water consumption method based on the crop water production function and compared it with the conventional water requirement method. The test showed that on average there was no significant difference between the estimation from the proposed water consumption method and the actual measurement of water use. However, the estimation from the conventional water requirement method was significantly higher than that of the water consumption method or the actual measurement at the Luancheng monitoring station as shown in Supplementary Figure1.

WF_{blue} and WF_{green}

WF_{blue} is the volume of consumed surface water and groundwater to produce goods or delivering services. WF_{green} is the volume of consumed rainwater during the production process. This is particularly relevant for agricultural and forestry products, including the total rainwater evapotranspiration (from fields and plantations) plus the water incorporated into the harvested products. The blue and green WF were calculated by the following equations (Zhang et al. 2008):

$$WF_{cons} = WF_{blue} + WF_{green} \tag{6}$$

$$WF_{blue} = \frac{ET_{blue} \times A \times B}{Y} \tag{7}$$

$$ET_{blue} = \max(0, ET_a - P_{eff}) \tag{8}$$

$$WF_{green} = \frac{ET_{green} \times A \times B}{Y} \tag{9}$$

$$ET_{green} = \min(ET_a, P_{eff}) \tag{10}$$

$$P_{eff} = \sigma P \tag{11}$$

Where ET_{blue} (mm) and ET_{green} (mm) are evapotranspiration of blue and green water, respectively; P_{eff} (mm) and P (mm) are effective rainfall and total rainfall within crop growth period, respectively; and σ is the effective utilization coefficient of rainfall.

WF_{grey}

The WF_{grey} is an indicator of freshwater pollution that is associated with a product over its full production chain. It is calculated as the volume of water required to dilute pollutants to meet water quality standards. We focused on the WF_{grey} of nitrogen because fertilizers were used intensively in the NCP and potentially caused the most severe pollution since nitrogen can easily be transported in soil, surface water, and groundwater (Sun et al. 2018). Soil phosphorus often easily generates chemical reactions with other soil minerals and produces chemical compounds that are not readily soluble, resulting in less pollution. Potassium ions are attracted by soil colloids and thus not easily filtered. Therefore, the pollution from phosphorus and potassium fertilizers can be ignored when assessing WF_{grey}. Supplementary Fig. 3 shows that the nitrogen application amount in the NCP, with an average amount of 435.99 kg ha^{-1} and a range from 179.76 to 879.11kg ha^{-1}. The spatial distributions of winter wheat and summer maize are similar; however, on average the nitrogen application amount of winter wheat (223.56 kg ha^{-1}) is higher than that of summer maize (212.43 kg ha^{-1}). The calculation functions for different types of grey WF are shown below:

$$WF_{grey} = \frac{(\alpha_{total} \times AR)/(C_{max} - C_{nat})}{y} \qquad (12)$$

Where α_{total} is the total leaching fraction, measured to be 25.0% (Zhao, Chen and Zhang 2009); a_{surf} and a_{ground} are run-off or leaching fractions of applied chemicals for surface water and groundwater respectively, measured as 9.6% and 15.4%, respectively (Xu et al. 2013); AR (kg ha^{-1}) *is* per hectare application amount of chemical fertilizers; C_{max} (g L^{-1}) and C_{nat} (g L^{-1}) are the maximum acceptable concentration and natural concentration of the chemical fertilizer, respectively.

Water scarcity

The water scarcity index of grain production from a WF perspective can be reflected through the ratio of agricultural water use to renewable agricultural water resources (I_{total}). The higher the water scarcity index, the less sustainable water use for grain production. The water scarcity index can be calculated as follows:

$$I_{total} = WF_{grain,total} / WR_{agri,\ total} \tag{13}$$

Where I_{total} is water scarcity due to agricultural use, $I_{total} > 1$ indicates unsustainable water use and $I_{total} > 2.5$ indicates severe water scarcity due to grain production. $WF_{grain,total}$ is the total WF for winter wheat and summer maize here; $WR_{agri,\ total}$ refers to the renewable agricultural water resources.

Crop water productivity

Crop water productivity refers to the amount of crop produced per unit of water used. We divided the amount of crop production by its corresponding water footprint in each county in 1986 and 2010 to get the crop water productivity at the county level over time. We also divided crop production by its corresponding water footprint in the whole NCP from 1986 to 2010 to obtain the average crop water productivity for the whole plain over time. To figure out to what extent increasing crop water productivity decreases the water footprint and water scarcity, we set the crop water productivity in 1986 (CWP_{1986}) as the baseline, and recalculated the water scarcity and water footprint during 1987-2010 by multiplying the amount of crop production during 1987-2010 with the CWP_{1986} to get the recalculated WF. Then we divided the recalculated WF from 1987-2010 by the renewable agricultural freshwater resource to get the recalculated water scarcity from 1987-2010 (Note: the amount of the renewable freshwater resource was kept constant during 1987-2010 since we used the average renewable water resource value across years. The change in water scarcity was determined by the change of WF). Then we compared the original WF and water scarcity with the recalculated WF and water scarcity to calculate the percent decrease in WF and water scarcity due to the change in crop water productivity.

Statistics and mapping

To test whether or not WF and crop water productivity changed with statistical significance over time, we performed the statistical significance test using the software SPSS Statistics 20 (Statistical Product and Service Solutions, IBM, USA). When P value < 0.05, it indicates significant change. We acquired GIS shape files for the NCP counties. We created the map of our study areas and mapped all the WF, water scarcity and productivity at the county level in ArcGIS.

RESULTS

Our results show the annual water footprint from irrigated agriculture increased in almost all counties (Figure 5.1). The southeast NCP had a larger water footprint and the central part had a smaller water footprint than other places in the NCP (Figure 5.1). Also, the water footprint of southeast NCP increased most while that of the central part increased the least over time (Figure 5.1).

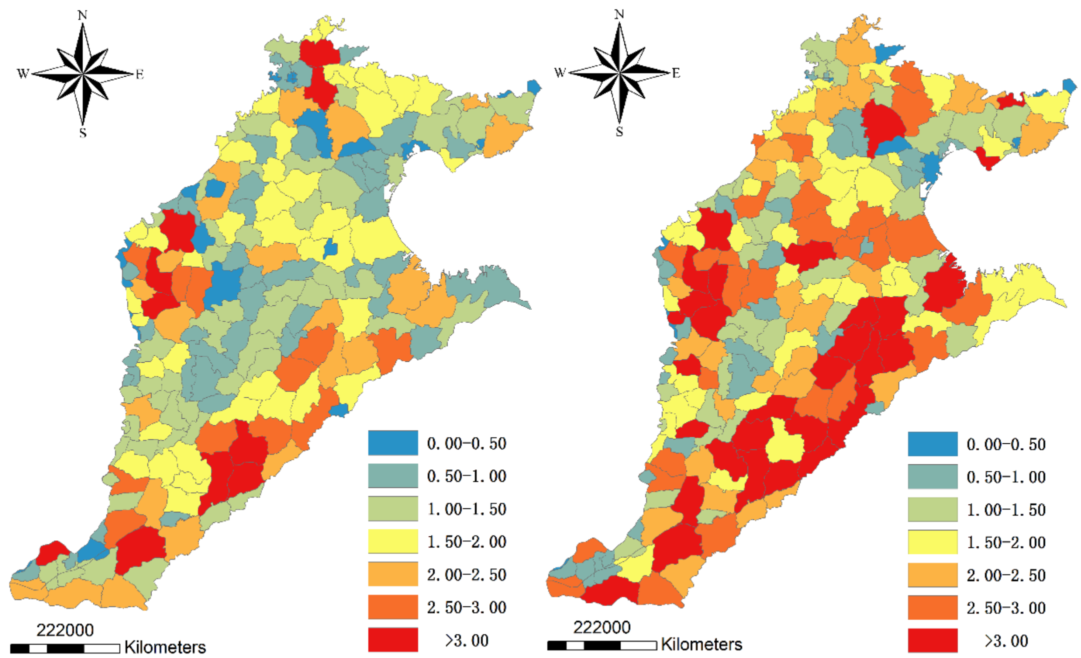

(a) (b)

Figure 5.1. Spatial dynamics of total water footprint (billion m^3) in irrigated agriculture from 1986 (a) to 2010 (b).

The annual water footprint in all counties together increased from 53 billion m^3 in 1986 to 78 billion m^3 in 2010 (Figure 5.2a). For the total amount of different types of WF, overall there were statistically significant increases in WF_{total} ($F = 17.97$, $p = 0.0003$), WF_{green} ($F = 22.17$, $p = 0.0001$), and WF_{grey} ($F = 21.88$, $p = 0.0001$) over time (Figure 5.2a; Table 5.1). The WF_{blue} gradually increased from 1986, peaked in 1997, then started to decline to the valley in 2003, and kept relatively stable between 2004 and 2010 (Figure 5.2a). Its overall temporal trend was not statistically significant ($F = 0.31$, $p = 0.5821$; Table 5.1). There are some potential reasons for the dynamics of the WF_{blue}. During 1986-1997, the rapid development of agriculture led to the WF_{blue} increase. But during 1998-2003, the water-saving policies were implemented in the NCP to reduce planting area and restrict the use of underground water and thus reduced the WF_{blue} (Xie and Zhang 2007, Liu, Cheng and Song 2008, Hu, Wu and Qi 2017). After 2004, the increasing demand for crop production in the NCP compensated for the effects of water-saving policies (Xie and Zhang 2007, Liu et al. 2008, Hu et al. 2017).

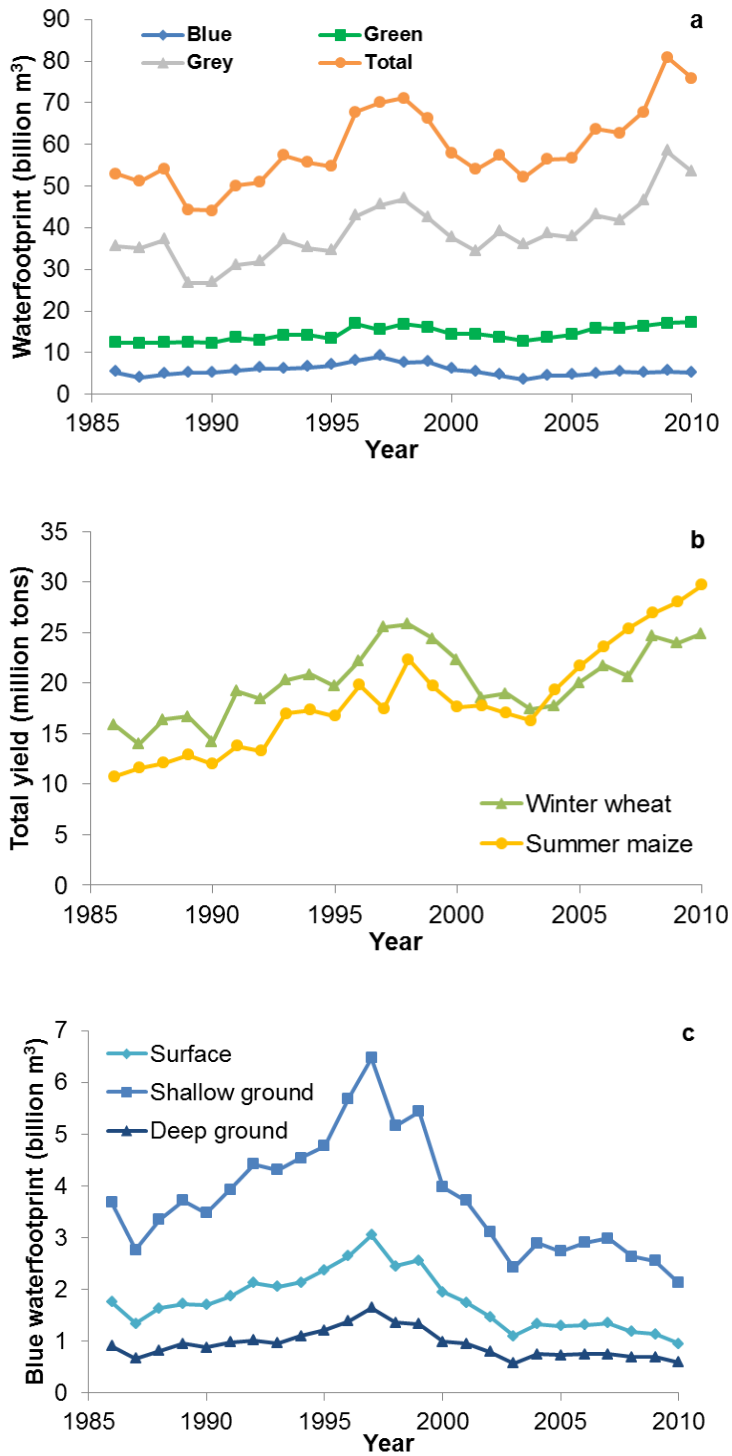

Figure 5.2. Temporal dynamics of different types of water footprint and annual total grain yield from 1986 to 2010. (a) the different types of grain production water footprint; (b) the total annual grain yield; and (c) the different sources of blue water footprint.

Table 5.1. Temporal trend analyses of grain production water footprint from 1986 to 2010 based on regression lines.

	WF_{total}	WF_{blue}	WF_{green}	WF_{grey}
Year	0.843^{***}	-0.021	0.161^{***}	0.703^{***}
	(0.181)	(0.027)	(0.023)	(0.164)
Constant	-1624.341^{***}	47.299	-306.696^{***}	-1364.944^{***}
	(361.346)	(53.088)	(45.378)	(327.980)
F statistics	21.65	0.62	49.89	18.29
R-Squared	0.44	0.01	0.49	0.49
N	25	25	25	25

Notes: Dependent variables are different types of grain production water footprint (10^9 m^3) in average values for the 207 analyzed counties, respectively. Numbers outside and inside parentheses are coefficients and robust standard errors, respectively. * $p < 0.05$; ** $p < 0.01$; *** $p < 0.001$.

Except for annual WF_{blue}, the whole NCP's annual irrigated agriculture WF, WF_{grey}, and WF_{green} increased due to the overall increase of total crop production over time (Figure 5.2b). By comparing Figure 5.2a and Figure 5.2b, it is easy to observe that the temporal dynamics of total crop production (either winter wheat or summer maize) were similar to the dynamics of WF of irrigated agriculture in NCP. The overall temporal dynamics of different sources of WF_{blue} fluctuated (Figure 5.2c).

Irrigated agriculture led to unsustainable water use in all evaluated counties (use intensity > 1 indicates unsustainable use) (Figure 5.3). Among the NCP's 207 counties, 174 counties faced severe water scarcity (use intensity > 2.5 indicates severe water scarcity). Our results show that the average water scarcity for total available water for agricultural use was as high as 10.14, indicating an unsustainable water usage pattern. There were 95.29% counties with water scarcity over 5.0 for total available water for agricultural use. Overall, there were 46.5% of counties with total agricultural water use intensity over 10.0 for grain production, covering almost the entire east of NCP (Figure 5.3).

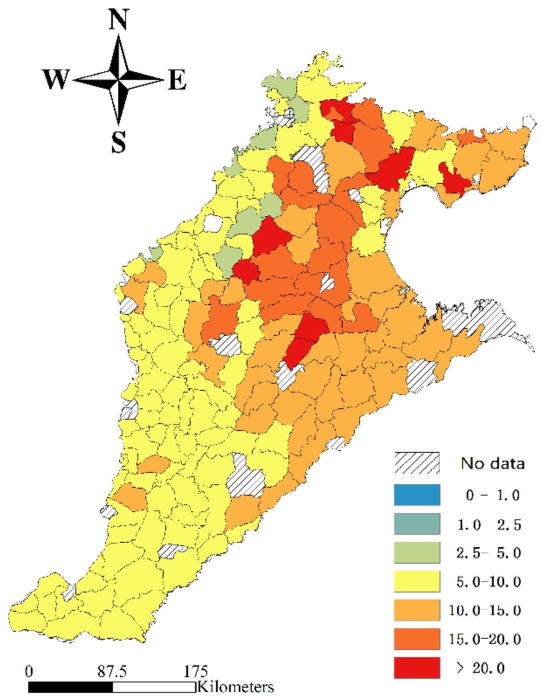

Figure 5.3. Spatial dynamic of water scarcity in irrigated agriculture from the water footprint perspective. Index greater 1 indicates unsustainable water use.

Crop water productivity increased in all counties, suggesting an irony with rising water productivity coupled with severe water scarcity (Figure 5.4-5.5). The average crop water productivity increased from 0.90 kg.m^{-3} in 1986 to 1.94 kg.m^{-3} to 2010. The central and western parts of the NCP had higher crop water productivity while its eastern part had lower crop water productivity. The central part's crop water productivity increased the most, while the eastern crop water productivity increased the least.

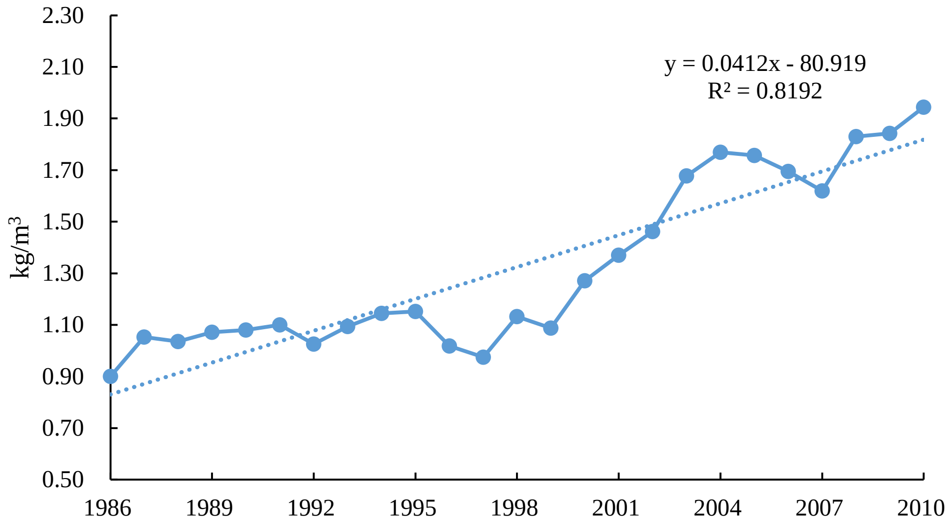

Figure 5.4. Temporal dynamics of average crop water productivity (kg/m^3) in the NCP from 1986 to 2010.

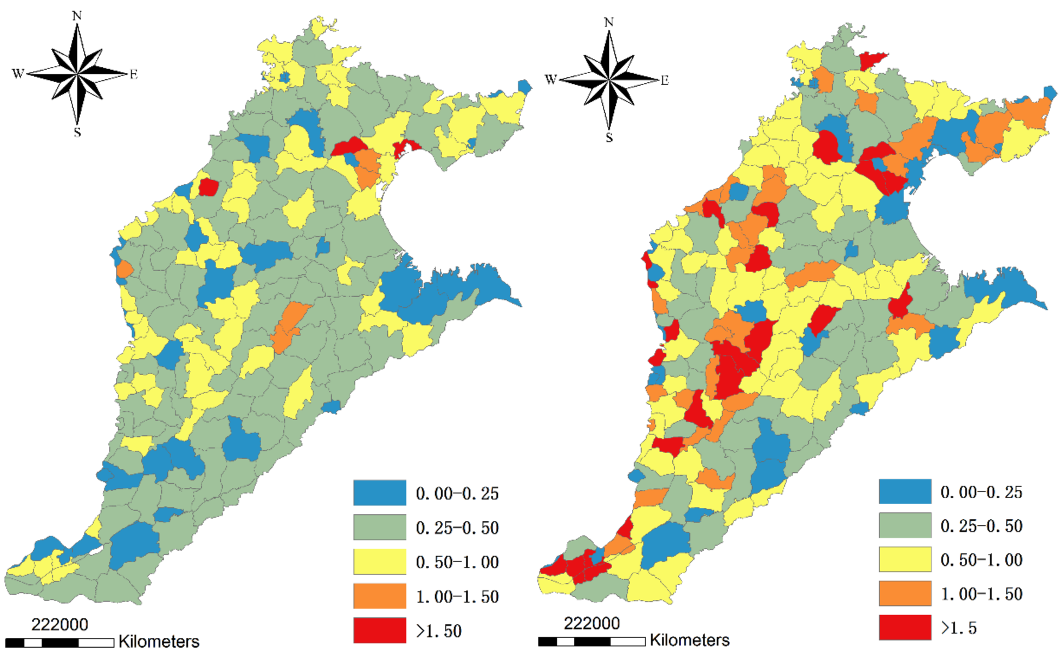

(a) (b)

Figure 5.5. Spatial dynamics of crop water productivity (kg/m^3) in irrigated agriculture from 1986 (a) to 2010 (b).

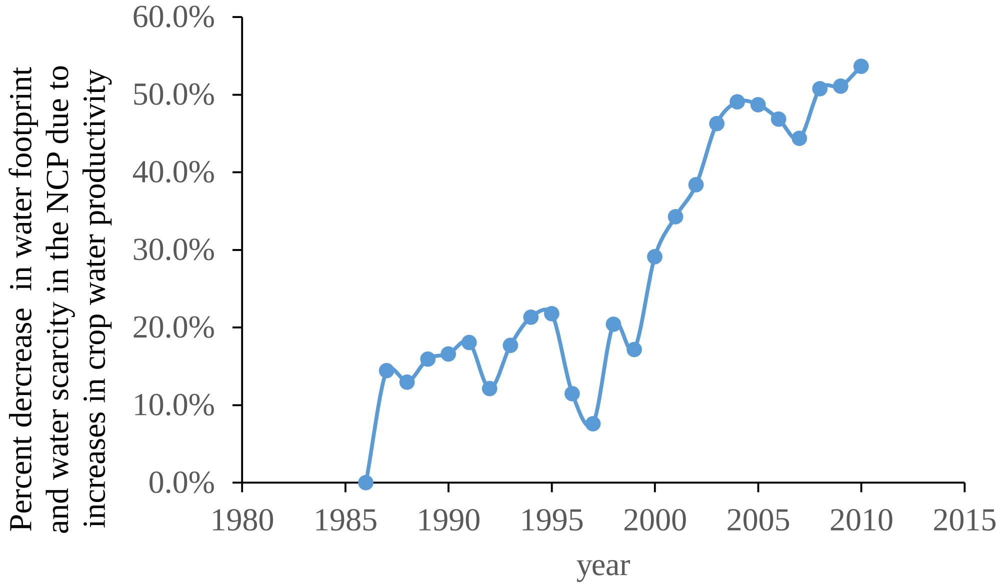

Figure 5.6. Percent decrease in water footprint and water scarcity in the NCP due to increases in crop water productivity from 1986 to 2010.

DISCUSSION

We find the increasing water footprint – worsening water scarcity as crop water productivity increased – in all 207 counties of the North China Plain over 1986-2010. The results show that the improving crop water productivity had increasingly positive influences on reducing WF and water scarcity over time (Figure 6). In 1987, an increase in crop water productivity dropped WF and water scarcity 14.5%, and this number increased to 53.7% in 2010 (Figure 6). However, the total grain production WF was still high and led to unsustainable water use in all evaluated counties. The underlying reasons for the persistence of unsustainable conditions include the soaring grain consumption driven by rapid economic development and a growing national population, extensive decline in cultivation areas in south China (Song, Sun and Dong 2007). With the growing population, an increasing water crisis and anticipated food shortages in the future, the contradiction in irrigated agriculture could be exacerbated, posing threats to national sustainability.

Spatial variations in WF of irrigated agriculture across the NCP reveals hotspot areas requiring special management. For example, the southeast part of the NCP showed higher WF than other parts, therefore, more agricultural water management should be planned for this area. Southeast NCP produced more crops due to its higher accumulated temperature, greater precipitation, and better soil organic matter than other areas in the NCP (Foster et al. 2004). Furthermore, because of its ineffective agricultural production management, excessive fertilization and waste of water, the southeast's WF was much higher than that in other areas of the NCP. On the other hand, the comparatively slow-growing crop productions WF in the central NCP was less than other parts of NCP. Since 1980, the government controls the agricultural production in the central part of the NCP to limit the groundwater exploitation since a groundwater funnel emerged (Wang et al. 2015). Moreover, since the precipitation in the central part of the NCP is smaller than that in other regions, the WF is much smaller.

Water transfer projects such as the South-North Water Transfer Project (Liu and Yang 2012) (SNWTP; the largest water transfer project in the world with a planned total investment of $80 billion USD and annual transfer amount of 48.4 billion m^3 water) has mixed impacts. By transferring physical water from southern China to northern China, the SNWTP can help alleviate the water shortages in northern China and indirectly enhance national food security. But the environmental cost of SNWTP is also large (Yin et al. 2001, Shao, Wang and Wang 2003, Zhang 2009, Liu, Yang and Li 2016). Therefore, for the NCP and China as a whole, the long-term water management strategies should target controlling and reducing total water use by improving water use efficiency rather than constructing more engineering projects to support the seemingly endless demand for water.

There are also many other specific measures to reduce total water consumption from grain production in the NCP. For instance, the total WF of NCP can be reduced by importing grain and other food products from water-abundant countries and reducing the cultivation area in the NCP. One way to reduce total WF is to mitigate WF_{grey}, which is the highest priority since it accounts for a large percentage of the total WF. The primary reasons for high WF_{grey} in the NCP are overuse and low efficiency in applying chemical fertilizers and pesticides. For example, the average per unit area amount of nitrogen applied (545 kg ha^{-1}) in a wheat-maize rotation system in the NCP during 1997-2005 was much higher than the nitrogen output with harvested crops of the system (311 kg ha^{-1}) (Zhao, Chen and Zhang 2009), meaning some nitrogen ended up polluting rather than boosting crop growth. Many studies (Ju et al. 2003, Zhang, Ma and Chen 2006, Zhang 2011) suggest that the applied amount of fertilizers and their use efficiency is negatively correlated, and thus controlling the use of fertilizers and improving their use efficiency are complementary. Using straw, livestock manure, biogas waste, and organic fertilizers instead of chemical fertilizers can not only reduce the applied amount of chemical fertilizers but also increase crop yield in the NCP (Zhang et al. 2006). Many nutrient management techniques, such as balanced fertilization, soil testing and formulated fertilization, application of slow-release fertilizers, and selection of fertilization timing, can also improve the use efficiency (Zhang et al. 2006, Quiñones, Martínez-Alcántara and Legaz 2007, Zhang 2011).

Crop production conditions can be altered (e.g., cultivar, water use efficiency, irrigation and tillage methods) to change the WF. The WF can be reduced by increasing per unit area crop yield or decreasing actual crop evapotranspiration. Field experiments confirm that using high yield cultivar improved crop water productivity and reduced water consumption (Zhang et al. 2010). Many techniques below are also documented to improve water use efficiency and thus reduce actual crop evapotranspiration. Currently, the common irrigation approach in the NCP is still surface irrigation with very low use efficiency of both water and fertilizers. The combination of integrated irrigation and fertilization technique with efficient water-saving irrigation systems (e.g., sprinkler irrigation, micro-irrigation) can reduce surface erosion, retain fertilizers in the crop root zone, mitigate fertilizers leaching into underground (Liu and Kang 2006, Man et al. 2014), and thus reduce both WF_{grey} and WF_{blue}. Research shows that the deficit irrigation approach and appropriate reduction of irrigation times for winter wheat can maintain or only slightly reduce crop yield but largely increase water use efficiency (Yang et al. 2006, Zhang et al. 2008). Covering the soil with straw can reduce soil evaporation while increasing rainfall infiltration and reducing surface runoff (Li et al. 2013). The use of soil tillage and subsoil tillage methods can improve soil moisture holding capacity, reduce ground infiltration, and increase water use efficiency (Salem et al. 2015). Greenhouse agriculture (e.g., covering the field with plastic films is much more common than glass greenhouses in China) also helps reduce water evaporation and water use (Chang et al. 2011).

Our work provides the first detailed and integrated assessment that analyzes water footprint, water scarcity and crop water productivity at the county level in a large plain over long term. It reveals the serious unsustainable water use across all counties in the NCP. The spatial variations of unsustainable water use, water footprint and crop productivity are uncovered. This information can help the government make more holistic and better-targeted policies to manage crop production and water consumption more sustainably in China's major crop production region. Future research can focus on the interactions between irrigated agriculture in the NCP and the environmental and socioeconomic development in the rest of China. Since much of the NCP harvest was transferred to the rest of China to enhance food security, and since much water was diverted from southern China through SNWTP to the NCP to alleviate the water shortage, the interactions between these two systems are complex and have great impacts on both systems. Cross-boundary studies can help get a comprehensive picture of drivers behind water use and thus provide holistic information for policy-making, therefore facilitating sustainable development and improvement of human well-being (Liu 2017, Liu 2018).

CONCLUSIONS

In this paper, we quantified water footprint, crop water productivity, and water scarcity from irrigated agriculture in China's major crop production region, the North China Plain's 207 counties, from 1986 to 2010. Our results indicated that even though crop water productivity grew over time, the water footprint in the NCP due to crop production increased sharply from 53 billion m3 in 1986 to 78 billion m3 in 2010, leading to unsustainable water use in all 207 counties. This study revealed the unsustainable state of irrigated agriculture in China's major crop production region, which has implications for global irrigated agriculture at the county level. The irrigated agriculture increased food security but increased the pressure on water use. There is tremendous pressure on water resources due to a huge food demand on the NCP under the context of a growing national population. Changing high water consumption cropping systems, developing efficient water-saving irrigation technology and reducing cropland area should be considered for the future agricultural management to help ensure water security and food security simultaneously.

CHAPTER 6. CONCLUSIONS

Below are main conclusions and research directions:

We found in Chapter 2 that the volumes of all these flows, except for land flow, increased over time. Financial capital flows increased most (188.9%), followed by flows of CO_2 (59.3%), energy (58.1%), water (50.7%) and nitrogen (10.5%), while land transfer decreased by 8.8%. Volumes of virtual material flows among distant countries were much higher than those among adjacent countries. The top five countries accounted for a surprisingly large proportion (47% to 80%) of total flow volumes. Our results suggest that it is important to pay particular attention to such fast-growing material flows, promote cooperation between distant countries and target countries with the largest flows to achieve global sustainable development goals. This finding also suggests that global trade hubs such as the United States and China dominate global networks. To manage global flows of virtual materials, policy-makers could consider driving forces from these hubs which can exert strong power over global trade dynamics. Safeguarding the environment through sustainable resource use will require a better understanding of the existing international mechanisms and structures of trade networks to target top trading countries.

The results in Chapter 3 unexpectedly showed that more than 40% of provinces gained one kind of resource (either water or energy) through trade at the expense of losing the other kind of internal resource (energy or water), and 20% of provinces suffered a double loss of both water and energy. The remaining provinces gained both water and energy. Surprisingly, approximately 40% of transferred water/energy was from relatively water/energy-scarce provinces to water/energy-abundant provinces, further deepening resource inequality. Overall, virtual water-energy networks tended to enhance each other. Trade largely shaped the nexus relationship between water and energy consumption in provinces. Our study suggests the urgent need to assess multiple virtual resource networks simultaneously in other countries to uncover unintended consequences and to develop cross-sectoral and holistic policies to achieve global sustainability and human well-being. More cooperation between distant areas should be built to deal with common and interrelated challenges. Our driver analysis also revealed that virtual water/energy trade may be motivated more by the demand side rather than by the supply side. Therefore, more demand-side policies should be developed to reduce resource consumption and environmental burden.

In Chapter 4, the total virtual energy transferred from energy-scarce to energy-abundant provinces increased from 43.2% to 47.5% from 2007 to 2012. Especially for virtual oil, its transfer from energy-scarce to energy-abundant provinces grew from 51.5% in 2007 to 54.0% in 2012. Surprisingly, the total virtual energy flowing from west China to east China was much greater than physical energy transferred through the West-To-East Electricity Transmission Project (WTEETP). We hope these findings will assist policymakers in crafting more efficient energy policy, since the current focus on physical energy supplies may overlook potential solutions virtual energy trade that can offer in addressing regional energy deficits. Government's energy management should target specific types of virtual energy, since the flow patterns of different types of energy differed from each other. Especially for the virtual oil, more than half virtual oil was flowed from energy-scarce to energy abundant provinces, which could exacerbate energy shortage and lead to more severe uneven energy distribution.

The results in Chapter 5 show that the irrigated agriculture's annual water footprint in the North China Plain increased over time. All counties faced unsustainable water use - local water consumption was greater than local renewable freshwater – even as the average crop water productivity doubled. The 173 NCP counties suffering severe water scarcity still produced significant crop yield with a high water footprint. This study has implications for exploring potential unsustainable conditions in irrigated agriculture worldwide. The spatial variations of unsustainable water use, water footprint and crop productivity are uncovered. This information can help the government make more holistic and better-targeted policies to manage crop production and water consumption more sustainably in China's major crop production region.

To sum up, in the context of globalization, the distant coupled human and natural systems are becoming more connected than ever before. The mechanisms with one local system cannot be separated from impacts of other systems. This connected world shapes the pattern of global challenges, which in turn affects many parts of the world. Understanding the interactions between telecouplings and global challenges can shed light on policymaking and management, and help achieve global sustainability and human well-being. This dissertation facilitates the comprehensive understanding about how telecouplings interact with global challenges.

Future research directions

How telecouplings at different scales interact with each other requires further exploration. For example, Guangdong Province in southern China received virtual water and energy flow from other provinces and other countries. Guangdong Province's demand for imported water and energy is limited. More import from other provinces indicate less import from other countries, and vice versa. Therefore, virtual resource flow from other provinces can affect and be affected by virtual resource flow from other countries. Studying interactions between telecouplings across different scales can help thoroughly reveal local mechanisms in a global context, and enhance the understanding of distant interactions and efficiency of policies for environmental and socioeconomic sustainability across local to global scales.

APPENDICES

APPENDIX A

SUPPORTING INFORMATION FOR CHAPTER 2

Supplementary Table S1. Code for each country or region

Code	Country/Region Name	Code	Country/Region Name
AUS	Australia	IRL	Ireland
AUT	Austria	ITA	Italy
BEL	Belgium	JPN	Japan
BGR	Bulgaria	KOR	Korea, Rep.
BRA	Brazil	LTU	Lithuania
CAN	Canada	LUX	Luxembourg
CHN	China	LVA	Latvia
CYP	Cyprus	MEX	Mexico
CZE	Czech Republic	MLT	Malta
DEU	Germany	NLD	Netherlands
DNK	Denmark	POL	Poland
ESP	Spain	PRT	Portugal
EST	Estonia	ROU	Romania
FIN	Finland	RUS	Russian Federation
FRA	France	SVK	Slovak Republic
GBR	United Kingdom	SVN	Slovenia
GRC	Greece	SWE	Sweden
HUN	Hungary	TUR	Turkey
SWE	Sweden	TWN	Taiwan, China
IDN	Indonesia	USA	United States
IND	India		

Supplementary Methods: Evaluating interactions between networks.

1. The Pearson correlation index for multiplex networks

Each material flow network is considered as one layer. A first method to investigate layers' correlations in a multiplex framework was proposed by Garlaschelli and applied to the commodity-specific trades (Barigozzi, Fagiolo and Garlaschelli 2010). Garlaschelli extended the Pearson correlation index to the multiplex by averaging over space instead of time. The Pearson correlation index $\rho^{AB}_{>>}$ between the layers A and B (at time t) of which flows going in the same direction will thus be:

$$\rho^{AB}_{>>} = \frac{\sum_{i\neq j}(w^A_{ij}-\mu^A)(w^B_{ij}-\mu^B)}{\sqrt[2]{\sum_{i\neq j}\left(w^A_{ij}-\mu^A\right)^2\left(w^B_{ij}-\mu^B\right)^2}} = \frac{cov_{AB}}{\sigma_A\sigma_B} \qquad (1)$$

It is noteworthy that the above definition of correlation can be applied both to flows going in the same direction (equation 1) and to flows going in opposite directions (equation 2).

$$\rho^{AB}_{><} = \frac{\sum_{i\neq j}(w^A_{ij}-\mu^A)(w^B_{ji}-\mu^B)}{\sqrt[2]{\sum_{i\neq j}\left(w^A_{ij}-\mu^A\right)^2\left(w^B_{ji}-\mu^B\right)^2}} \qquad (2)$$

2. A second correlation measure: multiplexity and multireciprocity

Recently, a more refined measure of correlation across layers in a (weighted) multiplex has been pro- posed (Gemmetto et al. 2016). This measure derives from the extension of concept of reciprocity in weighted networks (see Squartini et al. 2013 (Squartini et al. 2013)) to the context of multiple layers networks, and it is named multiplexity for flows in the same direction and mutireciprocity for flows in opposite direction. Multiplexity reads as follows:

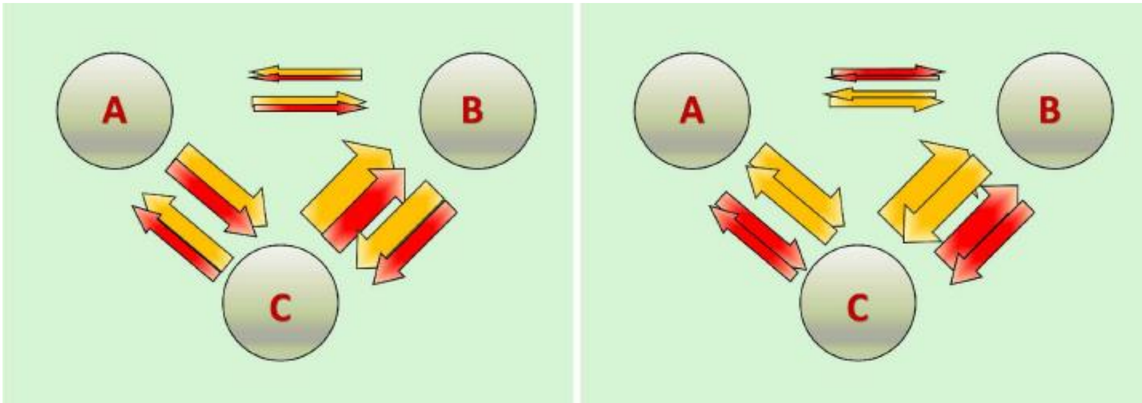

Supplementary Figure S1. Untangling correlation and reciprocity across layers

$$m^{AB} = \frac{2\sum_{i\neq j}\min[w_{ij}^{A}, w_{ij}^{B}]}{\sum_{i\neq j} w_{ij}^{A} + \sum_{i\neq j} w_{ij}^{B}} \qquad (3)$$

and multireciprocity:

$$r^{AB} = \frac{2\sum_{i\neq j}\min[w_{ij}^{A}, w_{ji}^{B}]}{\sum_{i\neq j} w_{ij}^{A} + \sum_{i\neq j} w_{ij}^{B}} \qquad (4)$$

Multiplexity and multireciprocity are both normalized measures, spanning from 0 to 1. In the former case layers A and B never overlap across all the network, in the latter they perfectly overlap and they are perfectly correlated.

A multiplex feature homogeneous layers - same units, or heterogeneous - different units. When a multiplex is heterogeneous all flows are normalized to the relative total flow W and become unit-less (scalar).

Any measure of correlation across layers (inter-layers) is sensitively dependent on the internal topology of each layer (intra-layer). Put it simply: if two layers share the same hubs, any correlation results trivially from the mere overlap the two internal structures. Figure 1 shows, by the means of a very simple and stylized multiplex with three nodes and two layers, to what extent the reciprocity structure within each layer can affect the observed correlation between layers (width of the arrows indicates the intensity of the flows). Prime facie, the red and the yellow layers seem to be very correlated when moving across nodes. Nevertheless, this is due the combined effect of the reciprocity level within each layer and the topology of the multiplex. For instance, node C is a hub in both layers and thus node A and B tend to exchange with C more than between each other.

Measures formalized in equations 3 and 4, differently from measure expressed by equations 2 and 1 permit the inclusion of suitable null models in the analysis and the development of an enhanced measure of correlation, cleaned by the intra-layer topological effects.

In Gemmetto et al. 2016 (Gemmetto et al. 2016), we proposed the following enhanced measure of multiplexity between two generic layers A and B and denoted as μ :

$$\mu^{AB} = \frac{m^{AB} - \langle m^{AB} \rangle}{1 - \langle m^{AB} \rangle} \tag{5}$$

and enhanced multireciprocity ρ:

$$\rho^{AB} = \frac{r^{AB} - \langle r^{AB} \rangle}{1 - \langle r^{AB} \rangle} \tag{6}$$

where

$$\langle m^{AB} \rangle = \frac{\sum_{i \neq j} \langle w_{ij}^{A} \rangle \langle w_{ij}^{B} \rangle}{\sum_{i \neq j} \langle w_{ij}^{A} \rangle \sum_{i \neq j} \langle w_{ij}^{B} \rangle} \tag{7}$$

and

$$\langle r^{AB} \rangle = \frac{\sum_{i \neq j} \langle w_{ij}^{A} \rangle \langle w_{ji}^{B} \rangle}{\sum_{i \neq j} \langle w_{ij}^{A} \rangle \sum_{i \neq j} \langle w_{ji}^{B} \rangle} \tag{8}$$

Where values comprised in <…> denote the expected values assessed over the graph ensembles (null model). Both μ and ρ can be positive or negative, indicating a positive or negative correlation in excess to the random correlation as captured by the null model and score 0 when the two layers are uncorrelated. It is noteworthy that μ and ρ, differently from customary correlation indexes, have no upper or lower limit. Hence, are measures suitable for comparing different networks or trends, but not for assessing the absolute correlation among variables (layers).

3. Null models

A null model is meant to test the statistics significance of results, on the one hand, and to enhance the correlation analysis by clearing them from undesired side effects generated by the complexity of the interactions' structure on the other.

In order to clear correlation measures across layers of the topological effects, we adopt the formalism of Exponential Random Graphs or p∗ models, which allow to obtain maximally random ensembles of networks with specified constraints.

The method is composed by two main steps: the first one is the maximization of the Shannon entropy over a previously chosen set of graphs, φ

$$s = -\sum_{G\in\varphi} P(G)\ln P(G) \tag{9}$$

under a number of imposed constraints (Garlaschelli and Loffredo 2008), generically indicated as

$$\sum_{G\in\varphi} P(G) = 1, \quad \sum_{G\in\varphi} P(G)\pi_a(G) = \langle\pi_a\rangle, \forall a \tag{10}$$

(note the generality of the formalism, above: G can be a directed, undirected, binary or weighted net- work). We can immediately choose the set φ as the grand canonical ensemble of BDNs, i.e. the collection of networks with the same number of nodes of the observed one (say N) and a number of flows, L, varying from zero to the maximum (i.e. N(N − 1)). This prescription leads to the exponential distribution over the previously chosen ensemble

$$P(G|\vec{\theta})=\frac{e^{-H(G,\vec{\theta})}}{Z(\vec{\theta})}, \tag{11}$$

whose coefficients are functions of the Hamiltonian, $H(G, \vec{\theta}) = \sum_a \theta_a \pi_a(G)$, which is the linear combination of the chosen constraints. The normalization constant, $Z(\vec{\theta}) \equiv \sum_{G\in\varphi} e^{-H(G,\vec{\theta})}$, is the partition function (Garlaschelli and Loffredo 2008). The second step prescribes how to numerically evaluate the unknown Lagrange multipliers θ_a. Let us consider the log-likelihood function $\ln\vartheta(\vec{\theta}) = \ln P(G|\vec{\theta})$ and maximize it with respect to the unknown parameters. In other words, we have to find the value $\vec{\theta}^*$ of the multipliers satisfying the system

$$\frac{\partial \ln\vartheta(\vec{\theta})}{\partial\theta_a}\bigg|_{\vec{\theta}^*}=0, \forall a \tag{12}$$

or, that is the same,

$$\pi_a(G) = \langle\pi_a\rangle(\vec{\theta}^*) = \langle\pi_a\rangle^*, \forall a \tag{13}$$

i.e. a list of equations imposing the value of the expected parameters to be equal to the observed one. Note that the term “expected”, here, refers to the weighted average taken on the grand canonical ensemble, the weights being the probability coefficients defined above. So, once the unknown parameters have been found, it is possible to evaluate the expected value of any other topological quantity of interest, $\langle X\rangle^*$:

$$\langle X\rangle^* = \sum_{G\epsilon\varphi} X(G)P(G|\vec{\theta}^*) \tag{14}$$

Because of the difficulty to analytically calculate the expected value of the quantities commonly used in complex networks theory, it is often necessary to rest upon the linear approximation method: $\langle X \rangle \cong X(\langle G \rangle^*)$, where $\langle G \rangle^*$ indicates the expected adjacency matrix, whose elements are $\langle a_{ij} \rangle^* = p_{ij}^*$. This is a very general prescription, valid for binary, weighted, undirected or directed networks: since the WTW has been considered in its binary, directed representation, the generic adjacency matrix G will be indicated, from now on, with the usual letter A. For the weighted directed version of the WTW, a very useful null model is the weighted directed configuration model (WDCM), that imposes the in and out strength sequence for every node (that is, the import and export sequence for every layer). The Hamiltonian will thus be:

$$H_{WDCM}=\sum_i (a_i s_i^{in} + \beta_i s_i^{out}) = \sum_{i \neq j} (a_j + \beta_i) w_{ij} \quad (15)$$

4 Z-score and statistical validation

The transformed quantities defined in equation 5 and 6 capture the similarity (correlation) between layers in a multiplex by comparing the empirical values with the expected values under a null model (the WDCM, equation 15). However, those quantities do not consider any information about the variances of the values of multiplexity and multireciprocity under the null model, thus giving no direct information about statistical significance. Given the absence of any parametric scale, it is difficult to untangle weak interlayer dependencies from pure noise. Put it simply, if 0 signals that two layers are uncorrelated, what is the band of decimal values that are acceptable (i.e. significant) under the constraints we imposed? Moreover, the random fluctuations around the expectation values will in general differ for different pairs of layers, making our choice even more difficult and arbitrary. A way to solve this problem is to accept only those values that exceed a given number (threshold) of standard deviations of the mean value, more formally, for the multiplexity:

$$\mathrm{Z}(m^{AB}) = \frac{m^{AB} - \langle m^{AB} \rangle}{\sqrt{\left\langle \left(m^{AB}\right)^2 \right\rangle - \langle m^{AB} \rangle^2}} \tag{16}$$

and for the multireciprocity:

$$\mathrm{Z}(r^{AB}) = \frac{r^{AB} - \langle r^{AB} \rangle}{\sqrt{\left\langle \left(r^{AB}\right)^2 \right\rangle - \langle r^{AB} \rangle^2}} \tag{17}$$

For the explicit analytical expressions for these z see Gemmetto et al. 2016 (Gemmetto et al. 2016). The z-scores have the same signs as the corresponding quantities (see Gemmetto et al. 2016 (Gemmetto et al. 2016) for demonstration), but in addition they allow us to test for statistical significance using, e.g., a threshold of $Z_C = 1$ as in our case.

APPENDIX B

SUPPORTING INFORMATION FOR CHAPTER 5

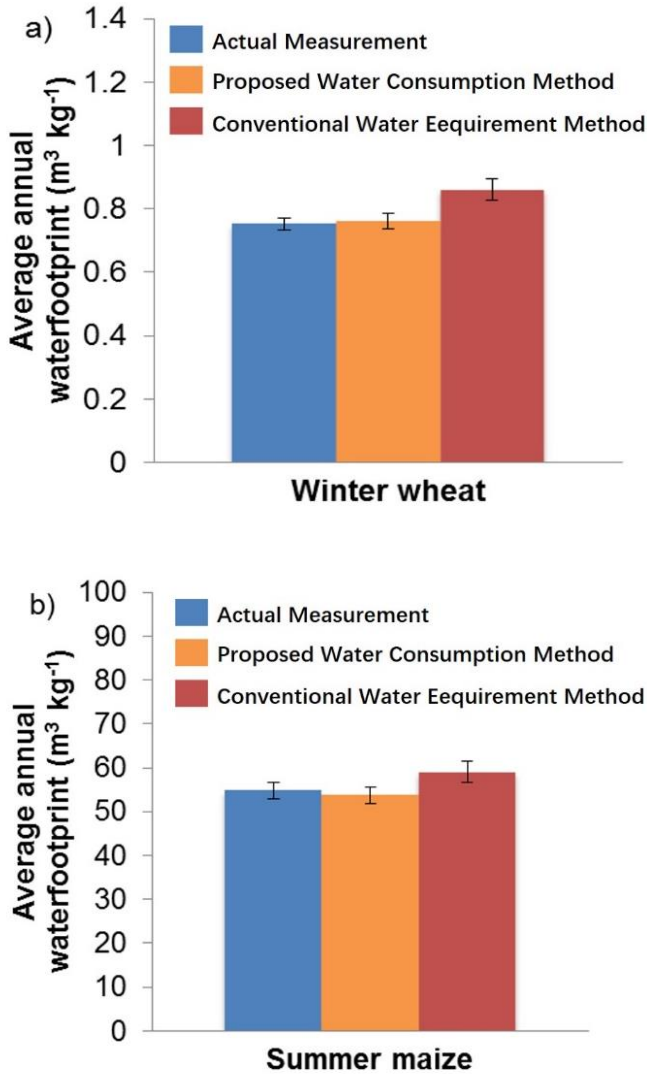

Supplementary Figure S2. Estimation results from water consumption method and water requirement method in comparison to actual measurement of water use at the Luancheng Agro-Eco-Experimental Station. The study periods range from 1986 to 2007 for winter wheat and 1986 to 2009 for summer maize, respectively. The error bars indicate standard errors.

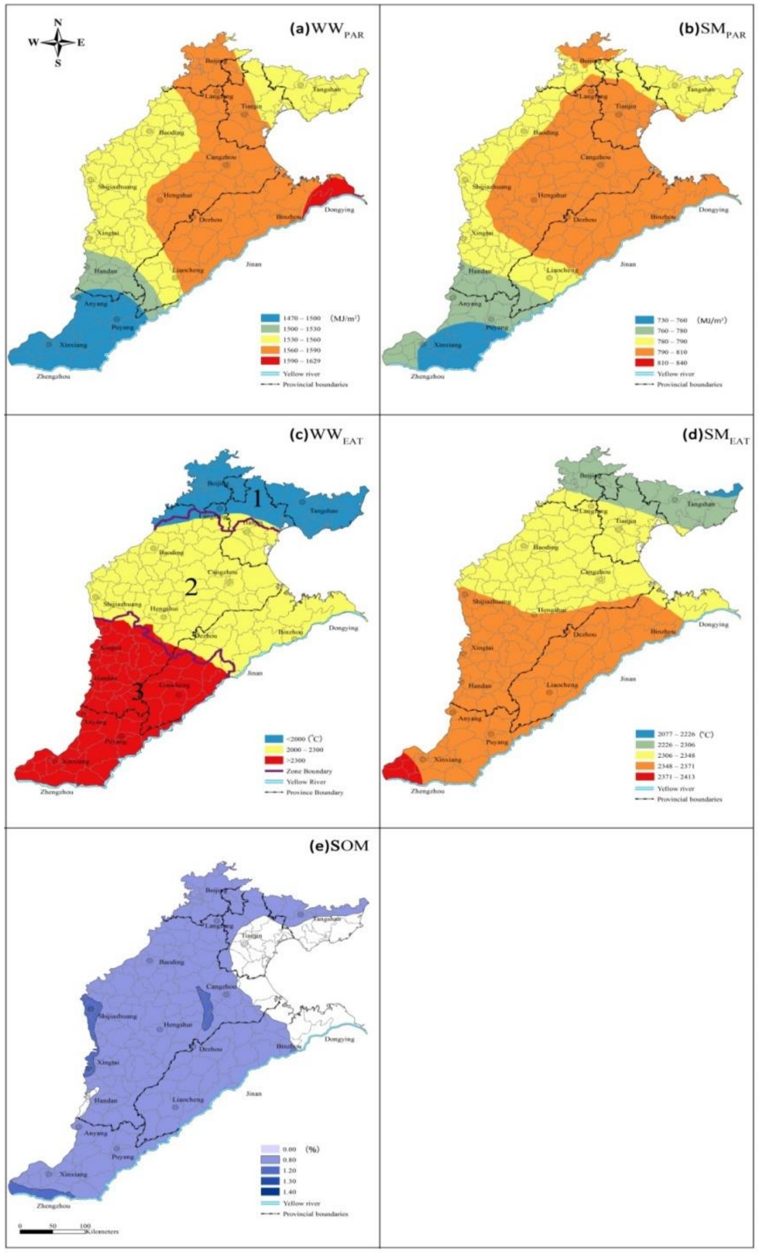

Supplementary Figure S3. Spatial patterns of agricultural factors that influence crop water consumption function (CWPF). WW stands for winter wheat, whose growth period is from September 25th to June 10th of the next year. SM stands for summer maize, whose growth period is from June 20th to September 20th. PAR stands for photo synthetically active radiation. EAT stands for effective accumulated temperature. SOM stands for soil organic matter. The multiple-year average values from 1986 to 2010 are displayed.

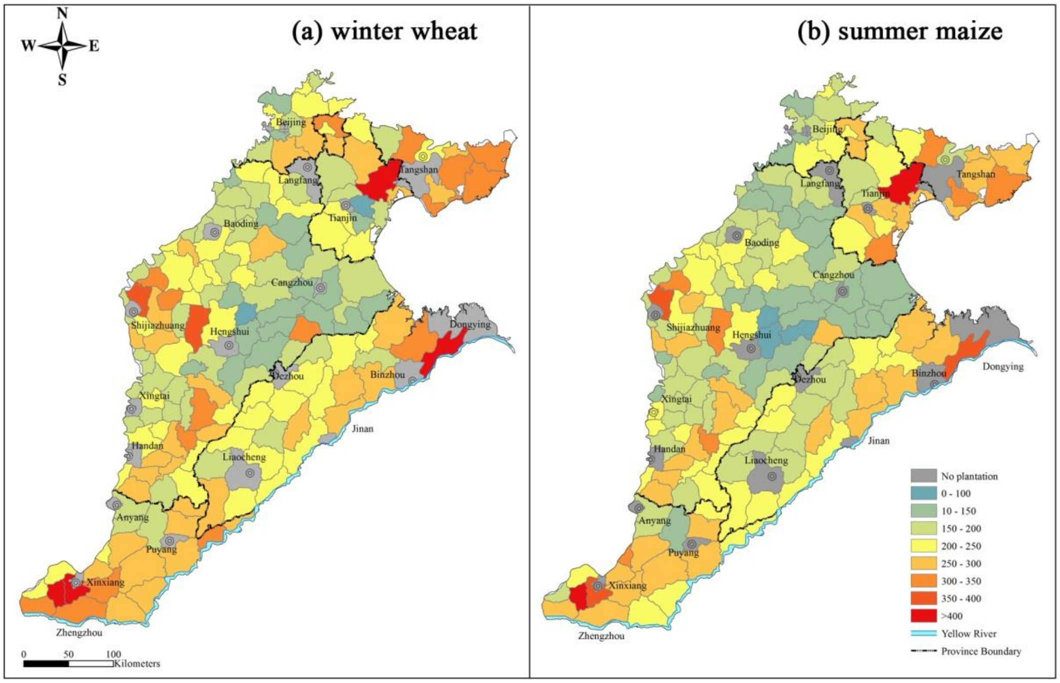

Supplementary Figure S4. Spatial patterns of per hectare application amount of nitrogenous fertilizers for winter wheat and summer maize.

Supplementary Methods.

Crop Water Production Function (CWPF) is the mathematical expression that describes the relationship between water use and crop production for a certain kind of crop. The function is mainly influenced by sunshine and heat factors such as photo synthetically active radiation and effective accumulated temperature, and agricultural production factors such as soil organic matter, crop types and varieties (Kang 2007). In the North China Plain (NCP), annual average photo synthetically active radiation ranges from 2290 to 2524 MJ m^{-2}. The effective accumulated temperature (EAT) of winter wheat and summer maize during their whole growth periods are 1298-2605 □ and 2077-2413 □, respectively. Soil organic matter in 82.90% of the area is between 0.5% and 1% (Supplementary Figure S3). These numbers suggest that for winter wheat there is only big difference of the EAT while little variation in other production factors. Thus, we divided the total plantation area of winter wheat into three zones based on the EAT (Supplementary Figure S3) and used different CWPFs to improve the estimation accuracy. Because the spatial distribution of EAT did not exactly match the administrative boundaries of counties, the EAT for the majority of a country's land area was used. For summer maize, given there is little variation for all production factors affecting the CWPF, the same CWPF was used for all counties for a certain year.

Meanwhile, the CWPF may vary in a long period due to changes in crop variety (e.g., drought resistance, unit area yield). In addition, data of CWPF may not be available every year. For this study, for winter wheat, we obtained CWPF data in years 1986 (Duan 2004) and 2007 (Zhao 2010) for zone 1, in years 1990 (Wang et al. 2001) and 2003(Zhang et al. 2008) for zone 2, and in years 1986 (Duan 2004) and 2008 (Kang, Yang and Pei 2013) for zone 3, respectively. For summer maize, we acquired CWPF data in years 1984 (Duan 2004), 2000 (Pei et al. 2004), and 2008 (Kang et al. 2013). Based on the obtained CWPF data in each two-consecutive time point, we then estimated the corresponding CWPF for each year with the assumption that the increment of crop yield per unit volume water consumption is equal across years.

In order to test the accuracy of the two methods, we took the measured data(Zhang et al. 2008) of ET_c (from Luancheng Agro-Eco-Experimental Station of the Chinese Academy of Sciences, which is located in the northern part of NCP.) to compare with data of ET_c calculated from CWPF method and water requirement method. We mapped a scatter diagram with a y-axis of CWPF method and water requirement method, an x-axis of the measured data of ET_c. The measured data is form 1986-2009 for summer maize and 1986-2007 for winter wheat. For both methods, the more discrete degree of the points, the less accuracy of the method.

‘

REFERENCES

REFERENCES

Ashraf Vaghefi, S., K. C. Abbaspour, M. Faramarzi, R. Srinivasan & J. G. Arnold (2017) Modeling crop water productivity using a coupled SWAT–MODSIM model. *Water,* 9**,** 157.

Barigozzi, M., G. Fagiolo & D. Garlaschelli (2010) Multinetwork of international trade: A commodity-specific analysis. *Physical Review E,* 81**,** 046104.

Bergstrand, J. H. (1985) The gravity equation in international trade: some microeconomic foundations and empirical evidence. *The review of economics and statistics***,** 474-481.

Census, T. S. C. L. G. O. o. S. C. E. 2008. *Chinese Economic Census Yearbook*. Beijing: China Statistic Press.

Chang, J., X. Wu, A. Q. Liu, Y. Wang, B. Xu, W. Yang, L. A. Meyerson, B. J. Gu, C. H. Peng & Y. Ge (2011) Assessment of net ecosystem services of plastic greenhouse vegetable cultivation in China. *Ecological Economics,* 70**,** 740-748.

Chapagain, A. K. & A. Y. Hoekstra. 2003. Virtual water flows between nations in relation to trade in livestock and livestock products. UNESCO-IHE Delft, The Netherlands.

Chapagain, A. K., A. Y. Hoekstra, H. H. G. Savenije & R. Gautam (2006) The water footprint of cotton consumption: An assessment of the impact of worldwide consumption of cotton products on the water resources in the cotton producing countries. *Ecological Economics,* 60**,** 186-203.

Chen, B., J. Li, X. Wu, M. Han, L. Zeng, Z. Li & G. Chen (2018) Global energy flows embodied in international trade: A combination of environmentally extended input–output analysis and complex network analysis. *Applied Energy,* 210**,** 98-107.

Chen, W., H. Li & Z. Wu (2010) Western China energy development and west to east energy transfer: Application of the Western China Sustainable Energy Development Model. *Energy Policy,* 38**,** 7106-7120.

Chen, W., S. Wu, Y. Lei & S. Li (2017) Interprovincial transfer of embodied energy between the Jing-Jin-Ji area and other provinces in China: A quantification using interprovincial input-output model. *Science of the Total Environment,* 584**,** 990-1003.

Chen, Z., J.-N. Wang, G.-X. Ma & Y.-S. Zhang (2013) China tackles the health effects of air pollution. *The Lancet,* 382**,** 1959-1960.

Cherniwchan, J., B. R. Copeland & M. S. Taylor (2016) Trade and the Environment: New Methods, Measurements, and Results. *Annual Review of Economics*.

Conway, D., E. A. Van Garderen, D. Deryng, S. Dorling, T. Krueger, W. Landman, B. Lankford,

K. Lebek, T. Osborn & C. Ringler (2015) Climate and southern Africa's water–energy–food nexus. *Nature Climate Change,* 5**,** 837.

Crippa, M., G. Janssens-Maenhout, F. Dentener, D. Guizzardi, K. Sindelarova, M. Muntean, R. Van Dingenen & C. Granier (2016) Forty years of improvements in European air quality: regional policy-industry interactions with global impacts. *Atmospheric Chemistry and Physics,* 16**,** 3825-3841.

Crompton, P. & Y. Wu (2005) Energy consumption in China: past trends and future directions. *Energy Economics,* 27**,** 195-208.

Cui, L.-B., P. Peng & L. Zhu (2015) Embodied energy, export policy adjustment and China's sustainable development: A multi-regional input-output analysis. *Energy,* 82**,** 457-467.

Dabrowski, J., E. Masekoameng & P. Ashton (2009) Analysis of virtual water flows associated with the trade of maize in the SADC region: importance of scale. *Hydrology and Earth System Sciences,* 13**,** 1967-1977.

Dalin, C., N. Hanasaki, H. Qiu, D. L. Mauzerall & I. Rodriguez-Iturbe (2014) Water resources transfers through Chinese interprovincial and foreign food trade. *Proceedings of the National Academy of Sciences,* 111**,** 9774-9779.

Dalin, C., M. Konar, N. Hanasaki, A. Rinaldo & I. Rodriguez-Iturbe (2012) Evolution of the global virtual water trade network. *Proceedings of the National Academy of Sciences,* 109**,** 5989-5994.

Dalin, C., M. Konar, N. Hanasaki, A. Rinaldo & I. Rodriguez-Iturbe (2012) Evolution of the global virtual water trade network. *Proc Natl Acad Sci U S A,* 109**,** 5989-94.

Dalin, C., Y. Wada, T. Kastner & M. J. Puma (2017) Groundwater depletion embedded in international food trade. *Nature,* 543**,** 700-704.

Damkjaer, S. & R. Taylor (2017) The measurement of water scarcity: Defining a meaningful indicator. *Ambio,* 46**,** 513-531.

Döll, P. (2009) Vulnerability to the impact of climate change on renewable groundwater resources: a global-scale assessment. *Environmental Research Letters,* 4**,** 035006.

Duan, A. W. 2004. *Irrigation water quota of main crops in North China*. Beijing: China Agricultural Science and Technology Press.

Duarte, R., V. Pinilla & A. Serrano (2018) Factors driving embodied carbon in international trade: a multiregional input–output gravity model. *Economic Systems Research,* 30**,** 545-566.

Erisman, J. W., J. N. Galloway, S. Seitzinger, A. Bleeker, N. B. Dise, A. R. Petrescu, A. M. Leach & W. de Vries (2013) Consequences of human modification of the global nitrogen cycle.

Phil. Trans. R. Soc. B, 368**,** 20130116.

Evans, A. 2009. *The feeding of the nine billion: global food security for the 21st century*. Chatham Historical Society Incorporated.

FAO. 2016. FAOSTAT.

Feng, K., S. J. Davis, L. Sun, X. Li, D. Guan, W. Liu, Z. Liu & K. Hubacek (2013) Outsourcing CO2 within China. *Proceedings of the National Academy of Sciences,* 110**,** 11654-11659.

Foley, J. A., R. DeFries, G. P. Asner, C. Barford, G. Bonan, S. R. Carpenter, F. S. Chapin, M. T. Coe, G. C. Daily & H. K. Gibbs (2005) Global consequences of land use. *science,* 309**,** 570-574.

Food and Agriculture Organization of the United Nations (2018) http://www.fao.org/nr/water/aquastat/water_use/index.stm.

Forbes, K. J. & F. E. Warnock (2012) Capital flow waves: Surges, stops, flight, and retrenchment. *Journal of International Economics,* 88**,** 235-251.

Foster, S., H. Garduno, R. Evans, D. Olson, Y. Tian, W. Zhang & Z. Han (2004) Quaternary aquifer of the North China Plain—assessing and achieving groundwater resource sustainability. *Hydrogeology Journal,* 12**,** 81-93.

Frankel, J. A. (2009) Environmental effects of international trade.

Garlaschelli, D. & M. I. Loffredo (2008) Maximum likelihood: Extracting unbiased information from complex networks. *Physical Review E,* 78**,** 015101.

Gemmetto, V., T. Squartini, F. Picciolo, F. Ruzzenenti & D. Garlaschelli (2016) Multiplexity and multireciprocity in directed multiplexes. *Physical Review E,* 94**,** 042316.

Godfray, H. C. J., J. R. Beddington, I. R. Crute, L. Haddad, D. Lawrence, J. F. Muir, J. Pretty, S. Robinson, S. M. Thomas & C. Toulmin (2010) Food security: the challenge of feeding 9 billion people. *Science,* 327**,** 812-818.

Hoekstra, A. & P. Hung. 2002. A Quantification of Virtual Water Flows Between Nations in Relation to International Crop Trade.–Value of Water Research Report Series 11. Delft.

Hoekstra, A. Y. & M. Mekonnen (2011) Global water scarcity: The monthly blue water footprint compared to blue water availability for the world's major river basins.

Hoekstra, A. Y. & M. M. Mekonnen (2012) The water footprint of humanity. *Proc Natl Acad Sci U S A,* 109**,** 3232-7.

Hu, H. J., X. M. Wu & C. W. Qi (2017) Using Multi-objective Optimization to Restructure

Agriculture with Consideration of the Constrains on Groundwater Extraction: Taking Hengshui as an Example. *Journal of Irrigation and Drainage,* 10, 95-99.

International Energy Agency. 2015. World energy outlook 2015. Vienna: IEA.

Jaramillo, F. & G. Destouni (2015) Local flow regulation and irrigation raise global human water consumption and footprint. *Science,* 350, 1248-1251.

Ji, Q., H.-Y. Zhang & Y. Fan (2014) Identification of global oil trade patterns: an empirical research based on complex network theory. *Energy Conversion and Management,* 85, 856-865.

Ju, X., J. Pan, X. Liu & F. Zhang (2003) Study on the fate of nitrogen fertilizer in winter wheat/summer maize rotation system in Beijing suburban. *Plant Nutrition and Fertilizing Science,* 9, 264-270.

Kampa, M. & E. Castanas (2008) Human health effects of air pollution. *Environmental pollution,* 151, 362-367.

Kan, S., B. Chen, X. Wu, Z. Chen & G. Chen (2019) Natural gas overview for world economy: From primary supply to final demand via global supply chains. *Energy Policy,* 124, 215-225.

Kander, A., M. Jiborn, D. D. Moran & T. O. Wiedmann (2015) National greenhouse-gas accounting for effective climate policy on international trade. *Nature Climate Change,* 5, 431-435.

Kang, S. 2007. *Introduction to agricultural water and soil engineering*. Beijing: China Agricultural Science and Technology Press.

Kang, S., J. Yang & Y. Pei. 2013. Farmland water cycle and high-efficient water use mechanism in agriculture of the Haihe River Basin. 329. Beijing: Science Press.

Kang, S., J. Yang & Y. Pei. 2013. *Farmland water cycle and high-efficient water use mechanism in agriculture of the Haihe River Basin*. Beijing: Science Press.

Konar, M., C. Dalin, S. Suweis, N. Hanasaki, A. Rinaldo & I. Rodriguez-Iturbe (2011) Water for food: The global virtual water trade network. *Water Resources Research,* 47.

Konar, M., C. Dalin, S. Suweis, N. Hanasaki, A. Rinaldo & I. Rodriguez-Iturbe (2011) Water for food: The global virtual water trade network. *Water Resources Research,* 47.

Lamastra, L., P. P. Miglietta, P. Toma, F. De Leo & S. Massari (2017) Virtual water trade of agri-food products: Evidence from italian-chinese relations. *Science of the Total Environment,* 599, 474-482.

Lambin, E. F. & P. Meyfroidt (2011) Global land use change, economic globalization, and the looming land scarcity. *Proceedings of the National Academy of Sciences,* 108**,** 3465-3472.

Lenzen, M., D. Moran, K. Kanemoto, B. Foran, L. Lobefaro & A. Geschke (2012) International trade drives biodiversity threats in developing nations. *Nature,* 486**,** 109-112.

Lenzen, M., D. Moran, K. Kanemoto, B. Foran, L. Lobefaro & A. Geschke (2012) International trade drives biodiversity threats in developing nations. *Nature,* 486**,** 109-12.

Li, S., Z. Wang, S. Li, Y. Gao & X. Tian (2013) Effect of plastic sheet mulch, wheat straw mulch, and maize growth on water loss by evaporation in dryland areas of China. *Agricultural Water Management,* 116**,** 39-49.

Liu, G., M. Casazza, X. Tian, Y. Zhang, Y. Hao, L. Zhang, S. Liang & B. F. Giannetti (2017) Tracing the inter-regional coal flows and environmental impacts in Jing-Jin-Ji region. *Ecological Modelling,* 364**,** 98-112.

Liu, H.-J. & Y. Kang (2006) Effect of sprinkler irrigation on microclimate in the winter wheat field in the North China Plain. *Agricultural water management,* 84**,** 3-19.

Liu, J. (2014) Forest sustainability in China and implications for a telecoupled world. *Asia & the Pacific Policy Studies,* 1**,** 230-250.

--- (2017) Integration across a metacoupled world. *Ecology and Society,* 22.

--- (2018) An integrated framework for achieving Sustainable Development Goals around the world. *Ecol. Econ. Soc.,* 1**,** 11-17.

Liu, J., T. Dietz, S. R. Carpenter, M. Alberti, C. Folke, E. Moran, A. N. Pell, P. Deadman, T. Kratz & J. Lubchenco (2007) Complexity of coupled human and natural systems. *science,* 317**,** 1513-1516.

Liu, J., V. Hull, M. Batistella, R. DeFries, T. Dietz, F. Fu, T. W. Hertel, R. C. Izaurralde, E. F. Lambin, S. Li, L. A. Martinelli, W. J. McConnell, E. F. Moran, R. Naylor, Z. Ouyang, K. R. Polenske, R. Anette, G. d. M. Rocha, C. S. Simmons, P. H. Verburg, P. M. Vitousek, F. Zhang & C. Zhu (2013) Framing sustainability in a telecoupled world. *Ecology and Society,* 18.

Liu, J., V. Hull, H. C. J. Godfray, D. Tilman, P. Gleick, H. Hoff, C. Pahl-Wostl, Z. Xu, M. G. Chung, J. Sun & S. Li (2018) Nexus approaches to global sustainable development. *Nature Sustainability,* 1**,** 466.

Liu, J., V. Hull, H. C. J. Godfray, D. Tilman, P. Gleick, H. Holger, C. Pahl-Wostl, Z. Xu, M. G. Chung, J. Sun & S. Li (2018) Nexus Appraoches to Global Sustainable Development. *Nature Sustainability,* in press.

Liu, J., V. Hull, J. Luo, W. Yang, W. Liu, A. Viña, C. Vogt, Z. Xu, H. Yang & J. Zhang (2015)

Multiple telecouplings and their complex interrelationships. *Ecology and Society,* 20, 44.

Liu, J., H. Mooney, V. Hull, S. J. Davis, J. Gaskell, T. Hertel, J. Lubchenco, K. C. Seto, P. Gleick, C. Kremen & S. Li (2015) Systems integration for global sustainability. *Science,* 347, 1258832.

Liu, J., A. Viña, W. Yang, S. Li, W. Xu & H. Zheng (2018) China's Environment on a Metacoupled Planet. *Annual Review of Environment and Resources,* 43, 1-34.

Liu, J. & W. Yang (2012) Water Sustainability for China and Beyond. *Science,* 337, 649-650.

Liu, J., W. Yang & S. Li (2016) Framing ecosystem services in the telecoupled Anthropocene. *Frontiers in Ecology and the Environment,* 14, 27-36.

Liu, J., A. J. Zehnder & H. Yang (2009) Global consumptive water use for crop production: The importance of green water and virtual water. *Water Resources Research,* 45, W05428.

Liu, J., D. Zhao, P. Gerbens-Leenes & D. Guan (2015) China's rising hydropower demand challenges water sector. *Scientific reports,* 5, 11446.

Liu, J. G., W. Yang & S. X. Li (2016) Framing ecosystem services in the telecoupled Anthropocene. *Frontiers in Ecology and the Environment,* 14, 27-36.

Liu, S. H., W. Q. Cheng & S. G. Song (2008) Development Trend and Prospect of Agricultural Water Saving Irrigation in the Mountainous area of Hebei Province. *Water saving irrigation,* 5, 47-50.

Lu, Y., A. Jenkins, R. C. Ferrier, M. Bailey, I. J. Gordon, S. Song, J. Huang, S. Jia, F. Zhang & X. Liu (2015) Addressing China's grand challenge of achieving food security while ensuring environmental sustainability. *Science Advances,* 1, e1400039.

Ma, H. & L. Oxley. 2012. *China's Energy Economy: Situation, Reforms, Behavior, and Energy Intensity*. Springer Science & Business Media.

Man, J., J. Yu, P. J. White, S. Gu, Y. Zhang, Q. Guo, Y. Shi & D. Wang (2014) Effects of supplemental irrigation with micro-sprinkling hoses on water distribution in soil and grain yield of winter wheat. *Field Crops Research,* 161, 26-37.

Maris, S., M. Teira-Esmatges, A. Arbonés & J. Rufat (2015) Effect of irrigation, nitrogen application, and a nitrification inhibitor on nitrous oxide, carbon dioxide and methane emissions from an olive (Olea europaea L.) orchard. *Science of the Total Environment,* 538, 966-978.

Mekonnen, M. M. & A. Y. Hoekstra. 2011. National water footprint accounts: the green, blue and grey water footprint of production and consumption. In *Value of Water Research Report Series No.50*. UNESCO-IHE.

Mekonnen, M. M. & A. Y. Hoekstra (2016) Four billion people facing severe water scarcity. *Science Advances,* 2**,** e1500323.

Meyfroidt, P., T. K. Rudel & E. F. Lambin (2010) Forest transitions, trade, and the global displacement of land use. *Proceedings of the National Academy of Sciences,* 107**,** 20917-20922.

Mi, Z., J. Meng, D. Guan, Y. Shan, M. Song, Y.-M. Wei, Z. Liu & K. Hubacek (2017) Chinese CO 2 emission flows have reversed since the global financial crisis. *Nature communications,* 8**,** 1712.

Miglietta, P. P., D. Morrone & F. De Leo (2018) The Water Footprint Assessment of Electricity Production: An Overview of the Economic-Water-Energy Nexus in Italy. *Sustainability,* 10**,** 228.

Ministry of water resources of China (2007) Water Resource Bulletin (in Chinese). *(China Water Power Press, Beijing)*.

---. 2014. General plan for development of water saving and reduction of water exploitation and high efficient water saving irrigation in North China (2014-2018); http://www.jsgg.com.cn/Index/Display.asp?NewsID=20209.

Morrison, W. M. (2014) CHINA'S ECONOMIC RISE: HISTORY, TRENDS, CHALLENGES, AND IMPLICATIONS FOR THE UNITED STATES*. *Current Politics and Economics of Northern and Western Asia,* 23**,** 493.

Mubako, S., S. Lahiri & C. Lant (2013) Input–output analysis of virtual water transfers: Case study of California and Illinois. *Ecological Economics,* 93**,** 230-238.

National Bureau of Statistics, P. s. R. o. C. 2008. *China Energy Statistical Yearbook 2007 (in Chinese)*. Beijing: China Statiscs Press.

National Development and Reform Commission of the People's Republic of China. 2013. China's Policies and Actions for Addressing Climate Change-the Progress Report 2013. National Development and Reform Commission Beijing.

Novo, P., A. Garrido & C. Varela-Ortega (2009) Are virtual water “flows” in Spanish grain trade consistent with relative water scarcity? *Ecological Economics,* 68**,** 1454-1464.

Oita, A., A. Malik, K. Kanemoto, A. Geschke, S. Nishijima & M. Lenzen (2016) Substantial nitrogen pollution embedded in international trade. *Nature Geoscience,* 9**,** 111-115.

Pei, D., S. Chen, X. Zhang, Y. Gao & Y. Wang (2004) Optimized irrigation scheduling for maize in the piedmont of Mt. Taihang of the North China Plain. *Chinese Journal of Eco-Agriculture,* 12**,** 144-147.

Peters, G. P. 2010. Policy update: Managing carbon leakage. Taylor & Francis.

Peters, G. P., J. C. Minx, C. L. Weber & O. Edenhofer (2011) Growth in emission transfers via international trade from 1990 to 2008. *Proceedings of the National Academy of Sciences,* 108**,** 8903-8908.

Pietz, D. A. 2015. *The Yellow River: the problem of water in modern China*. Harvard University Press.

Provincial Water Resources Bureau. 2007. *Water Resource Bulletin (in Chinese)*. Beijing: China Water Power Press.

Qiang, W., A. Liu, S. Cheng, T. Kastner & G. Xie (2013) Agricultural trade and virtual land use: The case of China's crop trade. *Land Use Policy,* 33**,** 141-150.

Qin, W., D. Wang, X. Guo, T. Yang & O. Oenema (2015) Productivity and sustainability of rainfed wheat-soybean system in the North China Plain: results from a long-term experiment and crop modelling. *Scientific Reports,* 5**,** 17514.

Quiñones, A., B. Martínez-Alcántara & F. Legaz (2007) Influence of irrigation system and fertilization management on seasonal distribution of N in the soil profile and on N-uptake by citrus trees. *Agriculture, ecosystems & environment,* 122**,** 399-409.

Raskin, P. D., E. Hansen & R. M. Margolis. 1996. Water and sustainability: Global patterns and long-range problems. In *Natural Resources Forum*, 1-15. Wiley Online Library.

Rudel, T. K., L. Schneider, M. Uriarte, B. L. Turner, R. DeFries, D. Lawrence, J. Geoghegan, S. Hecht, A. Ickowitz & E. F. Lambin (2009) Agricultural intensification and changes in cultivated areas, 1970–2005. *Proceedings of the National Academy of Sciences,* 106**,** 20675-20680.

Rulli, M. C., D. Bellomi, A. Cazzoli, G. De Carolis & P. D'Odorico (2016) The water-land-food nexus of first-generation biofuels. *Scientific Reports,* 6.

Ruzzenenti, F., A. Joseph, E. Ticci, P. Vozzella & G. Gabbi (2015) Interactions between financial and environmental networks in OECD countries. *PloS one,* 10**,** e0136767.

Salem, H. M., C. Valero, M. Á. Muñoz, M. G. Rodríguez & L. L. Silva (2015) Short-term effects of four tillage practices on soil physical properties, soil water potential, and maize yield. *Geoderma,* 237**,** 60-70.

Scheffer, M., S. Barrett, S. Carpenter, C. Folke, A. J. Green, M. Holmgren, T. Hughes, S. Kosten, I. Van de Leemput & D. Nepstad (2015) Creating a safe operating space for iconic ecosystems. *Science,* 347**,** 1317-1319.

Shao, X., H. Wang & Z. Wang (2003) Interbasin transfer projects and their implications: A China case study. *International Journal of River Basin Management,* 1**,** 5-14.

Song, Z., H. Sun & J. Dong. 2007. Solving China's North-South Grain Transfer problem.

Squartini, T., F. Picciolo, F. Ruzzenenti & D. Garlaschelli (2013) Reciprocity of weighted networks. *Scientific reports,* 3**,** 2729.

Steffen, W., K. Richardson, J. Rockström, S. E. Cornell, I. Fetzer, E. M. Bennett, R. Biggs, S. R. Carpenter, W. de Vries, C. A. de Wit, C. Folke, D. Gerten, J. Heinke, G. M. Mace, L. M. Persson, V. Ramanathan, B. Reyers & S. Sörlin (2015) Planetary boundaries: Guiding human development on a changing planet. *Science,* 347**,** 1259855.

Steinmann, Z. J., A. M. Schipper, M. Hauck, S. Giljum, G. Wernet & M. A. Huijbregts (2017) Resource footprints are good proxies of environmental damage. *Environmental science & technology,* 51**,** 6360-6366.

Sun, J., H. Mooney, W. Wu, H. Tang, Y. Tong, Z. Xu, B. Huang, Y. Cheng, X. Yang & D. Wei (2018) Importing food damages domestic environment: Evidence from global soybean trade. *Proceedings of the National Academy of Sciences,* 115**,** 5415-5419.

Sun, J., H. Mooney, W. B. Wu, H. J. Tang, Y. X. Tong, Z. C. Xu, B. R. Huang, Y. Q. Cheng, X. J. Yang, D. Wei, F. S. Zhang & J. G. Liu (2018) Importing food damages domestic environment: Evidence from global soybean trade. *Proceedings of the National Academy of Sciences of the United States of America,* 115**,** 5415-5419.

Sun, J., Y.-x. Tong & J. Liu (2017) Telecoupled land-use changes in distant countries. *Journal of integrative agriculture,* 16**,** 368-376.

Sun, S., C. Zhang, X. Li, T. Zhou, Y. Wang, P. Wu & H. Cai (2017) Sensitivity of crop water productivity to the variation of agricultural and climatic factors: A study of Hetao irrigation district, China. *Journal of cleaner production,* 142**,** 2562-2569.

Sun, X., J. Li, H. Qiao & B. Zhang (2017) Energy implications of China's regional development: New insights from multi-regional input-output analysis. *Applied energy,* 196**,** 118-131.

Swartz, S. & S. Oster (2010) China Tops US in Energy Use. *The Wall Street Journal,* 18.

Tamea, S., J. A. Carr, F. Laio & L. Ridolfi (2014) Drivers of the virtual water trade. *Water Resources Research,* 50**,** 17-28.

Tang, X., S. Snowden & M. Höök (2013) Analysis of energy embodied in the international trade of UK. *Energy Policy,* 57**,** 418-428.

Timmer, M. P., E. Dietzenbacher, B. Los, R. Stehrer & G. J. Vries (2015) An illustrated user guide to the world input–output database: the case of global automotive production. *Review of International Economics,* 23**,** 575-605.

Torres, S. M., E. F. Moran & R. F. B. d. Silva (2017) Property rights and the soybean revolution: shaping how China and Brazil are Telecoupled. *Sustainability,* 9**,** 954.

Viala, E. (2008) Water for food, water for life a comprehensive assessment of water management in agriculture. *Irrigation and Drainage Systems,* 22**,** 127-129.

Viña, A., R. Silva, H. Yang & J. Liu. 2017. Effects of the international soybean trade on the dynamics of Gross Primary Productivity in soybean-producing regions in China and Brazil. In *AGU Fall Meeting Abstracts*.

von Braun, J. & A. Mirzabaev. 2016. Nexus scientifi c research: Theory and approach serving sustainable development. In *The Water, Food, Energy and Climate Nexus*, 84-97. Routledge.

Vörösmarty, C., A. Hoekstra, S. Bunn, D. Conway & J. Gupta (2015) Fresh water goes global. *Science,* 349**,** 478-479.

Wang, D., G. Zhang, H. Feng, Y. Tian & J. Wang (2015) Spatial variation of groundwater guarantee extent in typical well irrigation area of North China Plain. *South-to-North Water Transfers and Water Science & Technology,* 13**,** 622-625 (in Chinese).

Wang, H., L. Zhang, W. Dawes & C. Liu (2001) Improving water use efficiency of irrigated crops in the North China Plain—measurements and modelling. *Agricultural Water Management,* 48**,** 151-167.

Wang, H. X., L. Zhang, W. R. Dawes & C. M. Liu (2001) Improving water use efficiency of irrigated crops in the North China Plain - measurements and modelling. *Agricultural Water Management,* 48**,** 151-167.

Wang, Y., P. Wu, B. Engel & S. Sun (2014) Application of water footprint combined with a unified virtual crop pattern to evaluate crop water productivity in grain production in China. *Science of the Total Environment,* 497**,** 1-9.

Ward, F. A. & M. Pulido-Velazquez (2008) Water conservation in irrigation can increase water use. *Proceedings of the National Academy of Sciences,* 105**,** 18215-18220.

Wicaksono, A., G. Jeong & D. Kang (2017) Water, energy, and food nexus: review of global implementation and simulation model development. *Water Policy***,** wp2017214.

Wiedmann, T. (2009) A first empirical comparison of energy footprints embodied in trade—MRIO versus PLUM. *Ecological Economics,* 68**,** 1975-1990.

Wiedmann, T. & M. Lenzen (2018) Environmental and social footprints of international trade. *Nature Geoscience,* 11**,** 314-321.

Wood, S. A., M. R. Smith, J. Fanzo, R. Remans & R. S. DeFries (2018) Trade and the equitability of global food nutrient distribution. *Nature Sustainability*, 34-37.

Wu, S., Y. Lei & L. Li (2015) Resource distribution, interprovincial trade, and embodied energy: A case study of China. *Advances in Materials Science and Engineering,* 2015.

Xie, J. F. & J. G. Zhang (2007) Groundwater Development Model in the Guantao County of Hebei Province. *Ground Water,* 6**,** 51-53.

Xu, J., X. Liu, S. Yang, Z. Qi & Y. Wang (2017) Modeling rice evapotranspiration under water-saving irrigation by calibrating canopy resistance model parameters in the Penman-Monteith equation. *Agricultural water management,* 182**,** 55-66.

Xu, Z., S. Chau, F. Ruzzenenti, T. Connor, Y. Li, Y. Tang, D. Li, M. Gong & J. Liu (2018) Evolution of multiple global virtual material flows. *Science of The Total Environment,* 658**,** 659-668.

Xu, Z., Y. Li, A. Herzberger, X. Chen, M. Gong, K. Kapsar, C. Hovis, J. Whyte, Y. Tang & Y. Li (2019) Interactive national virtual water-energy nexus networks. *Science of The Total Environment,* 673**,** 128-135.

Xu, Z., Y. Tang, T. Connor, D. Li, Y. Li & J. Liu (2017) Climate variability and trends at a national scale. *Scientific Reports,* 7**,** 3258.

Xu, Z., D. Zhang, P. McCord, M. Gong & J. Liu (2019) Shift in a national virtual energy network. *Applied Energy,* 242**,** 561-569.

Yang, Y., M. Watanabe, X. Zhang, J. Zhang, Q. Wang & S. Hayashi (2006) Optimizing irrigation management for wheat to reduce groundwater depletion in the piedmont region of the Taihang Mountains in the North China Plain. *Agricultural Water Management,* 82**,** 25-44.

Yergin, D. (2006) Ensuring energy security. *Foreign affairs***,** 69-82.

Yin, K., H. Yuan, Q. Liao & Y. Ruan (2001) Impact of Middle Route SN Water Transfer Project on Algae Bloom in Middle & Lower Reach of Hanjiang River. *Yangtze River (Renmin Changjiang),* 32**,** 31-50.

Yuan, X., M. Mi, R. Mu & J. Zuo (2013) Strategic route map of sulphur dioxide reduction in China. *Energy policy,* 60**,** 844-851.

Zhang, B., Z. Chen, X.-H. Xia, X. Xu & Y. Chen (2013) The impact of domestic trade on China's regional energy uses: a multi-regional input–output modeling. *Energy Policy,* 63**,** 1169-1181.

Zhang, B., H. Qiao, Z. Chen & B. Chen (2016) Growth in embodied energy transfers via China’s domestic trade: evidence from multi-regional input–output analysis. *Applied Energy,* 184**,** 1093-1105.

Zhang, C. & L. D. Anadon (2014) A multi-regional input–output analysis of domestic virtual water trade and provincial water footprint in China. *Ecological Economics,* 100**,** 159-172.

Zhang, F. 2011. Soil Testing and Fertilization Recommendation. 296. Beijing: China Agricultural University Press.

Zhang, F., W. Ma & X. Chen. 2006. Introduction to the theory and technology of integrated nutrient management. 329. Beijing: China Agricultural University Press.

Zhang, G., Y. Fei, J. Wang & M. Yan. 2012. *Study on the adaptativity of groundwater and irrigated agriculture in North China Plain*. Beijing: Science Press.

Zhang, G., Y. Lian, C. Liu, M. Yan & J. Wang (2011) Situation and origin of water resources in short supply in North China Plain. *Journal of Earth Sciences and Environment,* 33**,** 172-176.

Zhang, J. (2007) Who will meet China's import demand for forest products? *World Development,* 35**,** 2150-2160.

Zhang, J., N. Zhao, X. Liu & Y. Liu (2016) Global virtual-land flow and saving through international cereal trade. *Journal of Geographical Sciences,* 26**,** 619-639.

Zhang, Q. (2009) The South-to-North Water Transfer Project of China: Environmental Implications and Monitoring Strategy. *JAWRA Journal of the American Water Resources Association,* 45**,** 1238-1247.

Zhang, X., S. Chen, H. Sun, D. Pei & Y. Wang (2008) Dry matter, harvest index, grain yield and water use efficiency as affected by water supply in winter wheat. *Irrigation Science,* 27**,** 1-10.

Zhang, X., S. Chen, H. Sun, Y. Wang & L. Shao (2010) Water use efficiency and associated traits in winter wheat cultivars in the North China Plain. *Agricultural Water Management,* 97**,** 1117-1125.

Zhang, X. Y., S. Y. Chen, H. Y. Sun, D. Pei & Y. M. Wang (2008) Dry matter, harvest index, grain yield and water use efficiency as affected by water supply in winter wheat. *Irrigation Science,* 27**,** 1-10.

Zhang, Y., H. Zheng, Z. Yang, M. Su, G. Liu & Y. Li (2015) Multi-regional input–output model and ecological network analysis for regional embodied energy accounting in China. *Energy Policy,* 86**,** 651-663.

Zhang, Z., H. Yang & M. Shi (2011) Analyses of water footprint of Beijing in an interregional input–output framework. *Ecological Economics,* 70**,** 2494-2502.

Zhao, R., X. Chen & F. Zhang (2009) Nitrogen cycling and balance in winter-wheat-summer-maize rotation system in Northern China Plain. *Acta pedologica sinica,* 46**,** 684-697.

Zhao, X., J. Liu, Q. Liu, M. R. Tillotson, D. Guan & K. Hubacek (2015) Physical and virtual water transfers for regional water stress alleviation in China. *Proceedings of the National Academy of Sciences,* 112**,** 1031-1035.

Zhao, X., J. Liu, Q. Liu, M. R. Tillotson, D. Guan & K. Hubacek (2015) Physical and virtual water transfers for regional water stress alleviation in China. *Proceedings of the National Academy of Sciences,* 112**,** 1031-5.

Zhao, Y. 2010. Research on crop water consumption based on ISAREG model and crop water production functions. China Agricultural University.

Zhong, L. & A. P. Mol (2010) Water price reforms in China: policy-making and implementation. *Water resources management,* 24**,** 377-396.

Zhong, W., H. An, W. Fang, X. Gao & D. Dong (2016) Features and evolution of international fossil fuel trade network based on value of emergy. *Applied Energy,* 165**,** 868-877.

Zhou, Z. & D. Yang (2006) Virtual Energy: a New Visual Angle to Analyze the Hypernormal Growth Rate of Energy Consumption in China. *Advances in Earth Science,* 21**,** 320-323